HAW HAMBURG

MASTER THESIS

Lara Borsdorf [redacted]

# Development of a 3D-Printed Myoelectric Arm Prosthesis with a Rotational Wrist Joint

Faculty of Life Sciences
Department Biomedical Engineering

HOCHSCHULE FÜR ANGEWANDTE WISSENSCHAFTEN HAMBURG
Hamburg University of Applied Sciences

Lara Borsdorf [redacted]

# Development of a 3D-Printed Myoelectric Arm Prosthesis with a Rotational Wrist Joint

Master thesis submitted for examination in Master´s degree
in the study course *Master of Science Biomedical Engineering*
at the Department Biomedical Engineering
at the Faculty of Life Sciences
at University of Applied Sciences Hamburg

First Supervisor: Prof. Dr. Meike Annika Wilke
Second Supervisor: Prof. Dr. Thomas Schiemann

Submitted on: 02. July 2024

**Lara Borsdorf** [redacted]

**Title of Thesis**

Development of a 3D-Printed Myoelectric Arm Prosthesis with a Rotational Wrist Joint

**Keywords**

3D-Print, Prosthesis, Myolectric, Rotational Wrist, EMG, Machine Learning

**Abstract**

Prostheses can be highly expensive and often require a long manufacturing time, leading to limited accessibility to prosthetic devices for impaired individuals. This thesis aims to develop a low-cost, 3D-printed arm prosthesis controlled by electromyographic (EMG) signals. A MyoBand is attached to the residual limb to record eight EMG signals, which are used to differentiate between various hand gestures. The prosthesis features intuitive rotational control of the wrist which has not yet been implemented in other, similar devices. Therefore, the following research questions are asked: (1) To what extent can intuitive rotational movements of the hand be recognized using a MyoBand and differentiated from other gestures? (2) Can the data collected by the MyoBand be used to enable proportional and simultaneous control of the rotational movement along with other hand gestures in a 3D-printed arm prosthesis?

In order to answer the research questions, this thesis was conducted through the following steps: First, an appropriate 3D model was selected, which was adapted in order to be applicable as a prosthesis. Second, the required hardware components, such as motors and a microcontroller, were selected to match the design specifications and performance needs of the prosthesis. Third, the individual parts of the prosthesis were 3D-printed and assembled, and the hardware components were integrated. Fourth, the software for the control system was developed using MATLAB and Simulink. The control system comprised two programs: one for capturing various gestures, including flexion, extension, pronation, supination, and relaxation as a baseline, and another one featuring a Linear Discriminant Analysis (LDA) classifier for recognizing these gestures and controlling the prosthesis accordingly. Fifth, the control system was tested using a virtual prosthesis to validate its functionality, followed by a pilot test with the physical hardware.

The pilot test was conducted to evaluate the LDA classifier's gesture recognition and to determine whether the 3D-printed prosthesis could be controlled based on the recognized gestures. The results demonstrated that the system was capable of distinguishing between different intuitive gestures, including rotational movements. Furthermore, the motors of the prosthesis could be controlled proportionally to the user's muscle strength, allowing for a precise control of the prosthesis. Interestingly, the pilot test also revealed that the position of the arm influences the gesture recognition capabilities of the LDA classifier, with the suspended arm leading to higher accuracy compared the flexed arm.

# Table of Contents

# Table of Figures

# List of Tables

# Abbreviations

| | |
|---|---|
| **ABS** | *Acrylonitrile Butadiene Styrene* |
| **BBT** | *Box-and-Block Test* |
| **CLS** | *Closed-Loop Development Framework* |
| **DOF** | *Degree of Freedom* |
| **EMG** | *Electromyography* |
| **GPIO** | *General Purpose Input Output* |
| **$I^2C$** | *Inter-Integrated Circuit* |
| **LDA** | *Linear Discriminant Analysis* |
| **LR** | *Linear Regression* |
| **MVC** | *Maximum Voluntary Contraction* |

| | |
|---|---|
| **OPUS** | *Orthotics Prosthetics Users Survey* |
| **PCA9685** | *PCA9685 16-Channel 12-Bit PWM Servo Motor Driver* |
| **PLA** | *Polylactic Acid* |
| **PWM** | *Pulse-width modulation* |
| **QUEST** | *Quebec User Evaluation of Satisfaction with Assistive Technology* |
| **Raspberry Pi** | *Raspberry Pi 3B+* |
| **RCRT** | *Refined Clothespin Relocation Test* |
| **RMS** | *Root Mean Square* |
| **SCL** | *Serial Clock* |
| **SDA** | *Serial Data* |
| **SPI** | *Serial Peripheral Interface* |
| **SSC** | *Slope Sign Change* |
| **TPU** | *Thermoplastic Polyurethane* |
| **UML** | *Unified Modeling Language* |
| **WHO** | *World Health Organisation* |
| **WL** | *Wave Length* |
| **ZCR** | *Zero Crossings* |

# 1 Introduction

According to the World Health Organisation (WHO), only ten percent of individuals who could benefit from a prosthesis have access to one [31]. Arm prostheses are individually manufactured aids with substantial differences in costs, often reaching high prices. For example, a simple passive prosthesis for a toddler usually costs approximately 2,000 €, and a double-sided myoelectric shoulder prosthesis can cost up to 300,000 € [43]. The manufacturing time for such prostheses can take weeks or even months, depending on the type [21]. Therefore, it is crucial to develop affordable, and quickly available prostheses. In addition, temporary solutions should be provided to cover the waiting period for complex prostheses.

A promising solution to this problem could be 3D-printed prostheses. Printing the mechanical parts of a prosthesis in a 3D-printer takes comparatively little time. The printing time of the parts depends on the printer settings, such as the diameter of the nozzle, the layer height, and the degree of filling. It also varies depending on the filament material used [41]. When assembled from many small, individual parts, it is possible to further optimize the printing time by using several printers at the same time. Another advantage of 3D-printed prostheses is the overall substantially reduced costs compared to conventional prostheses. For instance, the 3D-printed prosthesis used in the work of S. Said et al., "Machine-Learning-Based Muscle Control of a 3D-Printed Bionic Arm", costs around $ 295 [75]. The cost efficiency, on the one hand, results from the comparatively low price per kilogram of the Polylactic Acid (PLA) filament commonly used for 3D-printing, which ranges from $ 20 to $ 40 per kilogram [47]. On the other hand, the required electrical components are mass-produced and, therefore, cheap and easily accessible.

Research in the area of 3D-printed prostheses has already been carried out. For example, self-actuated prostheses, which are controlled by movements of the shoulder, have been developed [56]. Other experiments have focused on externally powered prostheses that can be controlled using Electromyography (EMG) signals generated by the arm muscles

such as the study mentioned before [75]. Those studies that have researched EMG-controlled prostheses have mostly focused on the opening and closing of the hand, but little on the rotational movement of the wrist. Therefore, the main goal of this thesis is to develop a 3D-printed arm prosthesis, which is controlled using EMG signals while focusing on additional wrist movement to offer more functionality.

The Degree of Freedom (DOF) provided by the additional rotation unit gives the patient increased mobility and prevents postural deformities [48]. The prosthesis is externally powered and controlled with the help of EMG signals recorded of the arm muscles. For this purpose, a MyoBand is used, which is attached to the residual limb and records eight EMG signals. This enables the implementation of a control system with two DOFs for both the rotation of the wrist as well as the closing and opening of the hand. To develop this control system, machine learning approaches are used to find the complex relationships between the different hand gestures and the eight EMG signals. In contrast to similar 3D-printed arm prostheses featuring a rotation unit, the control mechanism for movements in this work's prosthesis is intuitive. A pilot test in the form of a self-experiment is carried out to validate the functionality.

As a result, the research questions addressed in this thesis are: (1) To what extent can intuitive rotational movements of the hand be recognized using a MyoBand and differentiated from other gestures? (2) Can the data collected by the MyoBand be used to enable proportional and simultaneous control of the rotational movement along with other hand gestures in a 3D-printed arm prosthesis?

The following sections offer a brief summary of the upcoming chapters in this work.

In Chapter 2, the theoretical background relevant to this thesis is presented. This includes an analysis of the general anatomy of the upper extremities followed by an overview of amputations. Furthermore, the basic types of prostheses are presented as well as a description of general aspects such as costs and accessibility of these prostheses. The chapter finishes with a description of the current state of research in the field of 3D-printing in prosthetics including the identification of existing research gaps.

Chapter 3 presents the methodology of this thesis. It begins with describing the requirements for the 3D-model of the prosthesis, followed by an explanation of the selection process and necessary adaptations. The chosen hardware is presented, explaining the reasons behind the selection. The additive manufacturing process of the prosthesis is described including the assembly of the prosthesis with the rest of the hardware. The

software used for programming the EMG-based prosthesis control and the program's structure are explained. Furthermore, the setup and execution of two experiments are discussed, starting with the pilot test and then progressing to the test with limb-impaired subjects. The final segment of the methodology is dedicated to ethical and safety-related aspects due to the prosthesis's skin contact with individuals.

Chapter 4 presents the results of this thesis. Firstly, the assembled prosthesis is illustrated, along with a description of the challenges encountered. Subsequently, the implemented control of the prosthesis is presented, including the code and the underlying logic. Finally, the results of the experiments are outlined, starting with the pilot test and followed by the tests with limb-impaired subjects. Various considerations, including wearing comfort, suitability for everyday use, prosthesis functionality, and customization capabilities are taken into account.

In Chapter 5, the interpreted results are discussed, comparing them with existing solutions. Likewise, the chapter addresses challenges and limitations. Based on this comparison, implications for practice are derived, alongside proposed future work and improvements.

Lastly, Chapter 6 serves as a conclusion of this thesis. It summarizes the most important results, addressing the initial thesis question along with an outlook into the future.

# 2 Theoretical Part

Below is an outline of the theoretical background of this thesis. Initially, the medical background is described, including the basic anatomical structures of the forearm and their role in controlling the hand. This is followed by an overview of upper limb amputations. Furthermore, the specific requirements and challenges involved in the development and adaptation of prostheses are explained. Likewise, the importance of prostheses and their various types are presented. Lastly, a comprehensive overview of the current state of research in the field of 3D-printing technology for upper limb prostheses is offered.

## 2.1 Medical Background

### 2.1.1 Degrees of Freedom of the Different Hand and Finger Joints

The movement of a rigid body in space is described using DOFs. A distinction is made between two types of movements: translational movements and rotational movements. The rigid body has a total of six DOFs, which are shown in Figure 2.1, using a ball in space as an example. Figure 2.1(a) shows the translational DOFs, and Figure 2.1(b) the rotational DOFs [76].

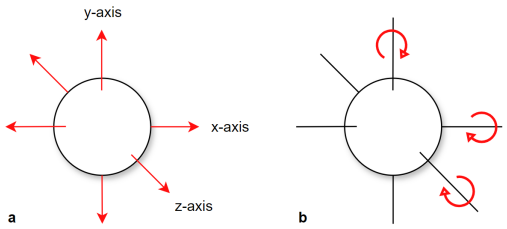


Figure 2.1: Degrees of freedom for a ball in space marked as red arrows (own figure based on [76]).

The DOFs are present in various degrees across the various joints of the body. The range of motion of a joint is determined by the shape of the articulating bones as well as by the muscular and ligamentous structures. A distinction is made between uniaxial joints with one DOF, biaxial joints with two DOFs, and triaxial joints with three DOFs. An example of a triaxial joint would be the shoulder joint [72].

The joints that enable the hand and fingers to move are described in the following paragraph.

There are two main joints at the base of the hand that allow the hand to move in relation to the forearm: the proximal and distal wrist joints [39]. The proximal wrist joint, which is located between the forearm and the proximal row of carpal bones, is an ellipsoid joint with two DOFs. This includes palmar flexion and dorsiflexion as well as ulnar abduction and radial abduction. In contrast, the distal wrist joint, which lies between the proximal and distal row of carpal bones, is an interlocking ginglymoid joint with a single DOF. This joint enables palmar flexion and dorsiflexion. The wrist movements can be seen in Figure 2.2 [76]. However, these movements will not be carried out by the prosthesis in this work.

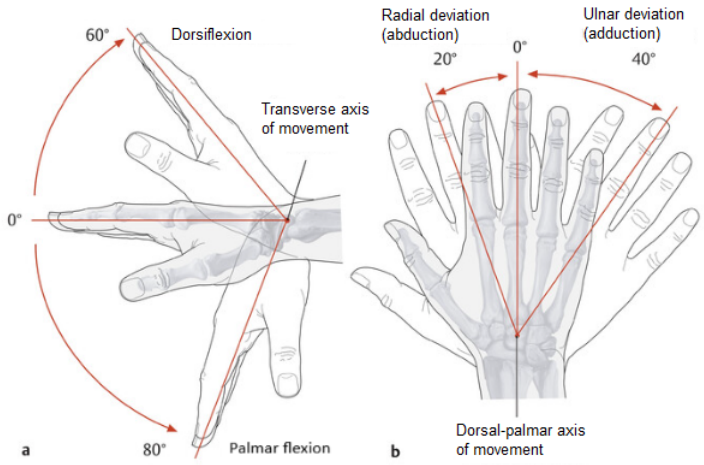


Figure 2.2: Range of motion of the proximal and distal wrist [76].

Pronation and supination of the forearm are of more importance, as these are intended to be performed by the prosthesis. These motions can be seen in Figure 2.3.

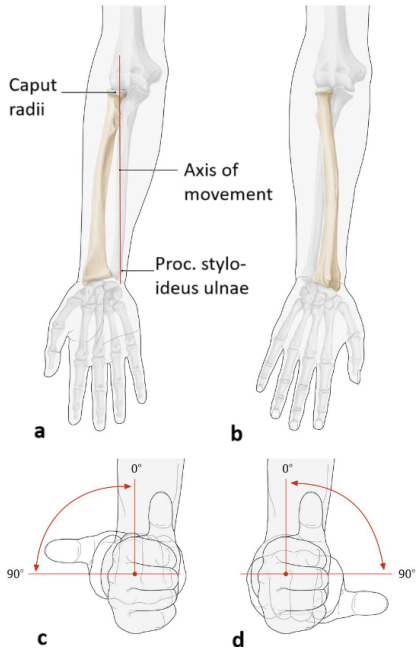


Figure 2.3: Supination and pronation of the forearm (adapted from [76]).

Figure 2.3 shows in (a) the supination position, in which the forearm bones are aligned parallel to each other, while in (b) it shows the pronation position, in which the radius crosses the ulna. The supination position of the hand can be seen in (c), whereas (d) shows the pronation position of the hand. In both (c) and (d), the elbow is flexed and the perspective is frontal [76]. The pronation and supination are made possible by the humeroradial, the proximal radioulnar, and the distal radioulnar joint, in which the radius moves around the ulna.
In simple terms, the wrist joint as a whole can perform flexion and extension as well as adduction and abduction movements. As pronation and supination movements are performed in one axis to the wrist, these form a theoretical third DOF of the wrist. Simplified, the mobility of the wrist joint therefore corresponds to that of a spheroid joint [39].

The number of DOFs in the individual joints of the fingers varies depending on the type of joint. Morphologically speaking, the carpometacarpal joint of the thumb has two DOFs that allow movements of the thumb around two vertically superimposed axes. These two axes can be seen in Figure 2.4(b). In Figure 2.4(a), the neutral zero position of the thumb is shown. The two axes allow the joint not only to adduct and abduct

(see Figure 2.4(c)), but also to flex and extend (see Figure 2.4(d)). Since the metacarpal bone of the thumb can also rotate around its longitudinal axis during the opposition movement (see Figure 2.4(e)), the carpometacarpal joint of the thumb has three DOFs from a functional point of view [39].

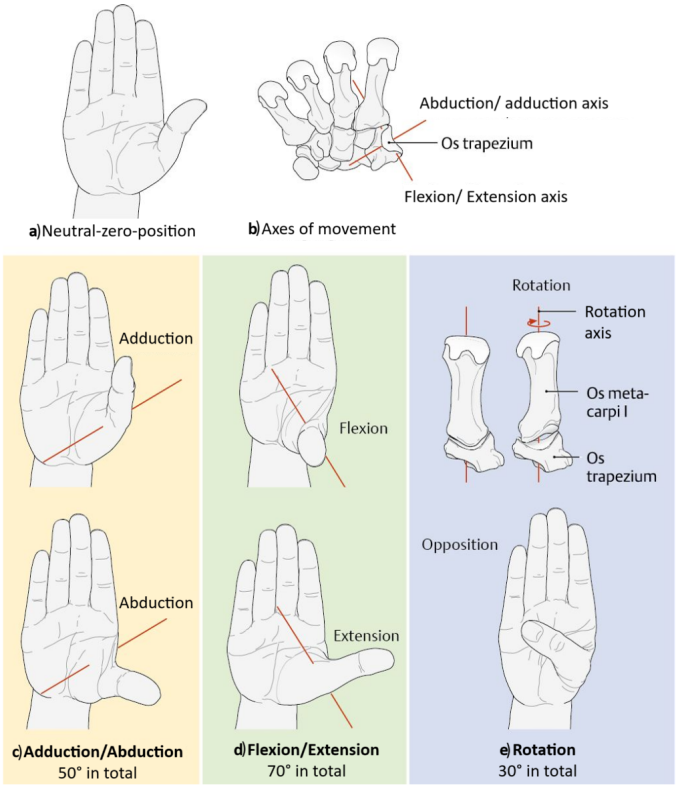


Figure 2.4: Movements in the carpometacarpal joint of the thumb (adapted from [70]).

Among the finger joints, a distinction is made between metacarpophalangeal, proximal interphalangeal, and distal interphalangeal joints. The metacarpophalangeal joints are located between the metacarpal bones and the proximal phalanges. From a morphological point of view, the metacarpophalangeal joints are spheroid joints. However, due to their tight ligamentous apparatus, they only have two DOFs, namely flexion and extension as well as abduction and adduction [76]. The movements of the metacarpophalangeal joints can be seen in Figure 2.5(a). The metacarpophalangeal joint of the thumb has a different structure, which is functionally similar to a hinge joint and only allows considerable extension and flexion [39].

The other joints in the fingers are classified as interphalangeal joints, which in turn are subdivided into proximal and distal interphalangeal joints. The proximal interphalangeal joints are located between the proximal and middle phalanges, while the distal interphalangeal joints are located between the middle and distal phalanges. In general, these joints are ginglymoid joints with a DOF limited to flexion and extension. Figure 2.5(b) shows the movement of these joints [76].

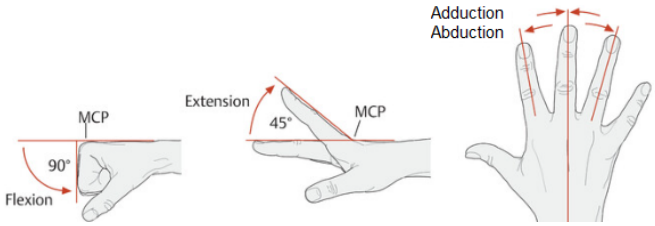


(a) Range of motion of the metacarpophalangeal joints.

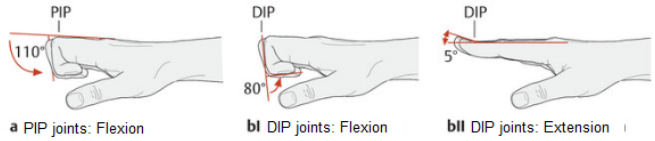


(b) Range of motion of the proximal and distal interphalangeal joints.

Figure 2.5: Range of motion of the finger joints (adapted from [76]).

### 2.1.2 Muscles of the Upper Limbs

Among other things, the muscles of the arm are responsible for the movements of the wrist and fingers. As the prosthesis is controlled with the aid of sensors attached to the forearm, the muscles of the forearm and their tasks are described in the following.

Based on their respective position, the forearm muscles are divided into five groups. A distinction is made between the muscles on the palmar side, which act as flexors, and the muscles on the dorsal side, which act as extensors. These flexor and extensor muscles can each be divided into superficial and deep muscle groups. Another group is the radialis group, which is classified as a group of extensor muscles due to their innervation and developmental history [39]. The superficial and deep flexor muscles are shown in Figure 2.6. The superficial and deep extensor muscles as well as the radial muscles are shown in Figure 2.7.

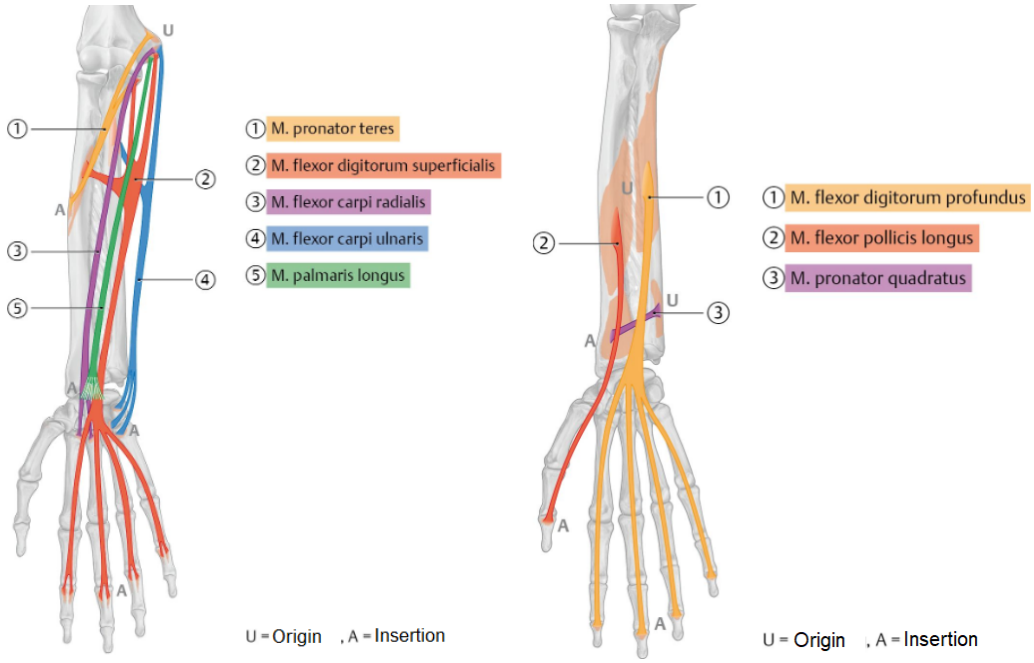


(a) Route of the superficial flexor muscles. (b) Route of the deep flexor muscles.

Figure 2.6: Flexor muscle routes in the forearm (adapted from [71]).

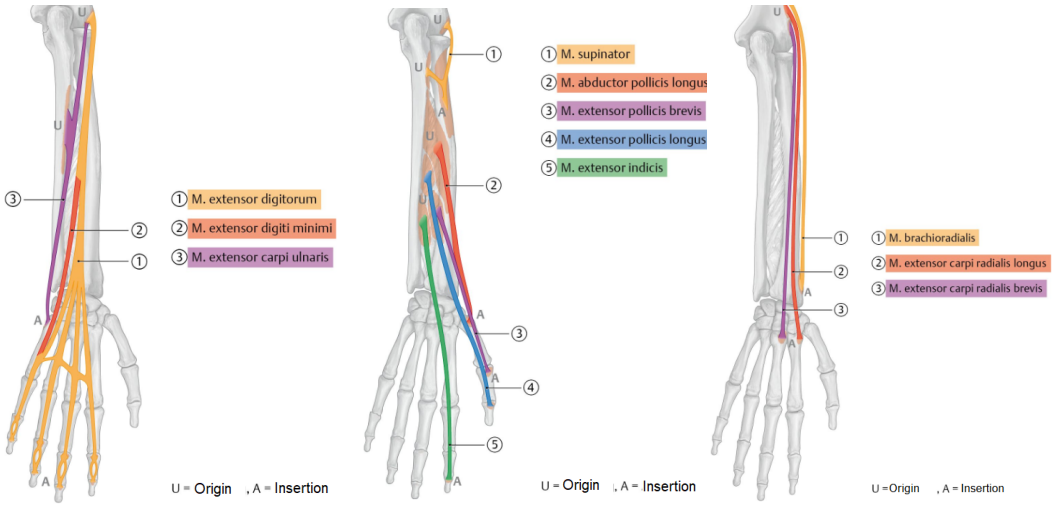


(a) Route of the superficial extensor muscles. (b) Route of the deep extensor muscles. (c) Route of the radialis muscles.

Figure 2.7: Extensor muscle routes in the forearm (adapted from [71]).

The muscles responsible for extension and flexion of the fingers are listed in Table 2.1. The individual fingers are numbered from 1 to 5, starting with the thumb.

Table 2.1: Muscles responsible for flexion and extension [39].

| **Muscle group** | **Muscles** | **Task** |
|---|---|---|
| **Superficial flexor** | M. flexor digitorum superficialis | Flexion of the metacarpophalangeal and proximal interphalangeal joints in the fingers 2-5. |
| **Deep flexors** | M. flexor digitorum profundus | Flexion of the metacarpophalangeal, proximal interphalangeal joints, and the distal interphalangeal joints in the fingers 2-5. |
| | M. flexor pollicis longus | Flexion and opposition of the carpometacarpal joint in the thumb, as well as the flexion of the metacarpophalangeal and distal interphalangeal joints in the thumb. |
| **Superficial extensors** | M. extensor digitorum | Extension of the joints in the fingers 2-5. |
| | M. extensor digiti minimi | Extension of the joints in the fifth finger. |
| **Deep extensors** | M. abductor pollicis longus | Abduction and extension of the carpometacarpal joint in the thumb. |
| | M. extensor pollicis brevis | Extension of the carpometacarpal and metacarpophalangeal joint in the thumb. |
| | M. extensor pollicis longus | Extension of all thumb joints and for the additional abduction of the carpometacarpal joint in the thumb. |
| | M. extensor indicis | Extension of the joints in the second finger. |

Table 2.2 displays which forearm muscles are substantially involved in pronation and supination.

Table 2.2: Muscles responsible for pronation and supination [39].

| **Movement** | **Muscles** |
|---|---|
| **Pronation** | M. pronator teres, M. flexor carpi radialis, M.pronator quadratus, M. brachioradialis, M. extensor carpi radialis longus |
| **Supination** | M. biceps brachii, M. supinator, M. abductor pollicis longus, M. extensor pollicis longus, M. brachioradialis |

### 2.1.3 Medical Background with respect to Amputations

In developed societies, arterial occlusive diseases and traumatic injuries are the predominant causes of amputations. For amputations caused by vascular disease, successful treatment requires the preservation of maximum residual limb length, early prosthetic fitting and the initiation of rehabilitation programs. In severely traumatized extremities, it is important to determine at an early stage, whether amputation is necessary, as unnecessary preservation can create risks. These include life-threatening conditions such as crush syndrom[1] or intoxication in gangrene[2], which in turn can delay rehabilitation by years [68].

Amputations of the upper extremities leads to more severe functional and psychological impairments than those of the lower extremities. This is due to the fact that the upper extremities perform more complex functions in everyday life in contrast to the lower extremities, which are primarily responsible for stability and movement. This results in different requirements for upper limb prostheses compared to lower limb prostheses. Consequently, prosthetic treatment of the upper extremities is more frequently rejected. The greater the degree of limb loss, the more likely it is that a prosthesis will not be accepted [68].

[1] Incidents, in which large amounts of muscle are destroyed, such as burns or severe bruising, and sometimes non-traumatic rhabdomyolysis (e.g. animal poisoning or statin therapy), can lead to crush syndrome. It is caused by the release of large amounts of myoglobin, potassium, metabolic products, and mediators of the inflammatory cascade during the destruction of skeletal muscles and can lead to kidney failure and electrolyte disturbances [85].

[2] Gangrene is a tissue necrosis, in which tissue dies due to a prolonged circulatory disorder. This occurs, for example, due to microangiopathy or peripheral arterial occlusive disease, particularly in the lower extremities [53].

The main function of an upper limb prosthesis is to provide a grasping function. However, a significant challenge is the absence of sensory feedback. Conventional prostheses allow a certain amount of sensory feedback via force-transmitting components. For example, via an active gripper arm, the force can be transmitted through a bandage and a cable pull. This option is not available with external power prostheses, which offer cosmetic advantages but do not provide any feedback [68].

Figure 2.8 shows the different amputation heights, which have a significant impact on the prosthetic treatment and its challenges.

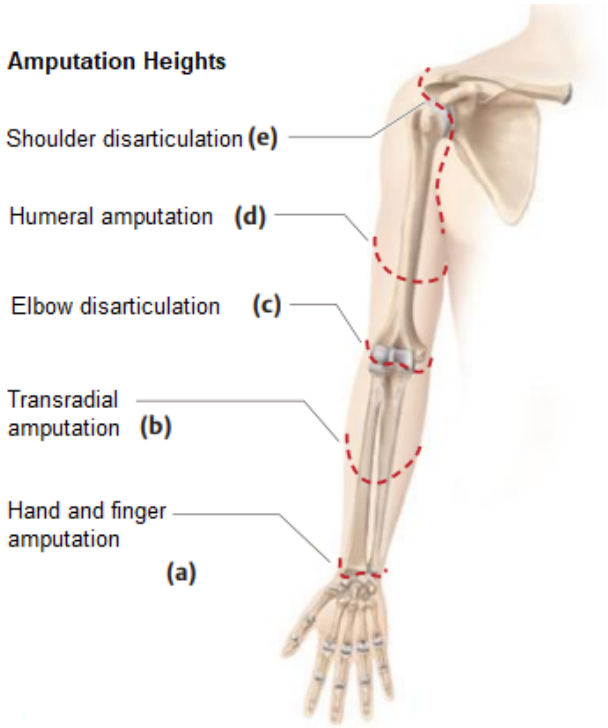


Figure 2.8: Different amputation heights of the upper limb (adapted from [68]).

An effective and functionally high-quality solution for shoulder disarticulations has so far been challenging. The amputation height is shown in the figure at position (e). At the next highest amputation level (d), the humeral amputation, the main challenge is attaching the prosthesis to the upper arm's residual limb. Surgical treatment, such as bending the distal residual limb, may be necessary. Active grasping arms are preferably

used for this form of amputation. Level (c) shows the elbow disarticulation in which myoelectric prostheses are often used. Myoelectric prostheses are also frequently used for transradial amputations, as shown in (b). For longer residual limbs, the Krukenberg technique is used, in which the ulna and radius are separated scissor-like from each other with a soft tissue sheath. This enables a gripping function as long as the sensitivity between the areas is retained. Wrist and finger amputations are performed at level (a) [68].

## 2.2 Classification and Accessibility of Prostheses

Prostheses can help people with physical impairments to lead more productive and self-determined lives. By overcoming functional limitations, prostheses not only help to restore mobility, but also enable a healthier life. However, access to prostheses is severely limited and only one in ten people who need assistive devices have access to them, according to the WHO. This restricted accessibility not only leads to individual limitations, but also contributes to social exclusion. People who are denied access to prostheses often suffer from poverty and become socially isolated. This leads to an increased risk of morbidity and disability [31].

The WHO estimates that on average around 0.5 % of the world's population require prosthetic or orthotic services, which means approximately 35-40 million people worldwide. Conflicts, accidents, and widespread diseases are factors that can increase the demand, while successful accident prevention and effective trauma care can help to reduce the number of people who need prosthetics [31]. The demand for orthoses and prostheses is expected to continue to increase due to the growing world population and increased life expectancy. The increasing incidence of musculoskeletal disorders and diseases such as diabetes will increase the demand. It is assumed that demand will rise to 1 % of the world's population in the future [31].

Upper limb prostheses can take the form of either exoskeletal prostheses or endoskeletal prostheses. Exoskeletal prostheses appear in the shape of the respective limb and are surrounded by an outer shell made of metal or plastic. These prostheses are permanently fixed and cannot be adjusted. Preferably, they are used by people who live in demanding environments or perform physical labor. In contrast, endoskeletal prostheses are less durable but can be adjusted. They have a central internal skeletal structure and are often covered with soft material or synthetic skin. Various types of upper limb prostheses

are available, including passive prostheses, body-powered prostheses, externally powered myoelectric prostheses, hybrid prostheses, and activity-specific prostheses [79].

A passive prosthesis helps with balancing and stabilizing objects. Visually, these prostheses resemble a natural limb, but do not have a usable joint or the ability to move the hand. They represent the lightest and most cost-effective form of prostheses [79].

The most common prosthesis is the body-powered type, which is favored due to its durability, comparably lower cost, and low maintenance requirements. This prosthesis is equipped with a belt and cable system that allows control of, for example, a hand, hook, or elbow joint by moving the shoulder. It is also possible for the prosthesis to be controlled by the opposite arm by attaching a strap in the armpit of the other arm, while the other side is connected to a cable that moves the hand, hook or elbow joint. People who work physically tend to prefer this type of prosthesis [79].

The externally powered myoelectric prosthesis enables active movements of the hand and joints without having to move the shoulder or body. The muscle movements of the residual limb are recorded by sensors or other inputs. The captured signals then control electrical actuators within the prosthesis, resulting in a higher gripping force compared to the previously mentioned prostheses [79].

Hybrid prostheses are normally used for higher-grade amputations of the upper limb. These prostheses combine myoelectric and body-powered elements. For instance, a body-powered elbow prosthesis is combined with an externally powered hand prosthesis [79].

Activity-specific prostheses have been developed to prevent fractures of the residual limb or the everyday prosthesis during certain activities. They are used when conventional prostheses cannot be used properly. These prostheses have a special design that usually consist of a customized interface, a socket, a suspension system, and a terminal device. They are designed to allow a person to hold tools such as a golf club or a baseball glove. Likewise, they also assist with special activities such as swimming or fishing. This type of prosthesis can be either passively or directly controlled [79].

The cost of a prosthetic arm or hand depends on the type of prosthesis. For a passive prosthesis, the costs are around $ 3,000 to $ 5,000. A body-powered prosthesis, which consists of a “split hook”, costs around $10,000. The cost of an externally myoelectric prosthetic hand ranges from $ 20,000 to $ 30,000 [51]. In addition to the type of prosthesis, the degree of limb loss also affects the cost of the prosthesis [45]. The costs for

externally powered myoelectric prostheses depending on the degree of limb loss can be seen in Table 2.3.

Table 2.3: Costs for externally powered myoelectric prostheses depending the degree limb loss [45].

| **Degree of limb loss** | **Costs** |
|---|---|
| Partial hand | $ 18,703 |
| Wrist | $ 19,922 |
| Transradial | $ 20,329 |
| Transhumeral | $ 59,664 |
| Shoulder | $ 61,655 |
| Forequarter disarticulation | $ 62,271 |

The duration of the manufacturing process of a prosthesis varies depending on the type of prosthesis. On average, the manufacturing process takes between one week and three months [55]. The considerable amount of time required to manufacture a finger prosthesis can be seen in Figure 2.9.

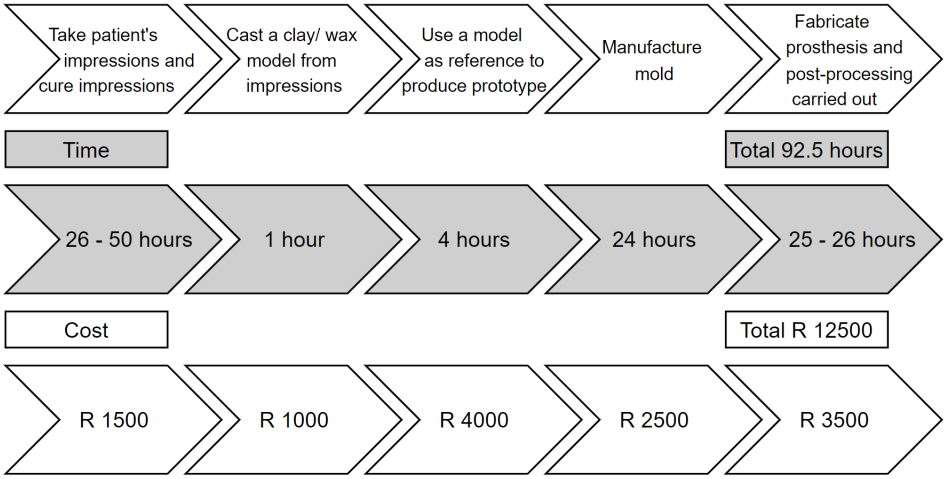


Figure 2.9: Manufacturing time of a prosthetic finger (own figure based on [57]).

In addition to the complexity and size of different prostheses, there are further aspects to be considered for the manufacturing of both body-powered and externally powered myoelectric prostheses. These include the integration of moving components and other elements such as cords and electronics. As a result, the manufacturing process not only

requires more time to complete the steps shown in Figure 2.9, but additional production steps are also necessary, leading to a longer manufacturing time.

Another important aspect to consider is the lifespan of a prosthesis, which depends on several factors. One of these factors is the material used. Different types such as plastic, various metals, or composite materials can be used. The durability of the prosthesis depends on the material. It is essential that the material used is selected according to the individual requirements of the individual and their level of activity. Therefore, another relevant factor is the user's level of activity, as prostheses are designed for normal everyday use. Heavy use leads to increased abrasion and a shorter lifespan. Regular and proper care is essential to maintain functionality and prevent damage to the prosthesis. It is also essential that the prosthesis is not exposed to extreme temperatures or moisture [74].
The lifespan of a prosthesis can vary widely due to these factors. Upper extremity prostheses like hands or arms typically last 3 to 5 years, longer than lower extremities which endure more stress and wear, lasting 1 to 3 years. High-activity prostheses also tend to have a shorter service life of 1 to 3 years on average due to the higher load. Prostheses for children require more frequent adjustments or replacements due to body growth, with an average lifespan and adjustment period of 6 months to 2 years [74].

## 2.3 State of the Art: 3D-Printed Prostheses

Between 1990 and 1999, scientists and doctors worked intensively on the development of 3D-printed prostheses. The breakthrough came after the first 3D-printed dental implants and organs were produced. However, despite these advances, research into 3D-printed prostheses for fingers, hands, and legs remains intensive [33].

In 2011, a significant milestone was reached with the "Robohand" project, where master carpenter Richard Van As, who had lost four fingers and could not afford a conventional prosthesis, created a prototype of a 3D-printed hand prosthesis [54]. Richard Van As received support from Ivan Owen, who worked with mechanical prop hands. Together, they worked on a prosthetic for a 5-year-old boy, the Robohand [44].
The design consisted of mechanical fingers that opened and closed with the movement of the wrist to grip objects. The movement was controlled by cables that ran from the fingers to the base of the hand. Depending on the tension of the wrist, the fingers were

opened proportionally via the cable system [49]. The Robohand can be seen in Figure 2.10.

Figure 2.10: Design of the Robohand (adopted from [54]).

Most of the Robohand's components were 3D-printed. Electronics and sensors were eliminated to facilitate maintenance and reduce costs. Each device cost less than $ 150, and the files for the Robohand were open source, allowing for home printing [49].

In their 2016 study "Development of novel 3D-printed robotic prosthetic for transradial amputees", K. F. Gretsch et al. [56] aimed to improve the Robohand by addressing its limitations. These included its restriction to users with a functional arm and the inability to control individual finger movements. The prosthesis was designed for individuals with transradial limb amputations. Their approach involved developing a 3D-printed prosthesis powered by an anthropomorphic end device and controlled by the patient's shoulder. An interactive measurement unit recorded the shoulder movement, and a microcontroller (ATmega32u4) controlled the motors of the prosthesis. Each finger was controlled by a micro-servomotor. By moving the shoulder up and down, the patient could open and close the complete hand. The thumb could also be moved individually by moving the shoulder back and forth. As soon as the respective condition for the movement was reached, the movement was executed up to the maximum stop [56]. Figure 2.11 shows the prosthesis.

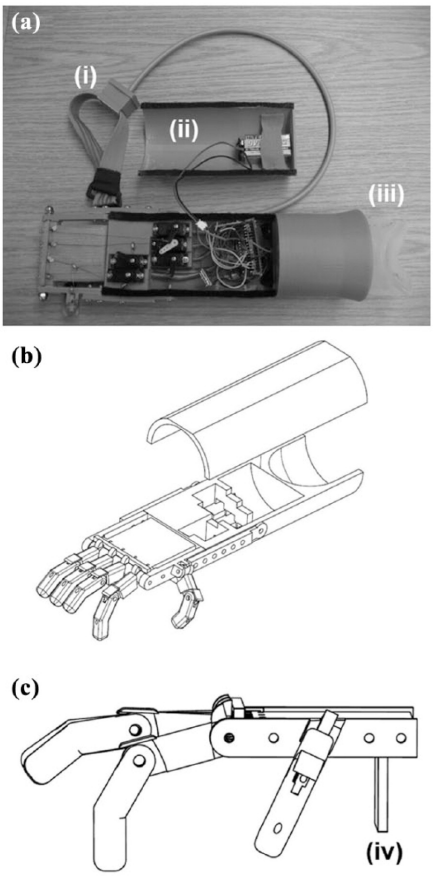


Figure 2.11: Design of the improved Robohand prosthesis (adopted from [56]).

The prosthesis was printed from Acrylonitrile Butadiene Styrene (ABS), had an estimated weight of 240 g, and cost around $ 300. Despite the advantages of this 3D-printed prosthesis, the challenges were also presented. The grip force was weak compared to other passive prostheses, the durability was limited, the battery life was insufficient, and the motor sound was audible. The study found that this 3D-printed prosthesis offered several advantages including lower weight, scalability in size, and easy adaptation to the growth of patients, making it particularly advantageous for use in children. [56].

The aspect of a rotation unit for the wrist was taken up by M. Hussein et al. [59]. In his bachelor thesis titled “3D Printed Myoelectric Prosthetic Arm” in 2014, M. Hussein et al. developed and tested a 3D-printed myoelectric prosthetic arm. The design was inspired by the InMoov robotic arm. Two EMG electrodes were used for control. Printed from ABS material, the prosthesis used a PIC18f25k22 microcontroller. Various gestures

had been implemented, which can be seen in Figure 2.12: “Power Grip”, “Pinch Grip”, and “Handle Grip”, whereby the fingers could each exert a force of 300 g [59].

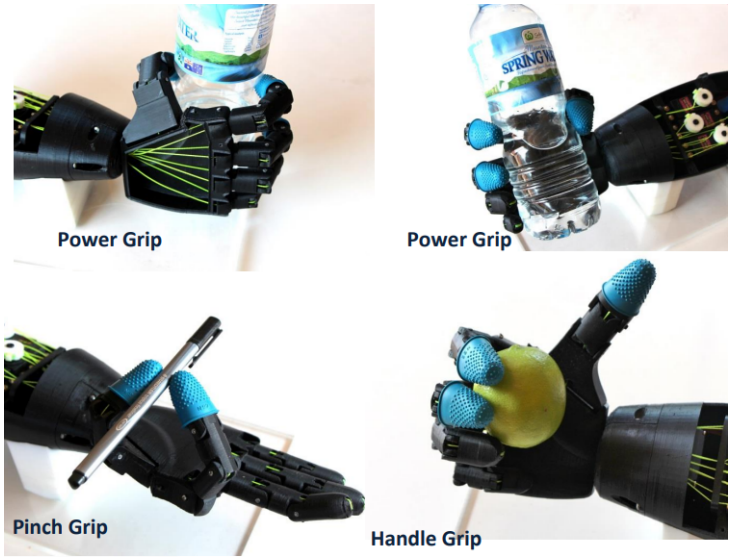


Figure 2.12: Different grips of the prosthesis (adopted from [59]).

In order to distinguish between different grip patterns, the movement of the M. biceps brachii was recorded. The EMG sensor of the forearm was used to control the actuators to close the hand or rotate the wrist, which can be seen in Figure 2.13 [59].

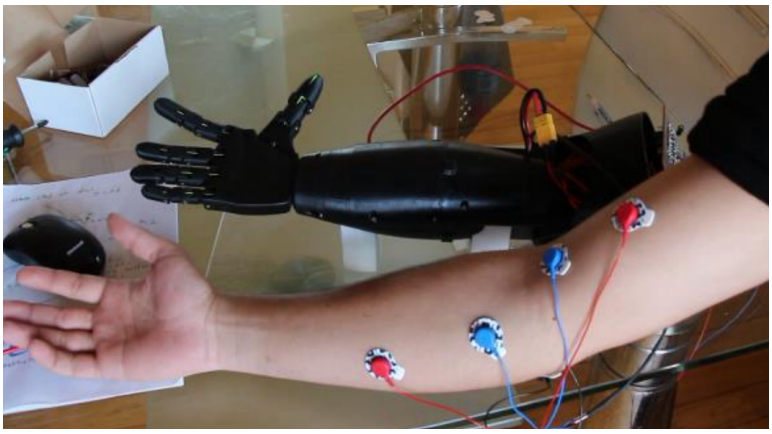

Figure 2.13: Testing of the prosthesis (adopted from [59]).

The intensity of muscle tension influenced the force of the movements and was thus controlled proportionally. In collaboration with his fellow student Michael Cerbara, an

extended control system was developed. Three electrodes instead of two were attached to the biceps, triceps, and chest. With the additional signal, eight separate control commands via a binary control system were integrated. This enabled the control of elbow flexion or wrist rotation using defined movement patterns without the need to switch between different modes. However, movements such as opening the hand and rotating the wrist could not be performed simultaneously [59].
The total cost of the prosthesis was about $ 250 and the battery life was around 6 hours. In total, the prosthesis weighed 970 g. For future improvements, M. Hussein et al. [59] suggested testing alternative printing materials such as nylon to achieve greater strength. The design of the finger could also be adjusted to provide more strength and reliability, even if this were to lead to a more complex design. Additionally, a DOF in rotation could be implemented. Another suggestion was to integrate a pressure sensor and a vibration motor for haptic feedback. In this context, a customized circuit board could also be used, which could be tailored to the requirements of the prosthesis and could minimize its dimensions. Another suggestion was the implementation of advanced EMG controllers that would enable simultaneous control and could be calibrated to the individual user to ensure reliable control [59].

In addition to technological advances in the field of prosthesis development, the important aspect of prosthesis fitting in the field of 3D-printed prostheses was studied in 2019. In their work “Remote fitting procedures for upper limb 3D printed prostheses”, J. M. Zungia et al. [88] focused on the development of a process for the remote fitting of prostheses. Therefore, patient satisfaction with remote fitting of their prosthesis was evaluated. The prosthesis used was based on a customized version of the “Cyborg Beast” called “Cyborg Beast 2”, which was created using Autodesk Fusion 360°. There were two versions of the prosthesis, one being a partial hand prosthesis, and the other one being a transradial prosthesis. Depending on the version, the prosthesis was controlled using cords by either flexing the wrist or elbow. According to the angle, the hand was closed proportionally. The movement was initiated with a 20° wrist flexion or 10° to 20° elbow flexion.
Relevant dimensions for the fitting were extracted from photos. To determine the range of motion, patients were first asked to extend the wrist to the maximum in both directions. In order to maintain symmetry, photos of the unaffected arm were used. The parametric design of the prosthesis allowed for standardization of certain part sizes, including the wrist mechanism of the transradial prosthesis and the forearm portion of the 3D-printed partial hand prosthesis. Finally, the design was reviewed by an orthopaedic

technician by placing a photo of the prosthesis on the patient's photo and examining it. The fitting process is shown in Figure 2.14 [88].

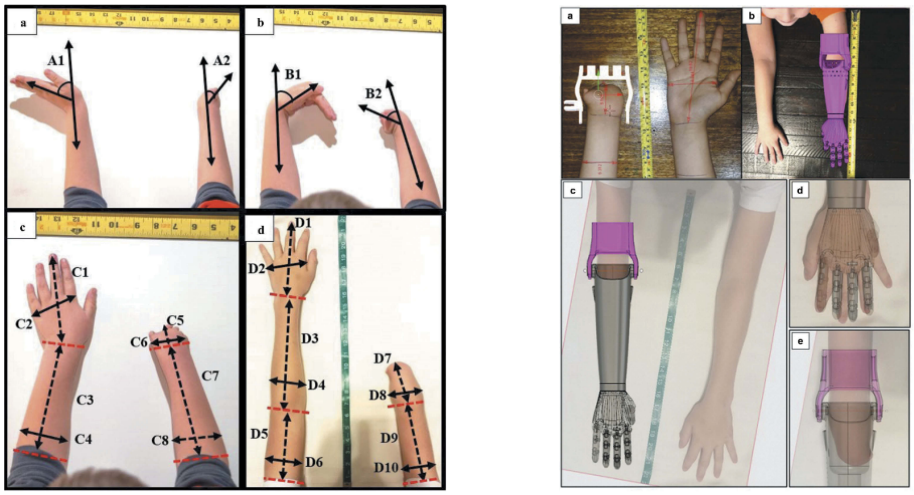


(a) Template photograph of the fitting procedure.

(b) Overlaid photographs of residual limb and prosthesis.

Figure 2.14: Remote fitting procedure (adopted from [88]).

Patient satisfaction was evaluated using the Quebec User Evaluation of Satisfaction with Assistive Technology (QUEST), which rates aspects such as dimensions, weight, and adjustments on a scale from 1 to 5, with 1 being "not satisfied at all" and 5 being "very satisfied". The Orthotics Prosthetics Users Survey (OPUS) was also used to assess satisfaction with the prosthetic appliance and associated services. OPUS comprises 28 questions in total on upper limb activities. Each question is rated on a scale from 0 to 5, where 1 means "very easy"/ "strongly agree" and 5 means "cannot perform activity"/ "strongly disagree". A 0 indicates "don't know"/ "not applicable" [88].
Six children, both male and female, aged 6 to 16 years and two adult males aged 25 and 59 years participated in the study. Of the participants, seven were congenitally impaired and one had an acquired impairment. The two types of prostheses can be seen in Figure 2.15 [88].

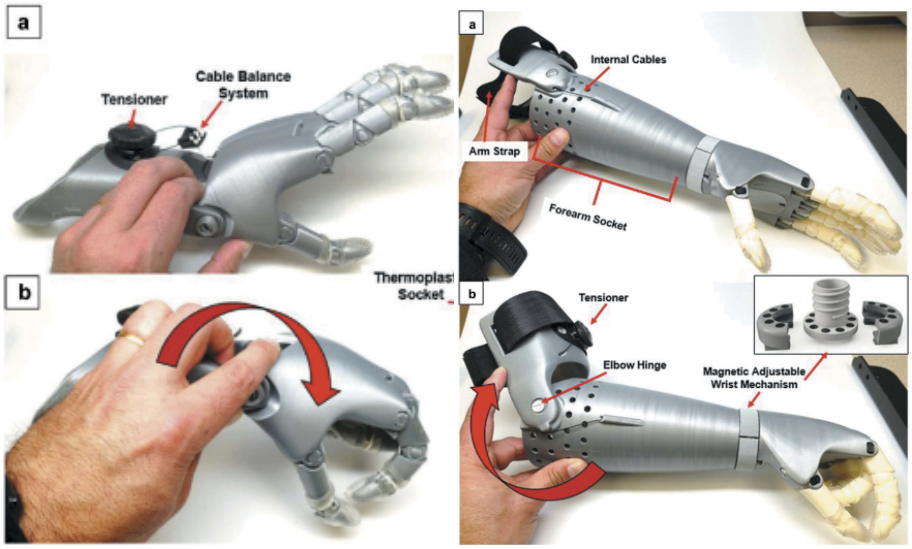


(a) 3D-printed partial hand prosthesis. (b) 3D-printed transradial prosthesis.

Figure 2.15: Printed prostheses (adopted from [88]).

The highest satisfaction according to the QUEST was found in the categories regarding weight (score of 4.50 ± 0.76), safety (score of 4.38 ± 0.52), and ease of use (score of 4.13 ± 0.64). According to OPUS, the simplest functional tasks were attaching and detaching the prosthesis (value of 1.5 ± 0.84) as well as drinking from paper cups (value of 1.75 ± 0.89) [88].
The study concluded that 3D-printed prostheses could be successfully adapted remotely. It was stated that this finding opened up promising opportunities, particularly in developing countries or rural areas. With the increasing availability of smartphones and other digital devices, access to trained technicians is significantly facilitated. [88].

Further progress on externally controlled prostheses was presented in the paper by S. Said et al. [75] entitled “Machine-Learning-Based Muscle Control of a 3D-Printed Bionic Arm” in 2020. This study was dedicated to the development of a 3D-printed bionic arm prosthesis for people with a right arm amputation that is controlled via machine learning algorithms. The prosthesis was controlled by surface EMG signals recorded with a MyoBand. A 24-year-old male with no other health restrictions was the target user of the arm. The prosthesis was manufactured at a total cost of $ 295. It featured an adjustable socket with a strap that provided a secure fit. The biceps support allowed the prosthesis to be worn for up to four hours, as it reduced pressure on the socket.

During construction, attention was paid to the symmetry between the left arm and the prosthesis in order to prevent muscle pain. The prosthesis is shown in Figure 2.16 [75].

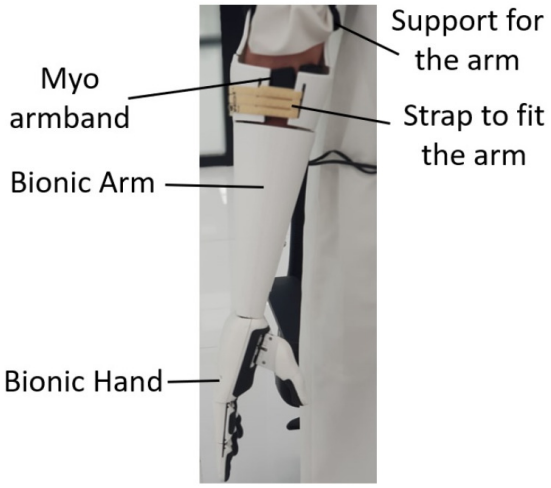


Figure 2.16: Amputee wearing the prosthesis (adopted from [75]).

To ensure a durable structure, most parts were printed from PLA. For soft padding and flexible movement, the outer layers and joints were printed in Thermoplastic Polyurethane (TPU). The total weight of the prosthesis was 350 g. With the actuators, the weight of the prosthesis was 428 g. The prosthesis was able to hold a weight of up to 4 kg for up to 10 seconds (including the prosthesis) and a weight of 1.5 kg for up to 60 seconds. The prosthesis was controlled by an ARM Cortex M0+ processor, which was connected to the MyoBand via Bluetooth [75].
In the course of developing the control system, the four different gestures “Open”, “Close”, “Wave-in” and “Wave-out” were recorded from 23 people. The test subjects were 12 males and 11 females between the ages of 18 and 45. A total of over 2000 gestures were recorded. The Open and Close gestures were used to open and close the hand of the prosthesis. Wave-in closed one finger, while Wave-out closed two fingers of the prosthesis. Depending on the recognized class, the respective actuators were controlled by the ARM Cortex M0+ processor. The actuators were controlled proportionally and could precisely set the position of the fingers through feedback. Various classifiers were trained using the features extracted from this data. Classifiers based on neural networks, support vector machines, and decision trees were created and compared to each other. The results showed that the support vector machine based classifier had an average accuracy of 89.93 %, outperforming the decision tree and neural network. The

study suggests that future extensions could include a wrist joint with multiple DOFs, by using two servomotors or a spherical manipulator, for instance. Additionally, the study proposes that attaching and detaching the arm could be simplified by an air-guided, adjustable mechanism [75].

In 2023, K. Avilés-Mendoza et al. [40] developed a hand prosthesis with a rotational unit in their study "A 3D Printed, Bionic Hand Powered by EMG Signals and Controlled by an Online Neural Network". The control was implemented with the help of EMG signals and neural networks. Three EMG surface sensors were used to record the signals. With the help of the recorded signals, a five-layer neural network was trained to recognize the different gestures. The prosthesis created in Fusion 360° was inspired by Ottobock's "SensorHand Speed" and consisted of three fingers that were controlled by a servo motor to open and close. Another servo motor rotated the base. An ESP32 developer board acted as the control board and was also responsible for signal processing. Figure 2.17 shows the prosthesis [40].

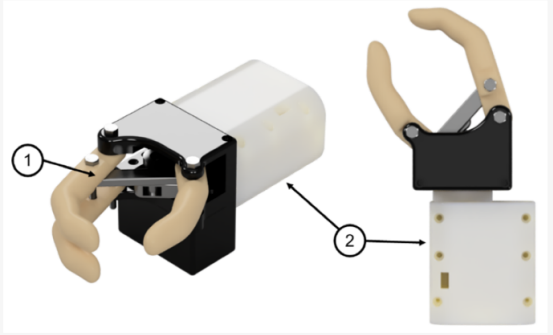


Figure 2.17: Model of the prosthesis (adopted from [40]).

The prosthesis was controlled using three classes. "Wrist Flexion" caused the axis of the gripping motor to rotate 20° clockwise, resulting in a gripping movement. In the second class, the second motor rotated 30° clockwise around the base each time the class was recognized. This class was recognized whenever a "Fist" was formed. In the third class, "Wrist Extension", the axis of the gripper motor rotated 20° counterclockwise, causing the prosthesis to open. The control was not proportional to the muscle movement, but was fixed to the number of degrees. Simulations and finite element analysis were carried out with the software Autodesk Inventor 2022 to validate the concept [40].
The tests to record the signals lasted 7 minutes. Visual signals were displayed for each movement, which the participant was supposed to imitate. Each muscle task was

performed within 5 seconds, followed by a 10-second long pause. The actions were displayed randomly on the screen and the sampling rate for recording was 1 kHz. Overall, 60 EMG recordings were obtained from the three different classes. The neural network was able to recognize the different classes with an accuracy of 78.67 %.
The first and third classes were classified with a higher accuracy, while the recognition of the second class tended to be less accurate. As a result, a binary model was created for the first and third classes only. This model achieved an accuracy of 95 %, which is significantly higher than the mentioned three-class model. Unlike class 2, class 1 and class 3 involved opposite muscles, with class 1 involving flexion and class 3 involving extension of the muscles. Wrist Flexion and Wrist Extension are opposite movements that are controlled by opposing muscles, namely the M. brachioradialis and the M. flexor carpi ulnaris. This clear muscular distinction made it easier to differentiate between the two movements. However, in the case of class 2, the Fist gesture, other muscles were addressed, which were more often confused with class 1 or class 3 during training. The study suggested that to overcome this problem, the algorithm could be trained using a more comprehensive database, which would generalize the processes more effectively and thus enable a more precise differentiation [40].
The prosthesis had a reaction time of 80 ms, could hold 500 g, and was able to grasp smaller objects. Overall, the prototype weighed 429 g. For future improvements, it was suggested to adapt the design to carry more weight, especially on the wrist. A lighter and more compact circuit was also suggested to improve portability. In addition, the connections on the development board could be redesigned to reduce noise in the EMG signals. By using deep neural networks to generalize data from different subjects and decrease pre-processing times, the accuracy of the model could be increased. Recurrent neural networks were suggested to be used to extend the time window analysis. The integration of a gyroscope sensor could also be useful because users of the prosthesis are normally not static during movement. Finally, dry electrodes instead of adhesive sensors were suggested to be used to minimize skin irritation [40].

### 2.3.1 Research Questions

In recent years, significant progress has been made in the field of 3D-printed prostheses. These developments range from the design of body-powered prostheses [54] to the introduction of remote fitting procedures, which enable access to 3D-printed prostheses in rural areas and allow customization according to individual needs [88]. Progress has also

been made in the field of externally controlled prostheses, ranging from simple electrical controls [59] to training of machine learning models to improve control and to adapt individual muscle movements [75].

Research on prostheses that allow wrist rotation has also been conducted in two studies. On the one hand, simple controls were realized by measuring the contraction of various muscles [59]. On the other hand, a prototype for prostheses with a rotation unit controlled by machine learning was implemented in another study [40].

However, it should be noted that these prostheses with rotational units have not yet been tested on people who are dependent on a prosthesis. Intuitive controls have also not yet been introduced, instead the rotation of the prosthesis' wrist has so far only been implemented using predefined gestures. This is partly due to the fact that the prostheses mentioned are prototypes for which no mechanism for attachment to the human arm has yet been realized or tested.

The aim of this work is therefore, to develop a 3D-printed prosthesis that can be intuitively controlled to open and close a hand as well as rotate the wrist using machine learning algorithms. Both movements should be able to be performed simultaneously and proportionally. Intuitive in this context means that the hand can be controlled like a natural hand and that the relevant muscles must be tensed in order to perform the corresponding movements[3]. This differs from the previously mentioned prostheses with rotational units, where specific movements such as biceps flexion in the upper arm controlled hand movements.
The movements should be proportional to the muscle contraction, whereby the intensity of the muscle contraction influences the intensity of the execution of the individual gestures. It should also be possible to control the different DOFs simultaneously.

Looking at the two existing studies that have already investigated prostheses with wrist rotation, only the proportional control was implemented in the study "3D Printed Myoelectric Prosthetic Arm" by M. Hussein et al. [59]. The other two objectives of this work (simultaneous and intuitive control) were not considered in either of the two studies [59, 40]. The functionality of the developed prosthesis will be tested with limb-impaired people in order to verify its suitability for practical use.

[3] It is possible that the gestures for the controls may be marginally adjusted, but this should be avoided as far as possible.

# 3 Methodology

The following chapter explains the methodology of this work. First, the selection of the 3D model and hardware is discussed. This is followed by a description of the additive manufacturing process and the assembly of the prosthesis. Furthermore, the framework for programming the control system is presented. Finally, the approach for the experiments is explained, including the ethical application required for the experiments.

## 3.1 Prosthesis Specification and Selection

At the beginning of this work a suitable 3D model for the prosthesis has to be selected. There are various freely available 3D models of the forearm. It is important that the 3D model can be used by people with impaired limbs and that it can be attached to the arm. In addition, the selected 3D model should have a rotation unit that allows the joint to rotate, simulating the pronation and supination of the arm. If the 3D model does not include a rotation unit, it should be possible to integrate one subsequently. The complete integration of all electrical components inside the 3D model is considered an advantage. Ideally, the 3D model should be variable in size so that it can be used by several people without major adjustments. In addition, the 3D model must be designed in such a way that it can be produced using a standard 3D-printer. Therefore, the dimensions of the 3D-printer's print bed must be taken into account as a limitation. The 3D model is printed with a Prusa i3 MK3S+ printer with a print bed measuring 25 cm x 21 cm x 21 cm [20].

Table 3.1 shows the printable parts of different 3D models that are potentially suitable. Only the printed parts are relevant, as the electrical components are selected individually according to different criteria. Therefore, only the DOFs, the weight and the availability of an integrated wrist function are taken into consideration. In addition, it is taken into account whether there is already an forearm included in the design or whether the design only consists of a hand.

Table 3.1: Different available 3D models.

| Prothesis | DOFs | Weight | Integrated wrist | Attachable forearm |
|---|---|---|---|---|
| **Brunel V1.0** | 4 DOFs[4] [78] | 371 g [78] | - | - |
| **InMoov V1** | 6 DOFs [63] | 475 g [38] | Rotational wrist [63] | Yes [63] |
| **Hackberry** | 3 DOFs [12] | 450-500 g [2] | - | Yes [12] |
| **Ada V1.1 [77]** | 5 DOFs [77] | 380 g [77] | - | - |
| **Dextrus** | 6 DOFs [7] | 393 g [38] | - | - |
| **Dextra** | 6 DOFs [84] | 405 g [38] | - | - |

The Hackberry arm has three DOFs. While the movement of the thumb and index finger can be controlled individually by one motor each, the remaining three fingers are controlled by a single motor [12]. The Brunel[4] hand has four DOFs. The thumb, index and middle finger can be controlled separately. An additional motor enables the movement of the ring and pinky finger [78]. In contrast, the Ada hand has five DOFs so that each finger can be controlled individually [77]. Both the Dextra and Dextrus hand have six DOFs each. The movements of the fingers can be controlled independently and the thumb has an additional motor that enables flexion, extension, adduction and abduction [7, 84]. The InMoov arm has six DOFs as well. In addition to the individual motors of each finger, it has an extra motor for the wrist, which enables a further DOF through rotation. The advantage of this hand is that it already features an integrated rotation unit. At the same time, this model already includes a forearm that can be attached to the patient's residual limb without major modifications [63]. Therefore, the InMoov arm will serve as the basis for the prosthesis. As this 3D model is originally designed for a robot, it has to be adapted in order to be used as a prosthesis. The adaptation is performed using the CAD software PTC Creo. Figure 3.1 shows the InMoov arm.

[4]The data sheet states that the prosthesis has nine DOFs and four degrees of actuation. This means that the individual fingers each have two joints, but the joints are not actuated individually. The thumb, index finger and middle finger are each actuated with separate motors and the ring finger and pinky finger are actuated together with one motor. As the DOF is equated with the number of individual movements in the other 3D models, the DOF is also considered to be four here [78].

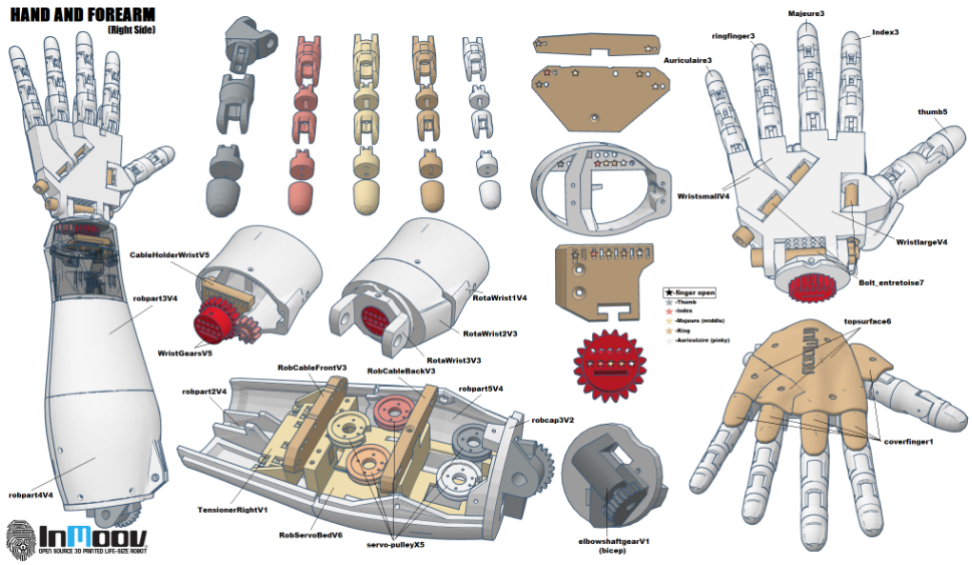


Figure 3.1: InMoov robotic arm (adopted from [86].)

In this 3D model, the motors are placed inside the arm as well as the wrist, as can be seen in Figure 3.1. However, to make the 3D model usable as a prosthesis, the number of motors used must be reduced to provide sufficient space for the residual limb.

The prosthesis should be able to perform four gestures. These gestures include flexion and extension of the hand, as well as supination and pronation of the hand. Pronation and supination are achieved through rotation of the wrist. To implement these gestures, two motors are required, one for flexion and extension of the hand and one for rotation of the wrist. The motor controlling rotation is placed inside the wrist, while the motor controlling flexion and extension is placed inside the forearm. To maintain the option of implementing additional gestures such as the Pinch Grip in the future, two additional motors are integrated in the forearm to control the thumb and index finger separately. In this work the three motors inside the forearm will only be used for flexion and extension.

Furthermore, the holder for the motors needs to be moved closer to the wrist to create enough space for the residual limb. In order to create further space, the orientation of the motors is adjusted. To achieve this, the three motors in the arm are rotated 90° around the x-axis and 90° around the z-axis. The motor holder is adjusted so that one motor is positioned in front of the other two motors, which are arranged vertically. In

addition, the rods within the arm must be reduced to a minimum in order to create sufficient space. A holder for the microcontroller that controls the motors is attached below the motor holder to ensure a compact design.

The part connecting the forearm to the upper arm is removed, as it is not needed. The prosthesis is attached to the residual limb with two elastic cable ties. The rear part of the forearm is extended and provided with bars, to which one of these elastic cable ties is attached. The other cable tie is attached to the bars of an additionally added upper arm part, which is placed on the back of the upper arm of the individual. Screws are used to connect the rear part of the forearm and the upper arm part through these bars.

To isolate the electrical components from the limb, a plate is attached behind the motors. Holes are added to connect the parts together to ensure modularity and allow easy disassembly without the need for permanent gluing. Figure 3.2 shows the adapted 3D model which will be used as the prosthesis. The microcontroller is displayed in white, and the motors are displayed in dark grey.

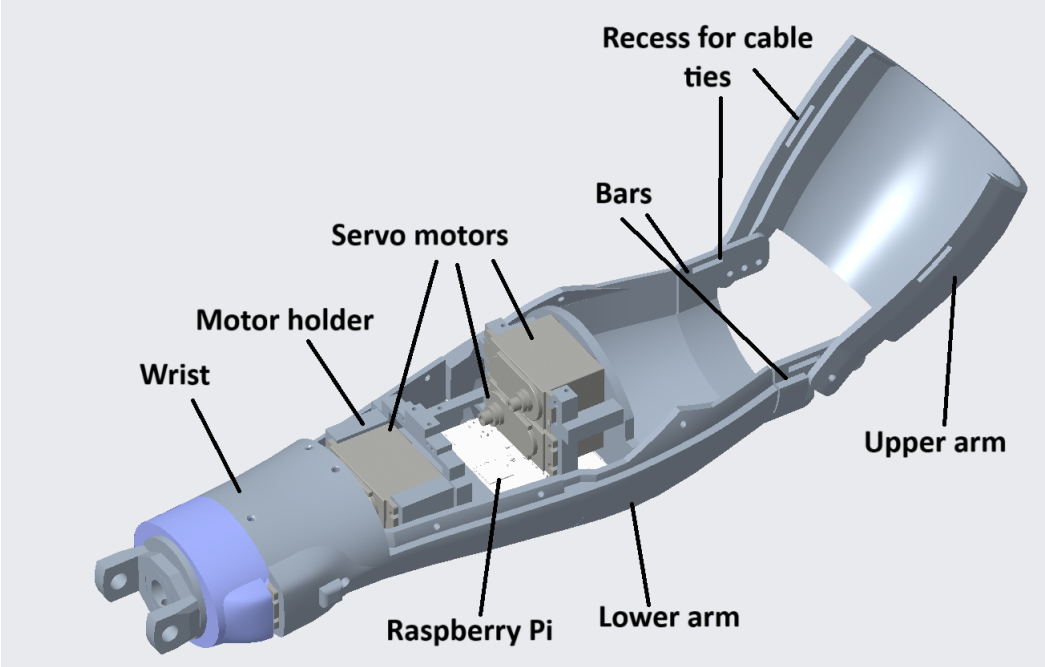


Figure 3.2: Model of the adapted prosthesis.

## 3.2 Hardware Criteria and Selection

In order to control the arm prosthesis, sensors, actuators, and other hardware need to be integrated. The required and selected components are explained in the following.

### 3.2.1 Sensors

A sensor is used to record the contraction of the arm muscles. In order to realize the desired two DOFs of the prosthesis, a MyoBand is used non-invasively to capture an 8-channel EMG signal. The MyoBand uses electromyographic sensors in conjunction with conventional movement sensors. EMG dry electrodes function as the electromyographic sensors and measure the electrical activity of the skeletal muscles. The movement sensors record both the rotation rate and acceleration. In order to recognize hand gestures, these sensors are placed at the lower end of the forearm, where the muscles used for extension and flexion movements are located. The recorded signals are transmitted via Bluetooth, to a Bluetooth dongle [5]. The MyoBand can be seen in Figure 3.3.

Figure 3.3: MyoBand from Thalmic Labs (adopted from [5].)

A significant advantage of the MyoBand compared to conventional adhesive electrodes is that no cabling is required as the data is transmitted via Bluetooth. The electrodes are firmly attached to the band and therefore have a predetermined arrangement, which can minimize the differences between sessions[5]. It also eliminates the need for adhesive strips, which not only reduces waste production but also avoids adhesive residue on the

[5]If not recorded at the same position, EMG signals can be session-dependent and vary for the same individual.

arm. Another positive aspect is that the prosthesis can be prepared more quickly, as only the MyoBand needs to be put on, rather than placing individual electrodes.

### 3.2.2 Actuators

Actuators are required to control the movements of the fingers and wrist of the prosthesis. The use of servo motors is a suitable solution, because the motor holder and the cut-out for the wrist motor are designed for servo motors and therefore do not need to be adjusted. Another advantage of a servo motor is that they are very precise and can control defined positions due to the feedback they provide [42, 87]. In addition, no torque is lost [42].

When selecting the servo motors, both the limited space within the prosthesis and the required gripping force must be taken into account. The gripping force of the Diymore MG996R servo motor ranges from 9 kg to 13 kg, depending on the supply voltage [8]. The servo motor can be seen in Figure 3.4.


Figure 3.4: Diymore MG996R servo motor.

One servo motor is used to control the index finger and another one is used to control the thumb. The remaining three fingers are controlled by an additional servo motor, leading to a total of three servo motors that are required to control the hand. The gripping force[6] results from the following equations:

[6]To calculate the gripping force, the prosthesis is viewed in simplified form as a parallel gripper with five gripper fingers. The gripping force $F_G$ is therefore calculated from the arithmetic sum of the individual gripper fingers [11]. The calculated gripping force should be verified by measurements since, among other things, the angle of the fingers to each other is not taken into account as well as the frictional forces caused by the cords and the individual parts of the respective fingers.

$$F_G = 9\ kg + 9\ kg + 3\ kg + 3\ kg + 3\ kg = 27\ kg \tag{3.1}$$

$$F_G = 13\ kg + 13\ kg + 4.33\ kg + 4.33\ kg + 4.33\ kg = 39\ kg \tag{3.2}$$

Therefore, the total gripping force ranges from 27 kg to 39 kg[7] depending on the supply voltage. Compared to the Michelangelo hand, which has a gripping force between 6 kg and 7 kg [19], the gripping force is higher and should therefore be sufficient for everyday activities. Each servo motor measures 40.5 mm x 20 mm x 39.5 mm and integrates into the forearm without difficulty, as the motor holder is designed for servo motors of this size. An identical servo motor is used for the wrist [8].

For stable control, a servo hat is required. This servo hat can be equipped with an external power supply to provide sufficient current and voltage to the servo motors. In this work, the PCA9685 16-Channel 12-Bit PWM Servo Motor Driver (PCA9685) is used as the servo hat, which can control up to 16 servo motors [52]. Figure 3.5 shows the PCA9685.

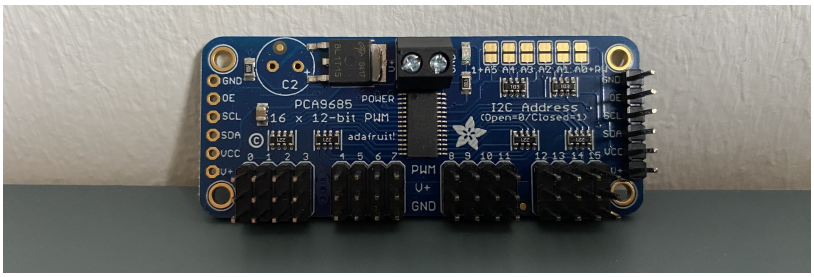


Figure 3.5: PCA9685 16-Channel 12-Bit PWM servo motor driver.

A power supply unit is used to ensure a stable and sufficiently long power source for all the servo motors during the implementation of the code and the tests. The stall current of one servo motor equals 1.300 A ± 10 % at a supply voltage of 6 V and 1.100 A ± 10 % at a supply voltage of 4.8 V[8] [8]. The stall current corresponds to the maximum current

[7] The servo motors delivered were not the ones that were ordered. According to research on the manufacturer's website, the torque of the servo motors supplied measures 13 kg when 4.8 V is applied and 15 kg when 6 V is applied. According to this, the gripping force should be between 39 kg and 45 kg [18].

[8] No information was found on the stall current for the servo motors delivered. Given that the upper gripping force limit of the ordered servo motors matches the lower gripping force limit of the received servo motors, it is assumed that both have the same stall current at this gripping force limit. The servo motors are therefore only operated at 4.8 V. For the future, either the correct servo motors should be purchased or a power supply unit with a higher current should be used. The stall currents should also be measured to verify if the power supply unit is sufficient [18].

required in the worst case [62]. The following equations show the maximum currents depending on the supply voltage [8]:

$$(1.300\ A + 10\ \%) \cdot 4 = 5.720\ A \tag{3.3}$$

$$(1.100\ A + 10\ \%) \cdot 4 = 4.840\ A \tag{3.4}$$

An adjustable power supply unit from Towisituati is used. The current output ranges from 1 A to 6 A, and the voltage is adjustable between 3 V and 24 V [1].

### 3.2.3 Other Hardware

In order to control the prosthesis, additional hardware is required. In particular, a microcontroller that can analyze the sensor, process the signals and control the actuators, is necessary. The microcontroller must have a Bluetooth interface in order to be able to communicate with the MyoBand. Moreover, the controller should have sufficient computing power to perform machine learning. To meet these requirements, a Raspberry Pi 3B+ (Raspberry Pi) is used. It features a 64-bit quad-core processor running at 1.4 GHz, along with support for 2.4 GHz and 5 GHz WLAN and Bluetooth 4.2 [35]. Similar to the PCA9685, the Raspberry Pi requires a power source, for which the official Raspberry Pi power supply unit is used [24]. The Raspberry Pi can be seen in Figure 3.6.

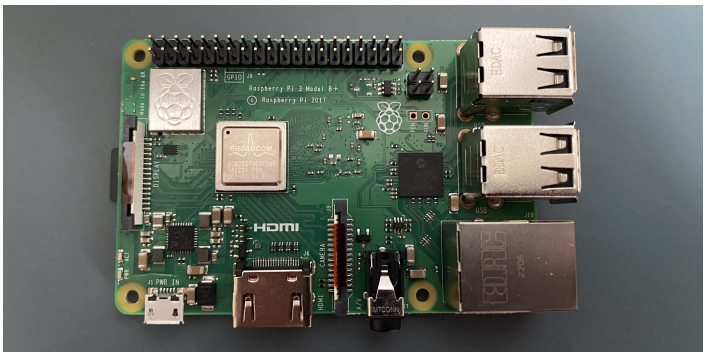


Figure 3.6: Raspberry Pi 3B+.

Various screws are necessary to join the individual parts of the prosthesis together. To assemble the parts of the fingers, 3.5 mm bolts are used [27]. Fishing line is used to

attach the motors to the fingers [14]. Elastic cable ties are used to attach the prosthesis to the residual-limb [28].

## 3.3 Outline for Additive Manufacturing and Assembly Procedure

The components of the prosthesis are manufactured using the Prusa i3 MK3S+ 3D-printer. After adapting the 3D model in the PTC Creo as described earlier, a Slicer software is used in order to generate a printing file that can be interpreted by the 3D-printer. The software used for this task is PrusaSlicer, which is an open source tool [22].

The individual components of the adapted 3D model are imported into PrusaSlicer. However, the number of imported components is limited by the space available on the print bed, necessitating multiple printing sessions. After importing, the parts need to be oriented and aligned on the print bed to maximize the utilization of available space and to ensure a high-quality print. It is advisable to place the parts in such a way that the use of support material is minimized, in order to save material and keep the additional work involved in separating the support material from the components to a minimum [10].

Next, the settings in the slicer software are selected, including choosing the 3D-printer to be used and determining the correct nozzle size. Likewise, the required printing material must be stored in the program [10]. In this work, the prosthesis will be fabricated entirely from PLA because of its favorable properties, including food-safeness, ease of fabrication, and low cost [29]. Therefore, it is usable for applications involving direct skin contact [29].
Furthermore, settings must be made for the desired layer height, which influences both the print quality and the printing time. A higher layer height leads to faster printing, but this can minimize the print quality, which is why a balanced average is aimed for. When parts require support material, for example due to large overhangs, appropriate settings must be made. Various options are available for this, including selecting the type of support material, positioning the support material on the print bed, and determining the level of overhang when support material is used [10]. Another configurable setting is the specification of the infill height and pattern. Since it is not always necessary to

print parts solid to achieve the desired stability, this setting can save both material and printing time. In addition, a margin can be defined to increase adhesion to the print bed and minimize deformation of the print [10].

Once the 3D-printer has been set up, a G-Code is generated as the printing file [10]. The G-Code is a programming language that consists of a sequence of G and M commands. With the help of these commands, a machine is able to interpret and execute the intended instructions or actions. Using this code, the 3D-printer understands and implements the movements required to produce the desired part [69].

As described earlier, not all components can be produced in a single printing process because the size of the printing bed is insufficient. The individual parts must therefore be split between different prints. This involves categorical sorting in order to enable step-by-step assembly and to be able to check any adjustments at an early stage. First, the hand is manufactured, followed by the wrist. The settings for the print of the wrist can be seen in Figure 3.7. The support material used for the print is visualized in green. The duration of the print can be seen at the bottom right. An estimated value is also given for the filament consumption as well as the associated costs. It takes 13 hours to print the wrist.

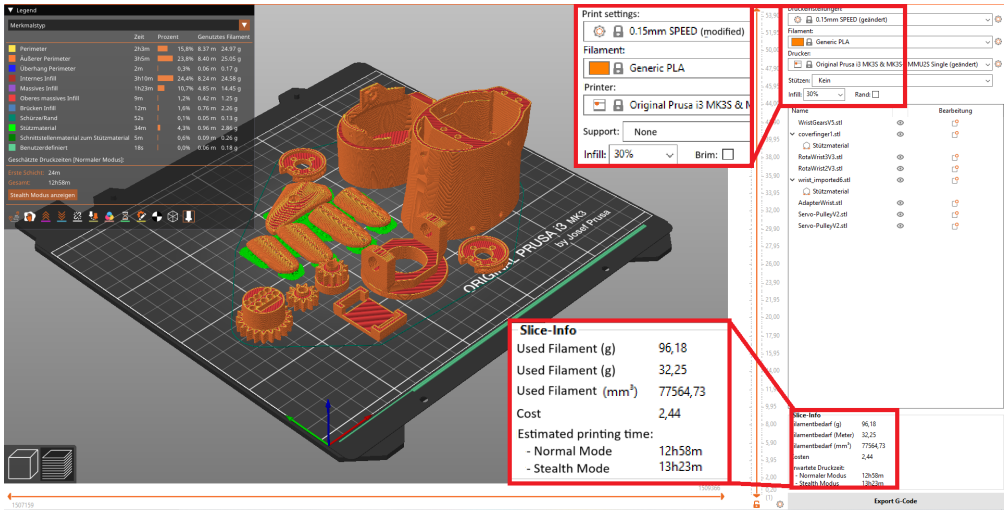


Figure 3.7: Settings in the PrusaSlicer for printing of the wrist.

The parts for the forearm are produced in the third printing session. In the final printing session, the inner components of the forearm, which enable the integration of the electronics, are printed. The total printing time is estimated to be 81 hours.

## 3.4 Software Specification

To integrate the controlling system, MATLAB is used in combination with Simulink. MATLAB offers the ability to interact with other programming languages such as Python, C, and C++ and can also be used for hardware programming. This makes MATLAB very versatile and therefore suitable for the implementation and testing of control systems, and signal processing applications. MATLAB also supports the use of machine learning [16].

Another advantage of MATLAB is the availability of various toolboxes. For this work, the MATLAB Support Package for Raspberry Pi Hardware [25], Simulink Support Package for Raspberry Pi Hardware [26] and Closed-Loop Development Framework (CLS) for Simulink [66] are used. The two support packages for the Raspberry Pi Hardware, enable remote access to the Raspberry Pi via a computer. It is also possible to write code that can independently run on the Raspberry Pi. This code can be used for processing data and for communicating with devices that are connected to the Raspberry Pi via General Purpose Input Output (GPIO), serial Inter-Integrated Circuit ($I^2C$) or Serial Peripheral Interface (SPI) pins. The code can also be simulated before it runs independently on the Raspberry Pi [25, 26]. To make the Raspberry Pi compatible with the toolboxes, the Raspbian OS image must be customized. This is done during the configuration of the toolboxes while the computer is connected to the Raspberry Pi [26].

The CLS can be used to configure and test closed control loops. It contains a number of generic blocks that can be controlled via standardized inputs and outputs. The settings of the blocks can also be customized [66]. Different models, including the Michelangelo hand with four DOFs or a virtual hand with three DOFs, are available to test programs virtually. Furthermore, the CLS offers input interfaces such as EMG sensors, including high-density EMG sensors [50].

The first step in developing the controlling system is to write a code that integrates the MyoBand and is able to record the EMG values. Subsequently, a machine learning model that can distinguish between different gestures is implemented. For this purpose,

either Linear Regression (LR)[9] or Linear Discriminant Analysis (LDA)[10] is used because classifiers for both are implemented in the CLS. To ensure reliable differentiation, the machine learning model must be trained with the previously recorded EMG signals. The following gestures should be recognized: extension and flexion of the hand, as well as pronation and supination. The trained machine learning model then sets a simulated hand in motion. In the next step, the model on the Raspberry Pi is used to actuate the corresponding motors based on the recognized gesture.

## 3.5 Outline of the Experimental Framework

The following section explains how the prosthesis and the implemented control system are tested.

### 3.5.1 Pilot Testing

To verify the functionality of the prosthesis and adjust the control system in order to ensure that it works according to the specified requirements, a self-experiment is carried out. This experiment consists of several steps. First, the different gestures are performed and recorded several times. The gestures are performed with different intensities so that they can be recognized during weaker and stronger contractions of the muscles. Once recorded, the gestures are saved in a file and loaded into the programmed machine learning model. Using the recorded data, the model learns how the EMG signals of the various muscle contractions differ and what characteristics they possess. This enables the machine learning model to differentiate between the various gestures. Then the trained machine learning model is tested online, using a simulation. Subsequently, the program is adapted to transition from the online simulation to a system where individual motors are activated in response to the specific gesture being performed. After these steps, the program is loaded onto the Raspberry Pi.

[9] In LR, a created machine learning model describes the relationship between one or more independent variables and a dependent variable. A distinction is made between simple linear regression, in which a value of a dependent variable is predicted by an independent variable, and multiple linear regression, in which a consideration of more than two independent variables can be taken into account [37].

[10] LDA can be used for classification problems with multiple classes. The dimensionality of the data is reduced, and thus several classes with multiple features are characterized. Linear feature combinations are then identified [36].

The prosthesis is then placed on a stable surface and connected to the MyoBand that is attached to the arm. This enables testing for the individual gestures. Each gesture is executed again several times with both high and low intensity. To evaluate the performance of the machine learning model, classification accuracy and recall are calculated for different gestures at different intensity levels. While the accuracy describes the overall correctly classified gestures, the recall describes how well the model can recognize the instances of a specific class.

The following equation is used to calculate the accuracy [3]:

$$Accuracy = \frac{C_{pred}}{A_{pred}} \tag{3.5}$$

with $C_{pred}$ being the correct predictions and $A_{pred}$ being all predictions.

The recall is calculated as follows [3]:

$$Recall = \frac{TP_{ClassN}}{TP_{ClassN} + FN_{ClassN}} \tag{3.6}$$

with $TP_{ClassN}$ being the true positive[11] predictions and $FN_{ClassN}$ being the false negative[12] predictions.

### 3.5.2 Testing on Limb-impaired Subjects

Once the pilot test has been completed, the prosthesis is tested on a limb-impaired individual. The prosthesis socket must initially be adapted so that it can be worn by the subject. The measurements of the residual limb have to be taken in order to adapt the prosthetic socket. This can be done either in person or with the help of photos. Afterwards, the customized parts of the prosthesis must be printed and integrated into the already manufactured parts.

The experiment can be carried out after these individual adjustments. Firstly, the muscle contractions of the individual's limb are recorded with the MyoBand, which is attached just below the elbow. If necessary, hair is removed, and the skin is treated with a skin cleansing gel (Everi, Spes medica) in order to optimize electrical conductivity.

[11] Correct class was classified.
[12] Another class was classified.

After these preparations, the subject is asked to contract the arm muscles as if they wanted to perform the specified gesture. If necessary, this procedure can also be carried out with the non-amputated arm. As described earlier, each contraction should be performed several times with varying intensity. The subject is informed of the intensity with which they should perform the respective gesture. Using these recorded signals, the model is trained to the individual muscle contractions of the subject. In the next step, the prosthesis is attached to the arm along with the MyoBand. The subject is now asked to use the arm muscles to control the prosthesis with the help of the MyoBand. This involves trying to grasp and move objects in order to evaluate the functionality, suitability for everyday use, and comfort of the prosthesis.

To evaluate the opening and closing function of the prosthesis, a modified version of the Box-and-Block Test (BBT) is carried out [67]. In this test, an open wooden box with two compartments is used. A total of 150 wooden blocks are provided for the test. The box is positioned lengthwise on the edge of the table with the test subject standing in front of it. An examiner sits opposite the test subject. The subject is given a trial phase of 15 seconds beforehand. The unused hand is placed on the table next to the box. As soon as a signal is given, the subject has one minute to transfer the blocks, one after the other, from one compartment to the other. Figure 3.8 shows the box [65].

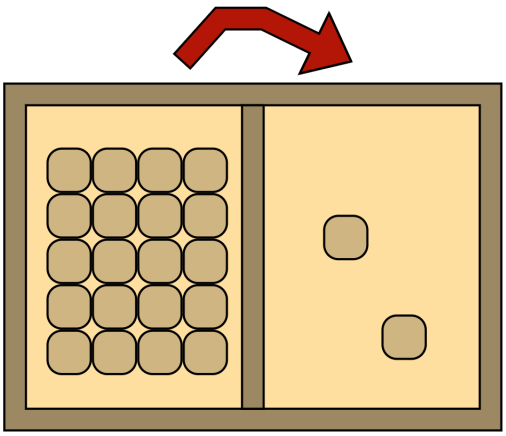

Figure 3.8: Structure of the Box-and-Block Test (own figure based on [65]).

If several blocks are moved at the same time, the extra blocks are counted separately, and subtracted from the total number so that only the transfer of one block is counted.

After passing the blocks over the wall that separates the two compartments, they can be released and do not need to be set down [67, 65]. The dimensions of the box and the blocks differ from those of the original test. Both the healthy and the prosthetic hand are used for the test and the number of blocks transferred is compared directly.

To evaluate the wrist's ability to rotate, the Refined Clothespin Relocation Test (RCRT) is carried out, in which a graded pinch exerciser with three clothespins and a timer are placed in front of the subject [58]. When placed on the table, the device should be at hip height (height of the upper iliac spine). The device consists of one vertical and two horizontal bars. During the test, the clothespins are moved back and forth between the vertical bar and the lower horizontal bar. The vertical bar is adjustable and can be moved to the side where the prosthesis is attached. Adhesive tape is attached to the bars to mark the positions for moving the clothespins [58]. Prior to the experiment, the direction (upwards or downwards) and the order in which the clothespins are moved must be determined and communicated. Figure 3.9 shows the test setup including the moving directions of the clothespins [58].

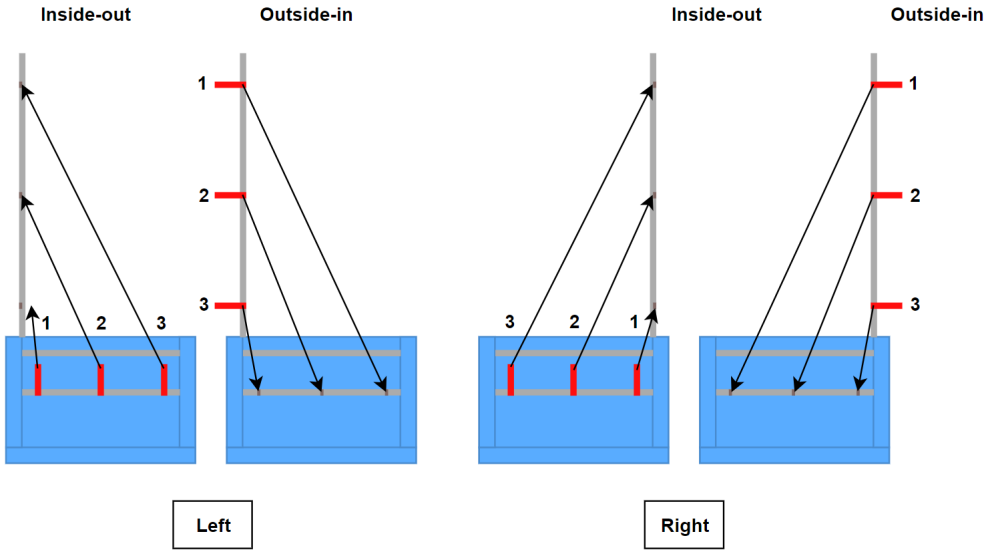


Figure 3.9: Order of the up- and downward movements for the left and right side (own figure based on [58]).

During the experiment, the subject starts the timer, moves the clothespins according to the predetermined sequence and then stops the timer. This process is performed

five times for the upward movements and five times for the downward movements. The experiment is carried out with both the prosthesis and the healthy hand.
The evaluation is based on the RCRT score, which takes into account both the average time of all the runs and the average degree of compensation [58]. Points between 1 and 4 are assigned for compensation, with 1 meaning strong compensation and 4 meaning no compensation[13]. During the upward movements, the inclination of the torso is assessed, while during the downward movements, shoulder abduction is included in the score, as these are typical compensations during these movements. If there are movements of the feet or other undesirable movements, the score is reduced accordingly. The first two clothespins are relevant when assessing the upward movements and the last clothespin when assessing the downward movements, as increased compensation occurs during these movements.
The RCRT score is calculated using different variables. The time is rounded to the nearest hundredth, while the degree of compensation is rounded to the nearest whole number. The average degree of compensation of the upward and downward attempts is described using $LateralTilt_{avg}$ and $Shoulder_{avg}$. The average time required for the upward attempts is described using $TimeUP_{avg}$. $TimeDown_{avg}$ is used to describe the average time for the downward attempts.

The variables are used to calculate the RCRT score as follows [58]:

$$RCRT\ Score = (LateralTilt_{avg} + Shoulder_{avg}) \cdot (\frac{1}{TimeUP_{avg} + TimeDown_{avg}}) \cdot 100 \tag{3.7}$$

In this work, flexing the entire hand serves as the primary gripping movement. As this involves a rather gross motor movement, grasping small items such as clothespins might be complicated. This challenge can potentially be addressed by using clothespins of sufficient size. Should this approach prove ineffective, the flexion mechanism should be adjusted so that only the thumb and index finger are flexed for the test, enabling a precise Pinch Grip.

### 3.5.3 Ethics

The experiments that are carried out involve human subjects, which is why compliance with certain regulations is crucial to ensure that ethical standards are maintained. To

[13] Which movement leads to which degree of compensation is shown to the test subject beforehand, either in person or with a picture.

ensure this, an ethics application is submitted. This application must be presented to the ethics committee from the HAW Hamburg for approval.

The application includes a detailed description of the experiment and answers to various questions relating to the experiment. The questions include, for example, details of the collected data and information about the environment in which the experiment is conducted. A subject information sheet is also prepared in advance. The sheet sets out the aim of the study, the course of the experiment, potential risks, the data relevant to the experiment, the conditions for participation and information about potential compensation. In addition, it is emphasized that the study can be discontinued at any time. It is also stated that the experiment has been approved by an ethics committee.

Furthermore, a declaration of consent is required, which must be obtained before the start of the experiment. This declaration confirms that the subject has been informed about the risks and the general procedure of the experiment in accordance with the subject information.

The subject information and the declaration of consent are also submitted to the ethics committee. The ethics application and all relevant documents prepared for conducting the experiment can be found in the appendix. The approval of the ethics committee of HAW Hamburg was received on November 29, 2023, before the pilot test was carried out. The approval can also be found in the appendix.

# 4 Results

## 4.1 Assembly of the Prosthesis

The following section describes the assembly of the prosthesis in detail. The calculated printing time for all parts was 81 hours. The time could not be fully verified as many parts were printed overnight in a printing lab. However, the calculated time was relatively accurate for shorter test prints, so it can be assumed that the total time is approximately correct. During assembly, the holes for the 3.5 mm bolts, which serve as joints for the fingers and thumb, had to be widened with a drill first. This was necessary as the holes were not provided with support structures during the print, because of their small size, and therefore collapsed slightly. Drilling was not necessary with other holes in the prosthesis, as they could either be opened with screws, had sufficient clearance or were of sufficient size to be provided with support structures during the print. An illustration of the holes can be seen in Figure 4.1.

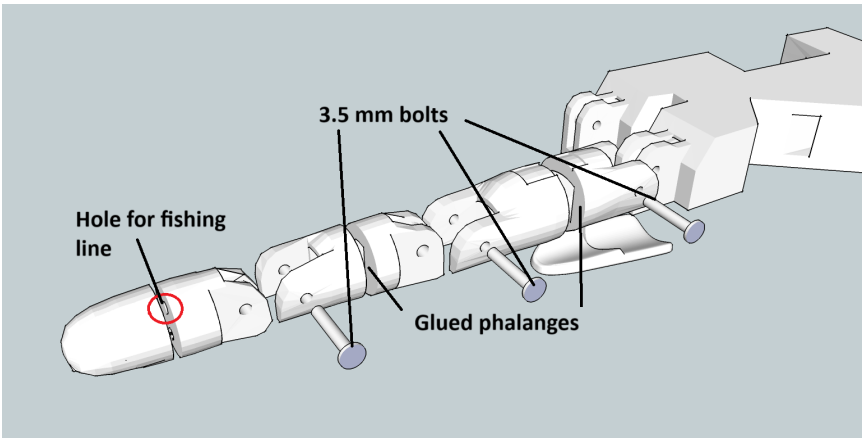


Figure 4.1: Exploded view of the finger (adapted from [13]).

As a preparation step prior to the assembly, the individual parts of the phalanges, except for the fingertips, were glued together (see Figure 4.1). The lower part of the thumb and the hand had to be glued together as well (see Figure 4.2(a)). The assembly was roughly divided into four steps: assembling the hand, assembling the wrist, integrating internal parts and electronics, and attaching the arm components. These steps are outlined below:

### Assembly of the Hand

The assembly of the hand can be seen in Figure 4.2.

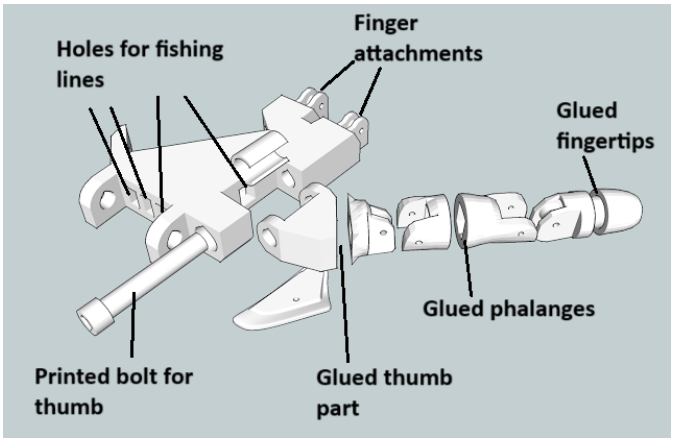


(a) Exploded view of the thumb (adapted from [13]).

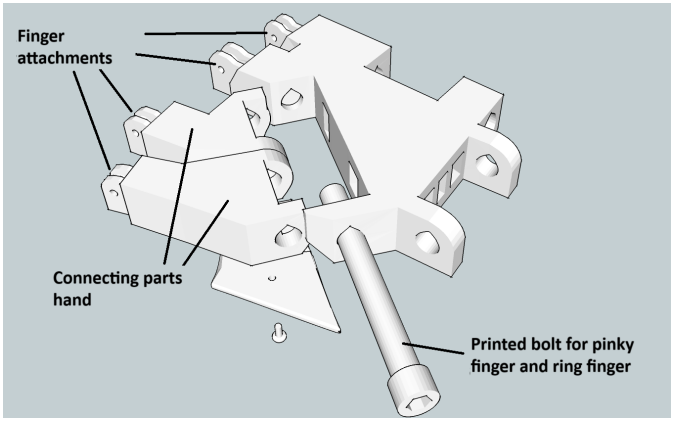


(b) Exploded view of the hand (adapted from [13]).

Figure 4.2: Exploded view of the thumb and the hand [13]).

1. The individual parts of the fingers were connected to each other using 3.5 mm bolts (see Figure 4.1).
2. The fishing lines were pulled through the individual fingers. The fishing lines that were pulled through thumb, pinky finger, and ring finger also had to be threaded through connecting parts, which are part of the hand. Eventually, all the fishing lines were threaded through the hand (see Figure 4.1 and 4.2(a)).
3. The index and middle finger were attached to the hand using 3.5 mm bolts (see Figure 4.2(a)).
4. The pinky finger, ring finger, and thumb were attached to the hand using printed bolts (see Figure 4.2(a) and Figure 4.2(b)).
5. Finally, the fingertips were glued to the fingers (see Figure 4.2(a)).

### Assembly of the Wrist

Figure 4.3 depicts how the wrist was assembled.

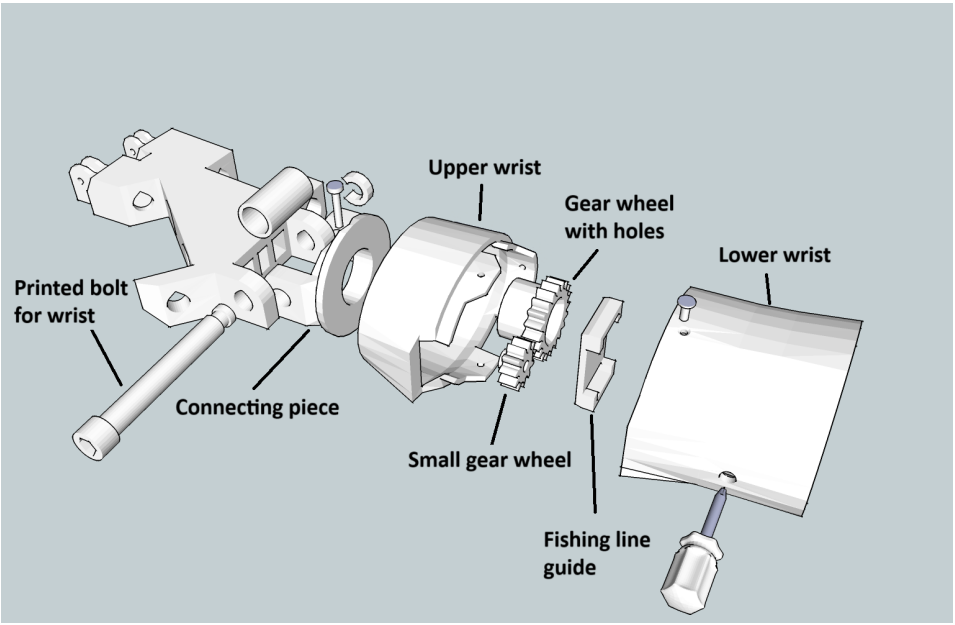


Figure 4.3: Exploded view of the wrist (adapted from [13]).

1. A gear wheel equipped with holes for the fishing lines was inserted into the upper wrist. The fishing lines were then passed through the said holes (see Figure 4.3).
2. The fishing lines were pulled through the upper wrist. A connecting piece was attached between the upper wrist and hand with a screw (see Figure 4.3).
3. A small gear wheel was attached to the motor, which serves for the rotation of the wrist, and then inserted into the lower wrist (see Figure 4.3).
4. The fishing line guide was attached on top of the motor in the lower wrist. The fishing lines were then pulled through the fishing line guide (see Figure 4.3).
5. The upper and lower wrist were connected using screws (see Figure 4.3).
6. The assembled wrist was connected to the hand using a printed bolt (see Figure 4.3).

### Integration of Internal Parts and Electronics

Figure 4.4 shows how the internal parts were assembled.

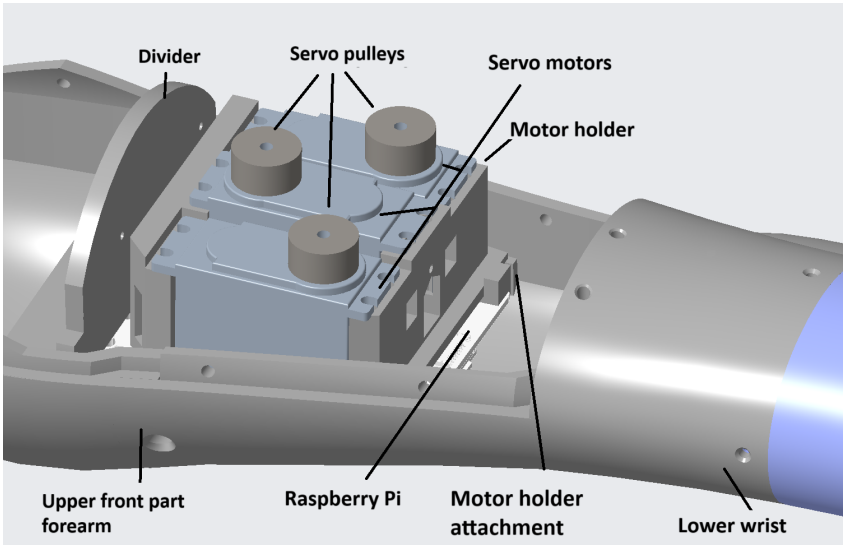


Figure 4.4: Integration of the internal parts.

1. The three remaining motors and the Raspberry Pi were attached to the motor holder. The motor holder was then inserted into the upper front part of the forearm [14] (see Figure 4.4).
2. The upper front part of the forearm was screwed to the lower wrist (see Figure 4.4).
3. The servo pulleys were attached to the remaining three motors. The fishing lines that had been pulled through the lower wrist were wound around the servo pulleys as follows: The fishing lines of the thumb and index finger were each attached to one servo pulley, while the other three fishing lines were attached to the remaining servo pulley (see Figure 4.4).
4. A divider was attached to the motor holder to separate the electrical components from the residual limb (see Figure 4.4).

**Attaching the Arm Components**

1. The remaining parts of the arm were attached to the prosthesis.
2. One of the two elastic cable ties was attached to the lower front part of the forearm, while the other elastic cable tie was attached to the upper arm part.

During assembly, it turned out that the fishing lines were not being wound up around the servo pulleys properly due to the pulleys' placement angle, which in turn stopped the fingers from moving. It was therefore decided to readjust the position of the servo pulleys and motors by rotating them back by 90° around both the x-axis and z-axis. Additionally, the three motors were aligned side by side and shifted as far as possible towards the wrist. However, it should be noted that after these adjustments, the Raspberry Pi and the PCA9685 could no longer be attached below the motor holder as there was no sufficient space. The two devices were therefore placed next to the prosthesis. The fully assembled prosthesis can be seen in Figure 4.5.

[14] The arm of the prosthesis is made out of multiple components that collectively form a casing. The forearm is composed of two front parts and two back parts. The remaining component is positioned on the back side of the upper arm and is connected to the forearm via its lower front part.

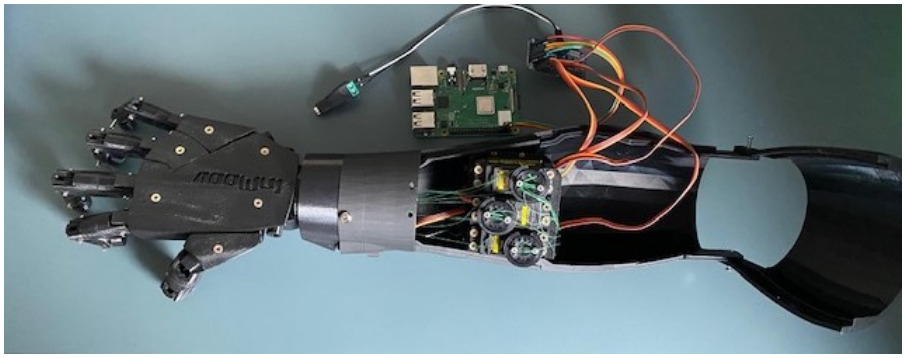

Figure 4.5: Picture of the assembled prosthesis.

During the pilot test, the back parts of the forearm were removed so that the electrical parts of the prosthesis were accessible, and changes could be made quickly if necessary. The overall cost of the prosthesis was about 216 €, the exact costs of the individual components are listed in the appendix.

## 4.2 Installation and Integration of the Electronics

The data for controlling the PCA9685 through the Raspberry Pi was transferred via an $I^2C$[15] interface using Pulse-width modulation (PWM)[16].

To enable communication with the PCA9685, the PCA9685 kernel module had to be activated on the Raspberry Pi. This module was activated by adding the line *dtoverlay=i2c-pwm-pca9685a* to the */boot/config.txt* file. After this modification, the Raspberry Pi was restarted. As the next step, the module had to be loaded by entering the command *sudo modprobe pwm-pca9685* in the terminal of the Raspberry Pi. Finally, it was checked whether the module had been loaded and integrated correctly by entering the command *i2cdetect -y 1*, which verifies whether the PCA9685 is connected to $I^2C$ bus 1.

Figure 4.6 illustrates the wiring and integration of the electrical components in a circuit diagram. The motors were connected to the PCA9685, which in turn was connected to

[15] With the $I^2C$ bus, communication takes place between one or more masters and one or more slaves. A major advantage is the fact that that only two wires are used. One interface is the Serial Clock (SCL), while the other is the Serial Data (SDA) [82].

[16] Rectangular pulses are generated with PWM, which have different widths. They are often used to control motors. Various parameters can be adjusted, such as the PWM period, pulse width offset, and the pulse delay time [46].

the Raspberry Pi. The motor on channel 0 managed pronation and supination, while those on channels 1, 2, and 3 managed flexion and extension. Specifically, the motor connected to channel 1 was responsible for flexion and extension of the thumb, the motor connected to channel 2 controlled the same movements for the index finger, and the motor connected to channel 3 controlled flexion and extension of the remaining fingers.

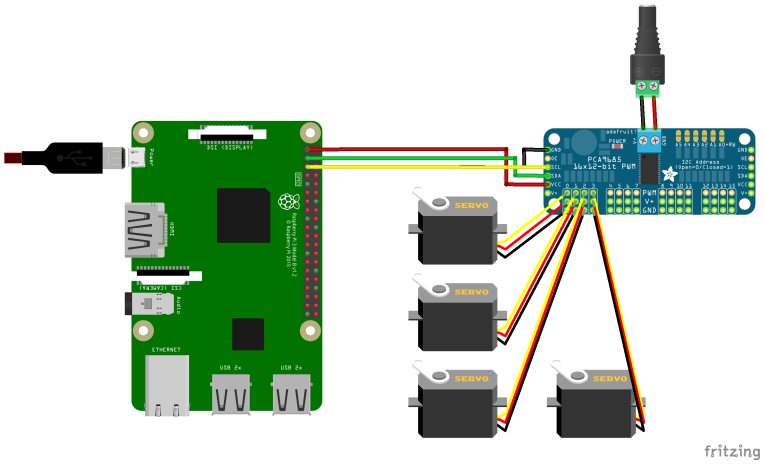


Figure 4.6: Circuit diagram of the electric components of the 3D-printed prosthesis (own figure based on [17]).

The PCA9685 was controlled via pin 3 and 5 using the $I^2C$ protocol. Pin 1 was used as a power supply, while pin 6 was used for grounding. Table 4.1 shows the pin assignment between the Raspberry Pi and the PCA9685. Before use, the pins had to be soldered onto the PCA9685.

Table 4.1: Pin assignment of the Raspberry Pi [17].

| **Raspberry Pi** | **PCA9685** |
|---|---|
| Pin 1 - 3,3 V | VCC / V |
| Pin 3 - GPIO 2 / SDA | SDA |
| Pin 5 - GPIO 3 / SCL | SCL |
| Pin 6 - GND | GND |

## 4.3 Implementation of the Software

The following section describes how the software used to control the prosthesis was created. Initially, a software was developed to control a virtual prosthesis, and later adapted for hardware integration. The software was almost exclusively based on blocks from CLS.

### 4.3.1 Software to Control the Virtual Prosthesis

The control software was divided into two programs: a recording program and a controling program. The recording program was used to record the various gestures. These gestures included flexion, extension, pronation, supination and relaxation (as a baseline). The recorded and stored data then served as a basis for the controlling program, which was used to perform the gestures in a virtual prosthesis. In this program, a machine learning model was trained using the stored data to execute the gestures. Both programs were developed using the LR and LDA demo programs from the CLS as a foundation. The recording program can be seen in Figure 4.7.

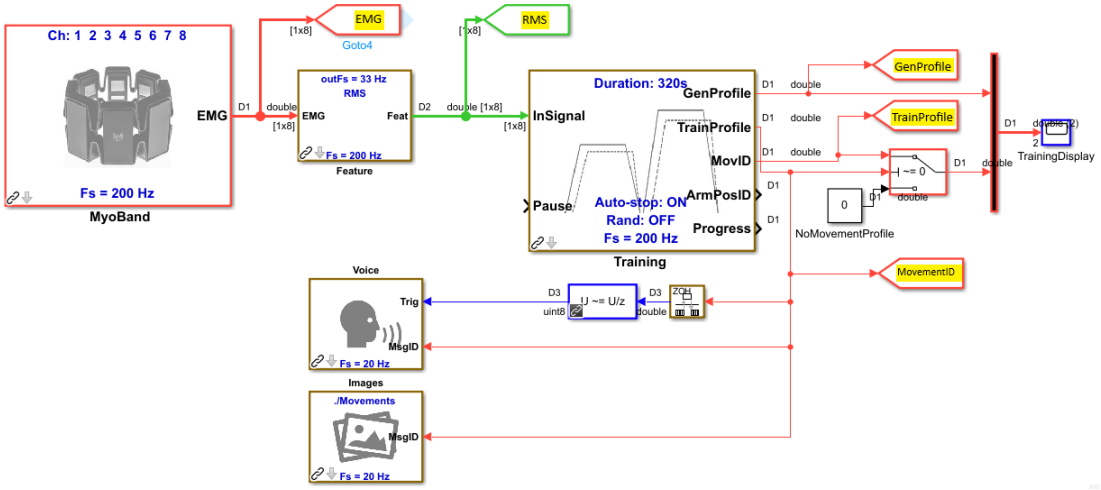


Figure 4.7: Program to record the gestures. The stored variables are highlighted in yellow.

Initially, the eight EMG signals of the muscles were recorded using the Myoband within the Simulink block labeled “MyoBand”. In the subsequent “Feature” block, a feature necessary for training the machine learning model was extracted from these signals. These

selectable features included Root Mean Square (RMS)[17], Zero Crossings (ZCR)[18], Wave Length (WL)[19], and Slope Sign Change (SSC)[20]. In this work, RMS was selected because it provides insight of the muscle activity [61].
A signal intended for gesture tracking during recording was generated in the "Training" block to specify the intensity of each gesture at specific time points. This signal represented the Maximum Voluntary Contraction (MVC)[21] of the performed gesture and consisted of two trapezoidal signals, indicating when the gesture should be performed with higher or lower intensity. In Figure 4.8, the red signal illustrates the generated signal. The blue signal represents the MVCs over time, which were calculated from the RMS values extracted from the recorded EMG signals. To support the transition between the gestures, images stored in the "Images" block were displayed. Furthermore, acoustic feedback was implemented to indicate which gesture should be performed at which time in the "Voice" block.

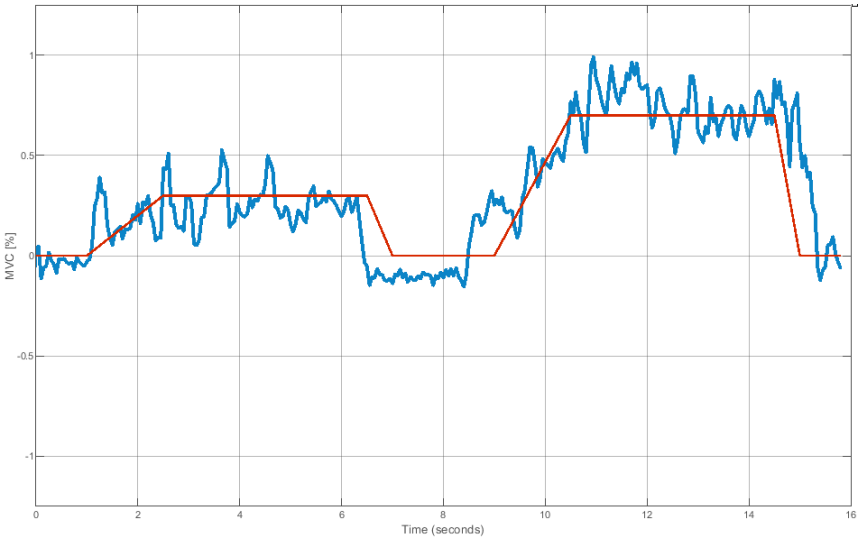


Figure 4.8: Generated signal which indicates the intensity to follow.

[17]The RMS parameter is used to evaluate the muscle activity level from the central nervous system. The RMS is influenced by the motor control as well as the peripheral properties of the muscle and the structure of the recording [61].
[18]The ZCR counts the number of times the signal passes through zero. This feature delivers an approximation of the signal frequency [81].
[19]The WL is a measurement for the complexity of the EMG signal and indicates the cumulative length within an analysis window [80].
[20]In the context of signal frequency, the SSC is the amount of sign changes within an analysis window in the slope of an EMG signal [80].
[21]MVC is used to measure muscle strength and to indicate the force-generating capacity of a muscle or muscle group. The MVC is expressed as a percentage [34].

In the Training block, it was also possible to specify how often each gesture should be performed by increasing the number of trapezoidal signals.
The data measured and calculated in the recording program were then saved in a training file. Specifically, the stored variables included the "EMG" signals, the extracted "RMS" values, the "GenProfile"[22], the "TrainProfile"[23], and the "MovementID"[24].

The controlling program trained a machine learning model using the training file and subsequently tested the machine learning model with a virtual prosthesis. The controlling program was implemented in Simulink and can be seen in Figure 4.9.

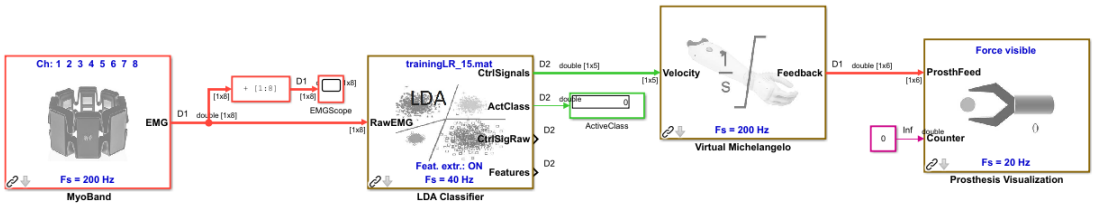


Figure 4.9: Program for controlling the virtual prosthesis.

In addition to the four gestures intended for the prosthesis, the machine learning model was also trained with a recorded baseline class named "relaxation". This baseline was included to ensure the machine learning model could consistently recognize a state of inactivity. Consequently, the LDA classifier of the CLS was used for the control system because the LR classifier of the CLS was restricted to training on a maximum of four classes, whereas the LDA classifier could be trained on up to ten classes. The LDA classifier was able to be trained with all five classes without requiring any modifications to the CLS.
To train the machine learning model, the training file was loaded into the "LDA Classifier" block. The LDA classifier learned to recognize the gestures and classified them using the stored variables in the training file. The distribution of the corresponding classes can be seen in Figure 4.10 in a feature space. The feature space shows the separation of the different classes using features that are based on the variables in the training file [32].

[22] MVC signal based on the extracted RMS.
[23] Signal of the MVCs generated in the Training block.
[24] An ID of 0-4 was assigned to each of the gestures mentioned earlier.

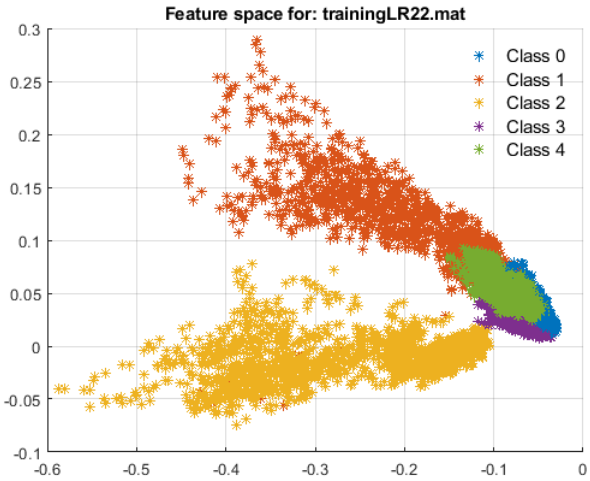


Figure 4.10: Feature space of the LDA classifier.

In the controlling program, the MyoBand block recorded the EMG signals of the performed gestures, which were used to control the virtual prosthesis. The EMG signals needed to be extracted into RMS values in the controlling program as well. In contrast to the recording program, the controlling program did not require a separate block for feature extraction because the LDA Classifier block could perform this task directly. After classification of a gesture, the signals were transferred into the "Virtual Michelangelo" block, which served as the virtual prosthesis using three DOFs and implemented the logic of a Michelangelo hand. In this block, it was necessary to map the classes to the corresponding movements. Specifically, class 1 and 2 corresponded to flexion and extension, while classes 3 and 4 corresponded to pronation and supination.
To visualize the virtual prosthesis, the "Prosthesis Visualization" block was used. The visualization of the virtual prosthesis can be seen in Figure 4.11. The control signals, which result from respective muscle contractions, can be seen in Figure 4.12.

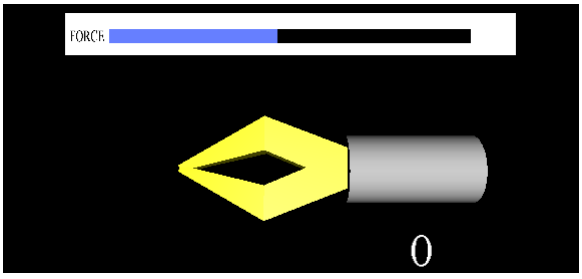


Figure 4.11: Calibration program implemented in Simulink.

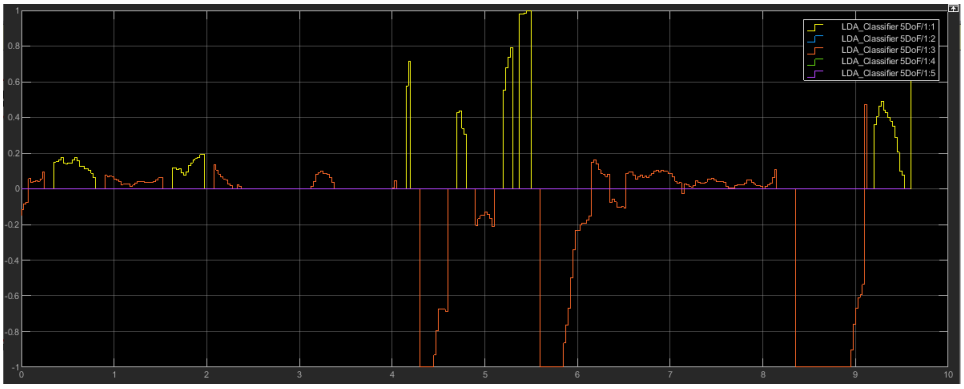


Figure 4.12: Control signals for the virtual prosthesis: The signal highlighted in yellow (Signal 1) represents flexion and extension within the range of -1 to 1, while the signal highlighted in orange (Signal 3) represents pronation and supination within the same range.

Typically, EMG signals are user-dependent and vary even when the electrodes are placed at the same position. Therefore, they were standardized by applying MVC normalization. This method analyzes the amplitude of EMG signals by using the mean RMS value [4]. To normalize the EMG signals recorded during the recording program, a calibration program was developed using the LR and LDA demo programs from the CLS. Figure 4.13 shows the calibration program.

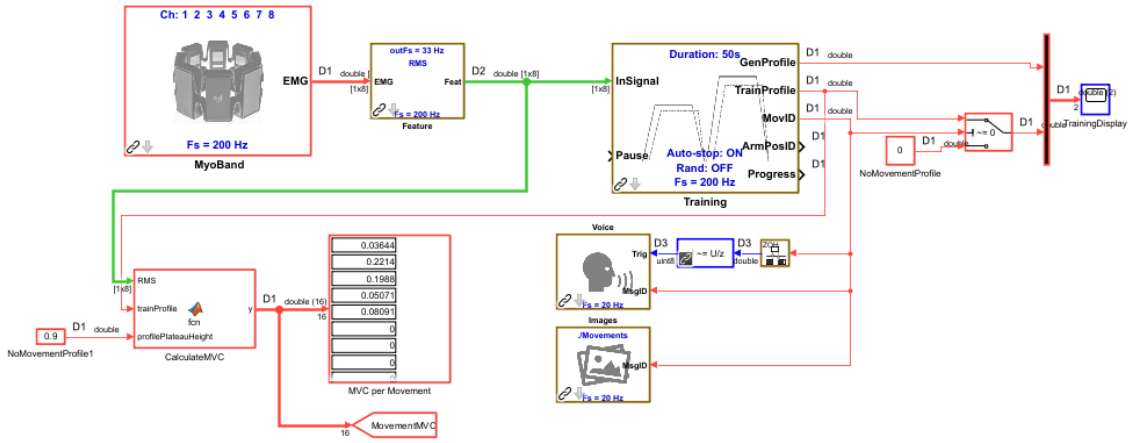


Figure 4.13: Calibration program implemented in Simulink.

The calibration program followed a structure similar to the recording program. The EMG signals from each gesture were recorded in the MyoBand block and then extracted

into RMS values in the Feature block. Similarly, a tracking signal was generated in the Training block. In the calibration program, however, the generated signal consisted of only one trapezoidal signal and was tracked once for each gesture instead of five times. Furthermore, no variables were stored in a file. In the calibration program, the extracted RMS values of one gesture were passed to the "CalculateMVC" block, where the mean RMS value, as well as the corresponding MVC, was calculated. This process was repeated for all gestures. The resulting MVCs were displayed individually for each gesture, as shown in Figure 4.13.
Eventually, the resulting MVCs were passed to the recording program, where they were used as normalization factors to make the recorded data compatible for training with other individuals. The calibration program had to be run once for every individual.

### 4.3.2 Software to Control the Hardware

The controlling program used to control the virtual prosthesis had to be adapted to control the hardware. The control signals were no longer used to control a virtual prosthesis, but instead to control the PCA9685 through the Raspberry Pi. Initially, the program was intended to operate independently on the Raspberry Pi. However, it was discovered that the MyoBand block was only compatible with Windows [73] and therefore could not be used on the Raspberry Pi, which operated on Linux. As a result, the program was executed on a Windows computer for initial testing. The control signals were then transmitted to the Raspberry Pi via Ethernet.

The controlling program was modified to transmit messages from the Raspberry Pi to the PCA9685 to control the motors. Initially, the classes identified by the LDA classifier were mapped to the gestures. The individual motors were controlled based on this mapping. This is shown in Table 4.2.

Table 4.2: Mapping classes to the corresponding gestures.

| **Class** | **Gesture** |
|---|---|
| Class 0 | Relaxation |
| Class 1 | Flexion |
| Class 2 | Extension |
| Class 3 | Pronation |
| Class 4 | Supination |

A state machine was implemented into the controlling program to distinguish between different classes. The logic of the state machine is shown in an Unified Modeling Language (UML)[25] diagram, which can be seen in Figure 4.14.

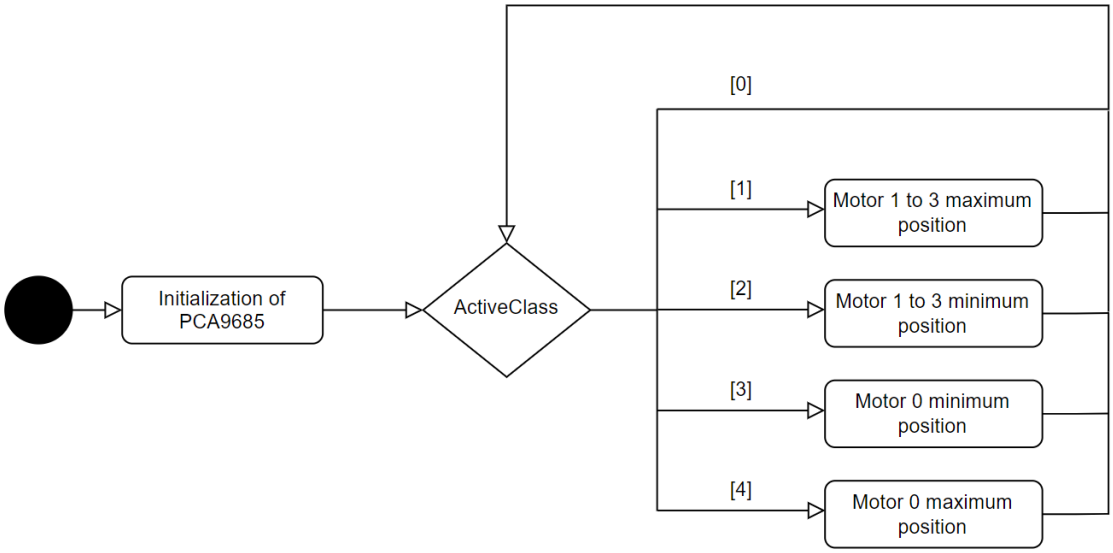


Figure 4.14: UML diagram of the state machine.

The motors in the prosthesis were actuated according to the states, which corresponded to the recognized classes. In class 0, motors maintained their previous alignment, serving as a resting state. Class 1 actuated motors 1 to 3, setting them at maximum position for flexion. Class 2 set motors 1 to 3 at minimum position for extension. Class 3 set motor 0 at maximum position for pronation, while Class 4 set the same motor at minimum position for supination.
The motors were controlled using an "Integrated MATLAB Function" block, which implemented the functionalities of a MATLAB script within Simulink. The adaptation of the controlling program can be seen in Figure 4.15.

[25] UML diagrams are based on Unified Modeling Language and are dynamic templates that visualize processes and workflows. In this case, an activity diagram was used to represent workflows. These workflows divide the activities into actions and decisions, and are well suited to represent code flows [83].

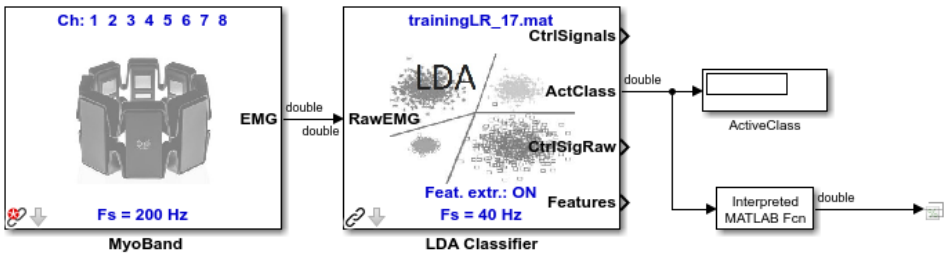


Figure 4.15: Program for controlling the hardware.

To control PCA9685 through the Raspberry Pi, the correct registers within the PCA9685 needed to be addressed [52]. First, the PCA9685 needed to be initialized, which can be seen in Figure 4.14. This initialization was performed in the "Intfnc"[26] of the Integrated MATLAB function block.

The following code illustrates the initialization process, where the green comments explains which configurations are set:

```
clear mypi
clear i2cpwm
mypi = raspi('169.254.189.243','protheseV1','SS22pro!');
i2cpwm = i2cdev(mypi,'i2c-1','0x40');
% Set all PWM to 0
write(i2cpwm,[hex2dec('FA') hex2dec('0')])
write(i2cpwm,[hex2dec('FB') hex2dec('0')])
write(i2cpwm,[hex2dec('FC') hex2dec('0')])
write(i2cpwm,[hex2dec('FD') hex2dec('0')])

% Set PWM frequency to 50 Hz
write(i2cpwm, [hex2dec('01') hex2dec('04')]);
% Activate "All Call" I2C address mode (default value)
write(i2cpwm, [hex2dec('00') hex2dec('01')]);
% Initialize PWM card
write(i2cpwm, [hex2dec('00') hex2dec('10')]); % Sets the MODE1 register to 0x10 (
    activates restart bit)
% Set default settings
write(i2cpwm, [hex2dec('01') hex2dec('04')]); % Sets the register for the PWM
    frequency
% Load presets
write(i2cpwm, [hex2dec('FE') 101]); % Sets the prescaler for the PWM frequency
% Activate PWM card
write(i2cpwm, [hex2dec('00') hex2dec('81')]); % Sets the MODE1 register to 0x81 (
    activates restart and sleep bit)
% Save required variables in the MATLAB Function Block Workspace
assignin('base', 'i2cpwm', i2cpwm);
```

[26] Initialization function.

The state machine was implemented as a switch case and is shown in the following code:

```
function y = ServoControl(x)
    controlSignal = x;
    servoMin = 150;  % Min pulse length
    servoMax = 600;  % Max pulse length
    coder.extrinsic("evalin");
    i2cpwm = evalin("base","i2cpwm"); %Read variables from workspace
    switch controlSignal
        case 0
                % Hold the servos 1-3 in the current position
        case 1
                % Move motors of channels 1, 2 and 3 to maximum position
            for channel = 1:3
                write(i2cpwm, [hex2dec('08') + channel * 4, bitand(servoMax,
                    hex2dec('FF'))]); % Lower 8 Bits
                write(i2cpwm, [hex2dec('09') + channel * 4, bitshift(servoMax, -8)
                    ]); % Higher 8 Bits
            end
        case 2
                % Move motors of channels 1, 2 and 3 to minimum position
            for channel = 1:3
                write(i2cpwm, [hex2dec('08') + channel * 4, bitand(servoMin,
                    hex2dec('FF'))]); % Lower 8 Bits
                write(i2cpwm, [hex2dec('09') + channel * 4, bitshift(servoMin, -8)
                    ]); % Higher 8 Bits
            end
        case 3
                % Move motor from channel 0 to minimum position
            write(i2cpwm, [hex2dec('08') + 0 * 4, bitand(servoMin, hex2dec('FF'))
                ]); % Lower 8 Bits
            write(i2cpwm, [hex2dec('09') + 0 * 4, bitshift(servoMin, -8)]); %
                Higher 8 Bits
        case 4
                % Move motor from channel 0 to maximum position
            write(i2cpwm, [hex2dec('08') + 0 * 4, bitand(servoMax, hex2dec('FF'))
                ]); % Lower 8 Bits
            write(i2cpwm, [hex2dec('09') + 0 * 4, bitshift(servoMax, -8)]); %
                Higher 8 Bits
    end
y = x;
```

Figure 4.16(a) shows the prosthesis in the maximum flexion position, while Figure 4.16(b) shows the maximum extension position. The maximum pronation position is shown in Figure 4.16(c), while the maximum supination position can be seen in Figure 4.16(d).

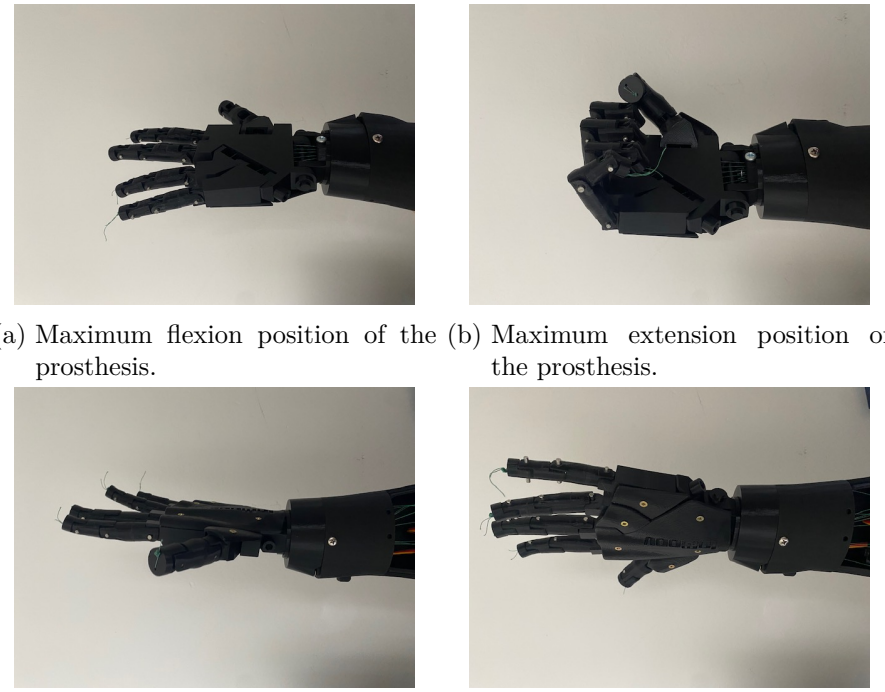

(a) Maximum flexion position of the prosthesis.

(b) Maximum extension position of the prosthesis.

(c) Maximum pronation position of the prosthesis.

(d) Maximum supination position of the prosthesis.

Figure 4.16: Maximum position of the different gestures of the prosthesis.

In the next step, proportional control of the fingers and wrist was integrated. To control the motors proportionally, the recognized classes were replaced by the control signals generated by the LDA Classifier block. The control signals varied proportionally based on the intensity of the executed gesture.
Next, the control signals were transformed into PWM signals that controlled the motors, using linear interpolation based on the following formula:

$$(x - x_1) \cdot \frac{(y_2 - y_1)}{x_2 - x_1} + y_1 \tag{4.1}$$

with $x$ being the control signal, $x_1$, $x_2$ being the lower and upper limits of the control signal, and $y_1$ and $y_2$ being the lower and upper limits of the PWM signal [15].

The transforming was performed using the “mappedH” and “mappedW” functions. Signal 1 controlled flexion and extension, while signal 3 controlled pronation and supination.

The following code shows how the proportional control of the fingers and wrist was implemented:

```
function y = ServoControl2(x)
    cntr = x;
    coder.extrinsic("evalin");
    i2cpwm = evalin("base","i2cpwm"); %Read variables from MATLAB Function Block
        workspace
    servoMin = 150;  % Min pulse length
    servoMax = 600;  % Max pulse length
    inpH = cntr(1); % Save signal 1 (extension/flexion) and
    inpW = cntr(3); % signal 2 (pronation/supination) inside a variable

                % Calculation of the motors movement of the fingers
    mappedH = (inpH - -1) * (servoMax - servoMin) / (1 - -1) + servoMin;
                % Calculation of the motor movement of the wrist
    mappedW = (inpW - -1) * (servoMax - servoMin) / (1 - -1) + servoMin;

                % Move motors of channels 1, 2 and 3
    for channel = 1:3
    write(i2cpwm, [hex2dec('08') + channel * 4, bitand(round(mappedH), hex2dec('FF
        '))]); % Lower 8 Bits
    write(i2cpwm, [hex2dec('09') + channel * 4, bitshift(round(mappedH), -8)]); %
        Higher 8 Bits
    end

                % Move motors of channels 0
    write(i2cpwm, [hex2dec('08') + 0 * 4, bitand(round(mappedW), hex2dec('FF'))]);
         % Higher 8 Bits
    write(i2cpwm, [hex2dec('09') + 0 * 4, bitshift(round(mappedW), -8)]); % Lower
        8 Bits

y = x;
```

With this code described, only one movement could be executed at a time. During a change of movement, the previous movement was reset to zero. This means, for example, that it was not possible to hold onto an object that had been grasped before when the wrist was turned. To solve this problem, the Virtual Michelangelo block was reintegrated. This block is capable of saving the previous control signal and adjusting it by adding or subtracting the current control signal. As a result, the hand remained closed even when switching to the next movement, because the intensity of signal 1 was set to zero when the wrist is turned. The previously developed code remained unchanged. The implementation in Simulink is shown below in Figure 4.17.

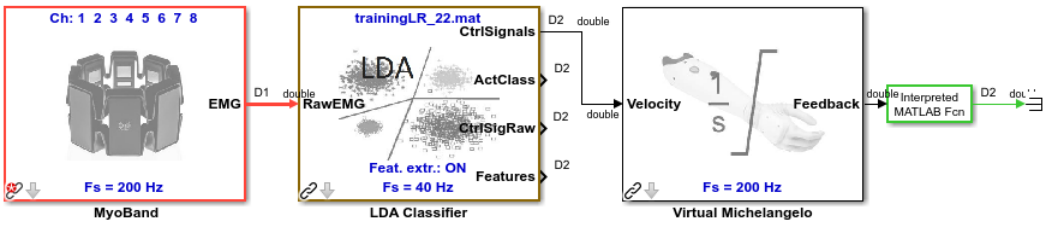


Figure 4.17: Adjusted program for proportional control.

## 4.4 Results of the Pilot Test

As the inputs and outputs of the Raspberry Pi had to be controlled, the simulation had to be carried out in I/O mode and could not be run in external mode. It was discovered that the simulation operated too quickly in I/O mode and that the response time of the Raspberry Pi was too slow, which led to so-called "missed ticks". In contrast to the external mode, the missed ticks led to an abortion of the program when the "maximum missed ticks" were exceeded. To reduce the amount of missed tick, the sampling frequency of the simulation would have to be reduced. However, the sampling frequency could not be adjusted in this simulation, as it was tuned to the fixed frequency of the MyoBand. Consequently, the maximum missed ticks in this simulation had to be set high enough to prevent the program from aborting during the pilot tests.
In addition to this, the latency resulting from the program's architecture contributed to a faster accumulation of missed ticks. The program was structured in such a way that the motors were actuated in proportion to the muscle movements. This increased the frequency of messages sent to the Raspberry Pi, which in turn led to higher latency. As a result, the muscle movements could no longer be correctly associated with the gestures performed by the prosthesis. Consequently, it was no longer possible to accurately check whether the correct movement was being executed. As a solution, the controlling program, in which the motors were controlled to fixed positions based on their corresponding classes, was used for the pilot test. This resulted in a lower frequency of messages sent to the Raspberry Pi, reducing both the accumulation of missed ticks and the latency.

During the pilot test, the recording program was executed initially, followed by the controlling program. In the recording program, 10 movements were recorded for each gesture. Five of these movements were performed at low intensity, while the other five

movements were performed at high intensity. The LDA classifier was then trained with these gestures.

In the controlling program, each gesture was performed 15 times at high intensity and 15 times at low intensity. The number of successful gesture executions was documented. Next, the recall for the recognition of the gestures and the accuracy for the LDA classifier were calculated. The pilot test was initially performed with a flexed elbow, as depicted in Figure 4.18, as many everyday movements, such as drinking or writing, are typically performed in this position.

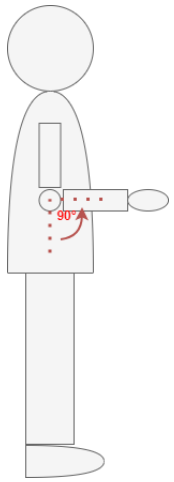


Figure 4.18: Flexed elbow during the pilot test (own figure based on [30]).

The results of the pilot test with a flexed elbow are shown in the confusion matrices in Figure 4.19 and Figure 4.20. On the diagonal of the confusion matrices, correctly classified gestures are represented. Wrongly classified gestures are displayed in the remaining fields, depending on which class was recognized. To calculate the accuracy, the numbers of the diagonal were summed up and divided by the total number of attempts. For the calculation of the recall for the different classes, the $TP_{ClassN}$ value was the one on the diagonal, while the $FN_{ClassN}$ value represented the sums of incorrectly recognized gestures in one row. Both the recall and the accuracy were first calculated separately for weak and strong intensity, and then for the whole LDA classifier. The calculated recall rates and accuracy are presented in Table 4.3.

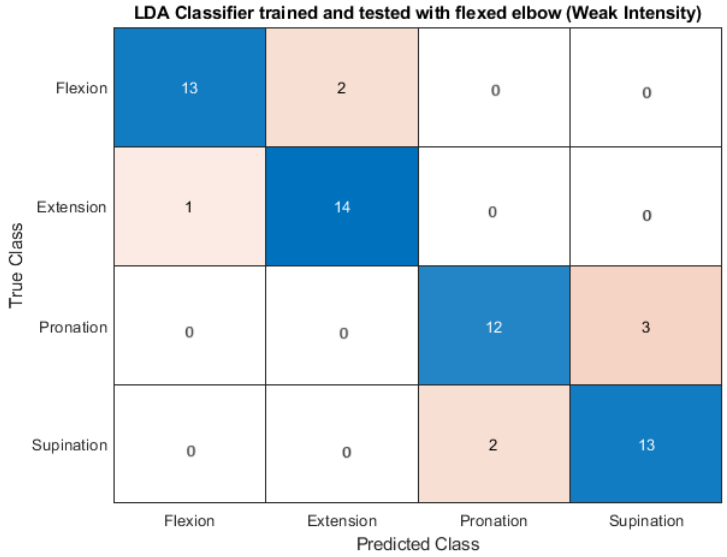


Figure 4.19: Confusion matrix for the LDA classifier trained and tested with a flexed elbow (Weak Intensity).

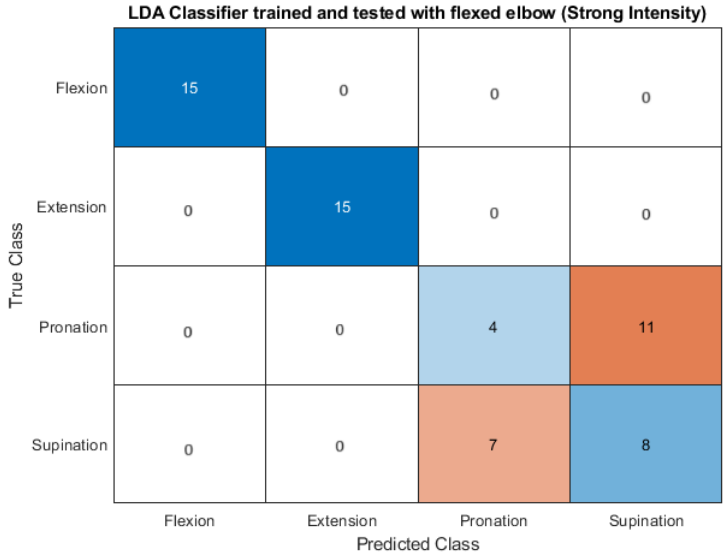


Figure 4.20: Confusion matrix for the LDA classifier trained and tested with a flexed elbow (Strong Intensity).

Table 4.3: Recall and accuracy for the LDA classifier trained and tested with a flexed elbow.

| **Class** | **Recall (Weak Intensity)** | **Recall (Strong Intensity)** | **Average Recall** |
|---|---|---|---|
| Flexion | 86.67 % | 100 % | 93.33 % |
| Extension | 93,33 % | 100 % | 96.67 % |
| Pronation | 80 % | 26 % | 53.33 % |
| Supination | 86.67 % | 53.33 % | 70 % |
| | **Accuray (Weak Intenisty)** | **Accuracy (Strong Intensity)** | **Average Accuracy** |
| | 86.66 % | 69.83 % | 78.33 % |

During the training and execution of the gestures, it was observed that over time the muscles tensed and trembled when the elbow was flexed. Therefore, the pilot test was carried out again with a suspended arm to test whether this leads to differences in accuracy. The position of the arm can be seen in Figure 4.21. The confusion matrices are shown in Figure 4.22 and Figure 4.23, while the calculated recalls and accuracy are shown in Table 4.4.

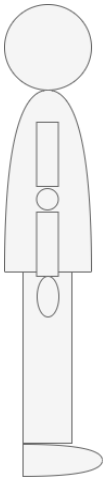

Figure 4.21: Suspended arm during the pilot test (own figure based on [30]).

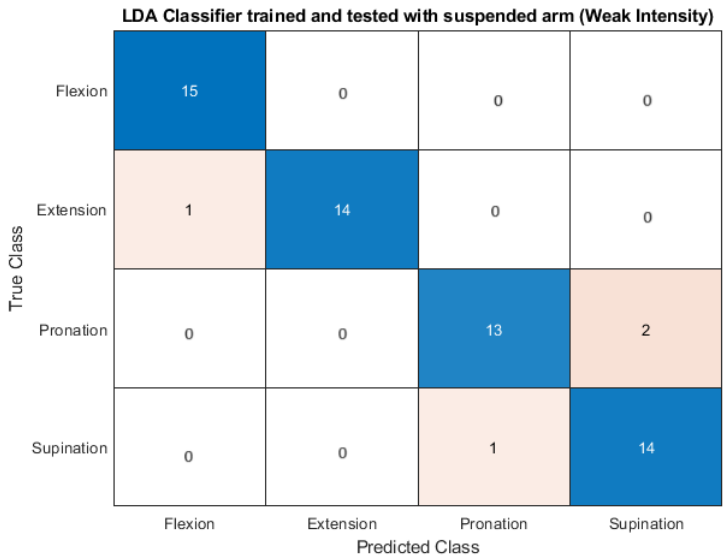


Figure 4.22: Confusion matrix for the LDA classifier trained and tested with a suspended arm (Weak Intensity).

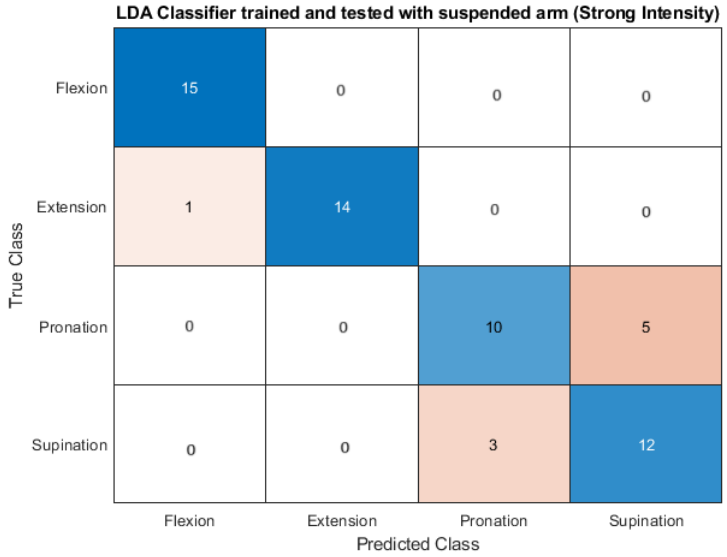


Figure 4.23: Confusion matrix for the LDA classifier trained and tested with a suspended arm (Strong Intensity).

Table 4.4: Recall and accuracy for the LDA classifier trained and tested with a suspended arm.

| **Class** | **Recall (Weak Intensity)** | **Recall (Strong Intensity)** | **Average Recall** |
|---|---|---|---|
| Flexion | 100 % | 100 % | 100 % |
| Extension | 93.33 % | 93.33 % | 93.33 % |
| Pronation | 86.67 % | 66.67 % | 71.56 % |
| Supination | 86.67 % | 80 % | 86.67 % |
| | **Accuray (Weak Intenisty)** | **Accuracy (Strong Intensity)** | **Average Accuracy** |
| | 91.66 % | 85 % | 87.89 % |

Finally, the same pilot test was performed once again with a LDA classifier that was trained with a suspended arm, but tested with a flexed elbow instead to see if there were any differences in accuracy compared to the previous tests. The confusion matrices can be seen in Figure 4.24 and Figure 4.25, and calculated recalls and accuracy for this test can be seen in Table 4.5.

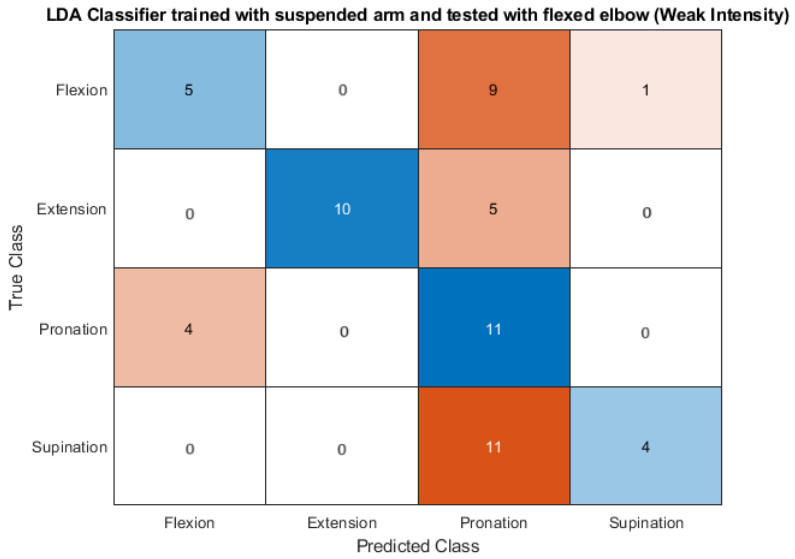


Figure 4.24: Confusion matrix for the LDA classifier trained with a suspended arm and tested with a flexed elbow (Weak intensity).


Figure 4.25: Confusion matrix for the LDA classifier trained with a suspended arm and tested with a flexed elbow (Strong intensity).

Table 4.5: Recall and accuracy for the LDA classifier trained with a suspended arm and and tested with a flexed elbow.

| **Class** | **Recall (Weak Intensity)** | **Recall (Strong Intensity)** | **Average Recall** |
|---|---|---|---|
| Flexion | 33.33 % | 46.67 % | 40 % |
| Extension | 66.67 % | 26.67 % | 46.67 % |
| Pronation | 73.33 % | 53.33 % | 63.33 % |
| Supination | 26.67 % | 53.33 % | 40 % |
| | **Accuray (Weak Intenisty)** | **Accuracy (Strong Intensity)** | **Average Accuracy** |
| | 50 % | 45 % | 47 % |

During these tests, it was noticeable that the transition from any gesture to the resting state often involved a subsequent brief switch to class 3 (pronation), before finally transitioning to the resting state. Similarly, switching from class 3 to the resting state involved a brief subsequent transition to class 4 (supination).

Tests on limb-impaired subjects were not conducted as part of this master's thesis.

# 5 Discussion

In this chapter, the results are discussed and compared with the current state of research. The challenges and limitations of this work are addressed, the impact of the results in practical applications is explained, and future extensions of this work are suggested.

## 5.1 Interpretation and Comparative Analysis with Contemporary Research

The adaptation of InMoov's design [63] to meet specific needs of a prosthesis has proven to be very promising. A few modifications allowed the robotic arm to be used as a prosthesis. Implementing a control system with only four motors instead of six resulted in a reduction of weight, cost savings, and the need for a less powerful power supply. The analysis of EMG signals recorded with the MyoBand enabled the recognition of different gestures. The RMS of the signals provided a solid basis for the application of machine learning models for gesture recognition. The LDA classifier was used as the machine learning model, because the LR classifier from the CLS could only be trained on four classes. The LDA classifier showed good results in gesture recognition and it was possible to realize a second DOF by adding rotation in addition to opening and closing the hand.

The validation of gesture recognition by controlling a virtual prosthesis with the MyoBand highlights the practical applicability of this approach. Additionally, the pilot test demonstrated that this technology can be implemented not only virtually but also that it can be used for controlling hardware. Successfully controlling individual motors with the Raspberry Pi to perform the desired gestures has demonstrated the suitability of the MyoBand as a sensor for controlling prostheses in real applications. The results indicate that the combination of 3D-printing technology, EMG signal analysis and machine

learning control offers promising opportunities for the development of advanced prosthetic systems. This work demonstrated that it is possible to control both flexion and extension, as well as pronation and supination, using an intuitive control mechanism. These gestures could be performed proportionally, but simultaneous execution of these movements was not possible. However, both DOFs could be executed sequentially, with the current position of the first DOF being maintained while executing the second.

Compared to the previous studies mentioned in Section 2.3, especially those involving a rotation unit, several improvements were integrated. Not only has the implementation of rotation in both directions been achieved, but also a proportional control of the motors based on muscle intensity. This is in contrast to the fixed control in the study by K. Avilés-Mendoza et al. [40], where only a 20° clockwise rotation was possible [40]. Furthermore, the rotation of the prosthesis can be controlled intuitively without resorting to predefined gestures, a feature which both M. Hussein et al. [59] and K. Avilés-Mendoza et al. [40] did not implement.
Using the MyoBand, it was feasible to operate the prosthesis even in cases of transradial forearm amputations, that were performed closer to the elbow. This contrasts with the work of M. Hussein et al. [59], where one of the electrodes was positioned near the wrist to target the forearm muscles (see Figure 2.13). Consequently, the prosthesis discussed in this work can also be employed for higher-level amputations. The MyoBand is attached in a similar position to the electrodes in K. Avilés-Mendoza et al.'s [40] work, but it utilizes eight electrodes in this work compared to only three used in their work. Additionally, since the EMG sensors in the MyoBand are firmly integrated into a band, that can be simply pulled over the arm, a more precise and quicker application was possible, especially between sessions. It was also not necessary to glue the electrodes.

The accuracy of machine learning models used for controlling prostheses was a topic discussed in two papers that were described earlier: In the first work, written by K. Avilés-Mendoza et al. [40], three classes were trained: Wrist Flexion (class 1), Fist (class 2), and Wrist Extension (class 3). Class 1 was used to close the hand, and Class 3 was used to open it. Class 2 was used to rotate the wrist. 20 movements were recorded per gesture, resulting in a total of 60 movements. The movements were performed by a single subject. An accuracy of 78.67 % was achieved. After the second class was removed, an accuracy of 95 % was achieved for a binary model. The removed class was responsible for the rotation of the wrist [40]. In the work of S. Said et al. [75], a total of four classes were trained. The gestures Open, Close, Wave-in and Wave-out were recorded from 23 subjects [75]. The Close and Open gestures were used to open the

hands of the prosthesis. Wave-in closed one finger, while Wave-out closed two fingers of the prosthesis. Each gesture was performed more than 10 times, creating a data set of 2000 gestures. It is noteworthy that the MyoBand was used in their work as well, although intuitive gestures were not implemented. Instead, the gestures implemented in the Software of the MyoBand were used. Overall, an accuracy of 89.93 % was achieved [75].

The feature space depicted in Figure 4.10 of this work demonstrates that class 1 (flexion) and class 2 (extension) can be clearly distinguished from each other and from the remaining classes. In contrast, class 0 (relaxation), class 3 (pronation), and class 4 (supination) are closely clustered together, making them difficult to differentiate. An accuracy of 78.33 % was achieved by a LDA classifier trained and tested with a flexed elbow, while an accuracy 87.89 % was achieved with by a LDA classifier trained and tested with an suspended arm. In a LDA classifier, that was trained with an suspended arm and tested with a flexed elbow, an accuracy of 47 % was archived. It should be noted that the training was conducted with a small data set and was performed by only one subject. 10 movements per gesture were performed, resulting in 40 movements in total and 50 movements, if the relaxing state is included. The LDA classifier was always trained and tested in one session, so neither session- nor subject-dependency were taken into account. The size of the data set is comparable to the work of K. Avilés-Mendoza et al., where the data were recorded for only one subject as well [40]. In S. Said et al.'s [75] study, data from different people were used, as well as a larger data set.

Since EMG signals are both session- and user-dependent, it was expected that the accuracy in this work would be higher than in S. Said's et al. study, which collected data from multiple subjects, although the specific methodology for addressing user-dependency in the data processing is not explicitly detailed [75]. However, the accuracy was higher in S. Said's et al. [75] study. This result suggests that rotational movements are more difficult to recognize than wrist extension and wrist flexion movements used in S. Said et al. study [75].

The higher difficulty in detecting rotational movements is illustrated in Figure 4.10. As mentioned earlier, the figure shows that the distribution of class 3 (pronation) and class 4 (supination) are very close to the distribution of class 0 (relaxation). The close alignment of the class features not only explains the transition to the opposite movement when changing to the resting state but also contributes to the confusion between pronation and supination by the LDA classifier. This confusion is evident in the confusion matrices

presented in Figures 4.19, 4.20, 4.22, and 4.23 from the first two pilot tests. The confusion matrices also show that gestures performed with a higher intensity lead to increased confusion between classes 3 and 4, suggesting that stronger execution of gestures also engages the muscles associated with the respective other movement. The difficulty is also reflected in the recall of these two gestures shown in Table 4.3 and 4.4. The recall of pronation and supination differs substantially from the recall of flexion and extension of the hand. This is especially noticeable when the elbow is flexed, resulting in differences of 10 % to 30 %. In comparison, S. Said et al.'s [75] confusion matrix shows that the recall rates for the gestures used in their study are very similar, with differences of less than 4 %, which allows for clear differentiation between the gestures.

Another potential cause for the lower accuracy observed in this work could be the substantially smaller data set used compared to the study of S. Said et al. [75], which may have impacted the training and performance of the LDA classifier, thereby explaining the discrepancies in accuracy. This assumption is supported by a comparison with the study of K. Avilés-Mendoza et al. [40], which used a similar small amount of data and achieved similar accuracy levels as observed in this work.

In the study of K. Avilés-Mendoza et al. [40], the gesture of closing the hand was excluded because it was frequently misclassified as other gestures. S. Said et al. [75] included the same gestures but achieved a much higher accuracy. One possible explanation for this discrepancy is the difference in the number of electrodes used. K. Avilés-Mendoza et al.'s [40] study utilized only three electrodes, whereas S. Said et al. [75] employed a MyoBand with eigth electrodes, which are distributed around the arm to capture a more comprehensive muscle activity profile. Therefore, the use of additional electrodes facilitates more accurate differentiation of gestures. This could explain why the accuracy achieved in this work is comparable to that reported by K. Avilés-Mendoza et al. [40], despite the more complex gestures of pronation and supination needed to be classified, as in this thesis also a MyoBand was used.

The higher accuracy of the LDA classifier trained and tested with a suspended arm is remarkable. This could be due to the fact that all gestures were recorded consecutively in a single session without interruptions. When the arm is suspended, the muscles are not subjected to the biomechanical constraints imposed by elbow flexion, thereby reducing muscle strain and minimizing involuntary tremors. This reduction in muscle strain leads to fewer involuntary movements in the EMG recordings, resulting in a cleaner and more consistent signal for each gesture.

Moreover, the observed decrease in accuracy of the LDA classifier trained with an suspended arm and tested with a flexed elbow highlights the substantial influence of arm position on gesture recognition. The confusion matrices of this test in Figure 4.24 and Figure 4.25 show that pronation was frequently misclassified into all other gestures, and flexion being identified more often when pronation was performed. It is noticed, that unlike before, where misclassification would often result in the opposite gesture being recognized, a completely different gesture was recognized instead. This suggests that the features for classification are different depending on the arm position.
The arm position was not considered in any of the reviewed studies and underlines the impact on muscle dynamics and, consequently, on the training and accuracy of machine learning models for gesture classification. This is particularly relevant in daily activities, as many movements involve a range of arm positions, including flexion or extension of the elbow, making robust machine learning model performance across varying postures necessary.

Compared to conventional prostheses, both the manufacturing time and the cost of the prosthesis developed in this work are substantially lower. The printing time of the developed prosthesis was 81 hours.
The time of assembling the prosthesis as well as the time of setting up the Raspberry Pi were not measured because several complications occurred. It is difficult to compare the production time directly with that of conventional prostheses, as the available information on conventional prostheses usually only provides broad timespans ranging from weeks to months. However, compared with the available information on the production time of a single finger of a conventional prosthesis, which takes a total of 80 to 105 hours [57], it becomes clear that the 3D-printing process is a faster method. The use of 3D-printing eliminates the need for molds, allowing for quick adjustments, leading to a shorter production time. In addition, printing multiple different versions simultaneously allows for direct comparison to find the best fit, without relying on molds.
The cost of the developed prosthesis in this work was around 216 €[27], which is substantially lower than the cost of conventional prostheses, where transradial myoelectric prostheses can cost up to $ 20,329, resulting in a difference of almost 200 %. However, electricity consumption and hourly rates for design adaptations, or gesture recording need to be taken into consideration regarding the overall cost as well. Nevertheless, the developed prosthesis is more affordable than conventionally manufactured prostheses.

[27] The cost of the MyoBand is not included, as this is no longer available for purchase and was provided for the master's thesis. A sensor for recording EMG signals would have to be included in future costs.

The cost is in a similar range to that of 3D-printed prostheses examined in comparative studies, such as Richard Van As' Robohand [49], which cost $ 150 and does not have any electrical components, or S. Said's et al. prosthesis, which cost around $ 250 [75].

## 5.2 Challenges and Limitations

During the course of this master's thesis, several challenges and limitations were encountered that impacted the prosthesis development process. One of the primary issues was the limited availability of 3D-printers, therefore the individual parts needed to be printed one-by-one. Consequently, the process of printing all the components was time-consuming, leaving little time for further customization. In total, only three 3D-printers were available, and their usage was restricted to 2-3 days per week due to limited access to the printing room. However, two of the 3D-printers were defective at times or were occupied by other projects.
Furthermore, since no tests were performed on the strength and distribution of forces in relation to the design and material of the prosthesis, the prosthesis could not be fully optimized for durability and effectiveness.

Space constraints within the arm, particularly due to the accommodation of motors and other essential hardware, posed substantial challenges. The need to house four motors and electronic components made it difficult to reduce the overall size of the prosthesis. Although two motors would have been sufficed to integrate the control system used for this work, further reducing weight and potentially lowering the cost of the prosthesis, the other two motors remained inside to keep maintain the option to implement additional grip types. Consequently, the prosthesis was primarily suitable for individuals with larger arms, limiting its applicability for people with smaller stumps or differing anatomical needs. Also placing the Raspberry Pi and PCA9685 inside the prosthesis was not possible. The prosthesis weighted 750 g. The increased weight caused by the large motors represents an additional burden to the user and is likely to impair both comfort and practicality. However, this could not be verified as the prosthesis was not tested on a limb-impaired individual. Additionally, the reliance on electrical power instead of a battery restricted user mobility, as the prosthesis had to remain tethered to a power source, limited its usability in real-world scenarios.

The compatibility of software tools presented another challenge. Integrating the CLS into the overall system was particularly problematic as it was development for Windows 7 and MATLAB 2019. Several steps had to be taken and different compilers had to be installed to make the toolbox usable on a newer system. Eventually, installation on Windows 10 was possible, but only with the MATLAB 2023a. The incompatibilities between Linux and the MyoBand further complicated the process of recording and processing muscle activity data. This issue occurred because the original software for the MyoBand was no longer available, as the device itself was no longer sold. The CLS block connected with the MyoBand used a third-party software, called "Myo-Python", that was only compatible with Windows [73]. As a result, the control software could not be run stand-alone on the Raspberry Pi and required a Windows computer for execution. The control commands then had to be transmitted via an Ethernet connection between the Windows computer and the Raspberry Pi.

While running on an external computer, it was not possible to run the control software in external mode, as the I/Os of the Raspberry Pi could not be addressed in this mode. To mitigate this, the control software was executed in I/O mode, allowing the Raspberry Pi's I/Os to be addressed. However, the high sampling frequency of the simulation caused delays in the Raspberry Pi, leading to missed ticks and eventual program termination. Theoretically, reducing the sampling frequency could prevent or reduce missed ticks, but since the simulation's sampling frequency could not be adapted, this was not feasible. The issue could only be temporarily bypassed by setting the maximum missed ticks high enough to perform the pilot test. This was merely a temporary solution, as the prosthesis lacked real-time capabilities and could only be operated for limited durations. As a result, it was not possible to conduct a more complex pilot tests, such as a brief version of the BBT or the RCRT. Tests on limb-impaired subjects were not conducted as part of this master's thesis primarily due to the extensive scope required to address all necessary aspects, which would have exceeded the constraints of a master's thesis.

Simultaneous execution of two DOFs was another limitation. The LDA classifier could only recognize a single gesture at a time, preventing simultaneously control of multiple movements. However, sequential control of gestures was possible, with the previously executed gesture maintaining its state. For instance, it was possible to close the hand and rotate it consecutively.

## 5.3 Implications for Practice

The results of this study demonstrate the potential of 3D-printed prostheses addressing accessibility challenges faced by individuals who lack access to conventional prosthetic devices. The combination of lower costs and rapid production times positions 3D-printed prostheses as viable alternatives, both as intermediate solutions and permanent replacements.
Moreover, the scalability of a 3D model presents a practical advantage, particularly beneficial for children during their growth phases. Minor adjustments to the attachment for the residual limb can be easily made, enabling a modular design approach. Besides, modularity also enables quick reprinting of spare parts, ensuring minimal downtime for users.

In addition, the utilization of MyoBand technology provides substantial advantages over traditional electrodes, including remote recording capabilities. The eight electrodes can be easily placed as a band. Furthermore, the intuitive control of two DOFs offered by the MyoBand, in combination with a machine learning model, may lead to increased acceptance among users by eliminating the need for relearning predefined gestures, enabling seamless integration into daily activities.
The implemented flexion of the hand allows for gripping movements, which are important for daily activities as they enable fundamental actions such as grasping object. Similarly, the rotation of the wrist provides additional mobility and prevents postural deformities [48]. However, other gripping movements that enhance fine motor skills, such as the pinch grip or handle grip, are required for tasks like opening a bottle or writing and could be considered for future implementation.
For the adoption of 3D-printed prostheses in combination with the MyoBand, it is also important to address practical challenges such as technological compatibility, the recording and processing of training data, and the longevity of materials used.

## 5.4 Prospects for Future Work

For future developments, the design of the prosthesis could be revised to create additional space within the arm. This change would make the prosthesis suitable for smaller individuals and allow for the integration of a battery and other electric components. Using less powerful and therefore smaller motors could not only reduce the overall weight

of the prosthesis but also enable the integration of a smaller and lighter battery. For this purpose, calculations and experiments could be carried out to find out how much power is required for the motors to carry out everyday tasks. Another possible improvement would be the relocation of the motors into the hand, thereby freeing up space within the arm. Integrating sensory feedback into the fingers would enable interactions with the environment, and could therefore substantially improve the acceptance and usability of the prosthesis. One potential approach is using the InMoov Hand i02 [64], which not only includes recesses for tactile feedback sensors but also a holder for motors inside the hand.

Ways to optimize thumb movement could be further investigated, particularly implementing a combination of flexion and adduction to increase grip strength and offer finer grip movements. The prosthetic hands Dextrus [7] and Dextra [84] each have an additional motor inside the hand to enable this combined movement. It could be tested whether a thumb movement, with an additional motor providing it two DOFs, is necessary for daily activities. Another potential improvement could be replacing fishing lines with springs to provide more consistent tension and flexibility, as springs maintain their tension over time. In future work also robust testing procedures could be conducted to ensure that the prosthesis can withstand everyday use and provide reliable performance.

The printing time of the prosthesis could be further reduced by using higher quality printers, adjusting the wall thickness or material, or pre-production of certain parts, as only the suspension of the residual limb needs to be customized. The printing time could also be further reduced by using additional printers. In future, the Raspberry Pi could be set up in advance, which would reduce the production time. The cost could be reduced by using less powerful motors that are sufficient for everyday use or by developing a processor specifically tailored to the requirements, as not every feature from the Raspberry Pi is necessary.

Different machine learning models could be evaluated in the future regarding their performance and adaptability, with a focus on determining which model is most effective at differentiating gestures. The LR classifier could be tested first, as it is already implemented in the CLS. To ensure its applicability, the LR classifier's code would need to be modified so that five classes can be trained. Alternatively, a cut-off could be implemented. This would allow only the gestures to be executed if the recognition confidence exceeds a certain percentage threshold. The first option is preferable because it would

not require changes to the MATLAB script controlling the motors, and the effort to add an additional class to the LR classifier is likely less.
A cut-off could also be implemented in the LDA classifier, which is already in use, to prevent the machine learning model from reverting to classes 3 or 4 when transitioning to the resting state. A threshold of around 5 % could be set, as this reversion occurs only for a very short duration.

To determine whether intuitive or predefined gestures should be used for implementing wrist rotation, a one-to-one comparison, where the same machine learning model is used, could be conducted. Intuitive gestures like pronation and supination used in this work could be compared with wrist flexion and wrist extension used in the studies by S. Said et al. [75] or K. Avilés-Mendoza et al. [40]. This could provide additional insight into the differences in accuracy and effectiveness regarding the recognition of different gestures.

Although the M. biceps brachii is the strongest supinator, it is currently not recorded with the MyoBand. In future work, this muscle could be recorded using an additional sensor on the upper arm and potentially used to better classify supination. It could also be investigated whether the M. pronator teres, responsible for pronation, and the M. supinator, responsible for supination, were optimally recorded to ensure that the classification is carried out correctly. The muscles originate very close to the crook of the arm. Therefore, the MyoBand could pick up stronger signals when placed closer to the crook of the arm. This could lead to a more precise classification of the rotation movement.

Future adaptations in the control software could enable independent control of several DOFs simultaneously. One approach would be to train two separate machine learning models for each DOF. One machine learning model would be used to recognizing either the opening or closing movements, while the other model would focus on identifying supination or pronation movements. Based on these recognitions, the first machine learning model would control motors 1-3 to execute the opening or closing movements of the prosthesis. Concurrently, the second machine learning model would control only the wrist motor, enabling simultaneous control of the prosthesis movements. With this approach, each machine learning model is only required to distinguish between two gestures (or three, if relaxation is considered a gesture) rather than recognizing two classes simultaneously or detecting combinations of different gestures with a single machine learning model. This simplifies the classification task for each machine learning model. However, it should be noted that the muscle movement may appear different if two gestures are

performed simultaneously. Therefore, the recording of gesture combinations would be essential for training each machine learning model.

Additionally, investigating the influence of different arm positions on prosthesis control could be a focus in future projects. In this regard, determining optimal training methods for various arm positions is important to achieve a high level of accuracy and reliable gesture execution. In addition, future work could consider other gripping movements. Implementing movements such as the pinch grip is feasible, as additional motors for the index finger and thumb are already integrated. One approach could involve replacing the flexion gesture with a pinch grip by controlling only the motors for the index finger and thumb rather than activating all motors. Another approach would be to add an additional class to the LDA classifier and train it with the new gesture.

In the future, the control software could be adapted in order to run independently on the Raspberry Pi, eliminating the need for an additional computer for execution. Either the block integrating the MyoBand could be reprogrammed so that it can run on the Raspberry Pi independently, or the entire control software could be completely written in another programming language, such as Python, so that it is compatible with Linux. A different programming language would also avoid the compatibility problems caused by the fact that CLS was written for an older version of Windows. However, since the MyoBand is no longer in production, an alternative for the sensor should also be considered in the future.

The prosthesis could be tested with limb-impaired individuals in the future. These tests could include a larger number of subjects to fully validate the functionality and usability of the prosthesis. Individuals with congenital limb loss could also be examined to study how their muscles movement is, as they never performed these gestures with their limb. However, many people with congenital limb loss often do not use prostheses, as they have learned to perform tasks effectively without them [60]. It is also essential to consider session- and subject-dependencies in future research. This will help assess whether the LDA classifier can reliably process data from different people and sessions, and accurately recognize gestures in different sessions. To evaluate these dependencies, the developed calibration program could be tested and modified as needed. It is essential to verify whether the implemented MVC normalization is effective and ensures that the data can be used across different subjects.

# 6 Conclusion

A major challenge in the field of prosthetics lies in the development of cost-effective, functional prostheses that are accessible to a broader population and can be produced in short time. This master's thesis aimed to develop a 3D-printed myoelectric arm prosthesis with integrated intuitive control for hand opening and closing movements as well as wrist rotation. This objective was successfully achieved, with adding a proportional control based on muscle contraction intensity. Compared to previous studies, this work succeeded in enabling intuitive rotation control without relying on predefined gestures, thereby advancing the research of M. Hussein et al. [59] and K. Avilés-Mendoza et al. [40]. As the applied LDA classifier can only recognize a single class at a time, it was not possible to control the rotational movement, and opening and closing of the hand simultaneously. Consequently, only a sequential control of hand opening and closing movements, and rotation was possible.

A functional design of a 3D-printed arm prosthesis was developed by adjusting the InMoov robotic arm model [63]. The adjustment included arranging additional space for the residual limb within the prosthesis and implementing attachments for secure fitting. Hardware components, including a Raspberry Pi, a PCA96895, and four servo motors, were thoroughly selected to form the control system. A recording program was implemented to record five gestures: flexion, extension, pronation, supination, and relaxation. Subsequently, a controlling program was implemented to control a virtual prosthesis using a LDA classifier, and a third program allowed to use the data across different subjects through a MVC normalization method.

Initially, the control system was evaluated in a virtual environment, where it demonstrated that EMG sensors and RMS signal processing could effectively differentiate between various gestures. Subsequently, pilot testing confirmed that these gestures could be successfully used to control the hardware. Pilot testing the hardware revealed that arm positions influenced the accuracy of the trained model. For instance, a flexed elbow

resulted in lower accuracy of the LDA classifier's gesture recognition compared to a suspended arm. This discrepancy can be attributed to muscle strain during arm bending. In comparison, studies by S. Said et al. [75] and K. Avilés-Mendoza et al. [40] demonstrated that factors such as data set size, number of electrodes used, and type of gesture substantial impact the accuracy of LDA classifier's gesture recognition. Particularly, the rotation gestures (pronation and supination) were often misclassified as each other, indicating that the muscle movements for these two gestures are similar or involve similar muscles.

Several challenges and limitations were encountered during the project, mainly related to software compatibility and real-time operation. The incompatibility of the MyoBand with Linux and the need to run the control software on an external Windows computer made it difficult to implement real-time control and to conduct complexer tests. Due to the effort required to conduct tests with limb-impaired individuals exceeding that of a master's thesis, these tests were not carried out. Consequently, the control system's everyday applicability and comfort design aspects could not be validated. Although the design modifications allowed the 3D model to be used as a prosthesis, limited space within the arm prevented the integration of the electronic components. Additionally, due to the size of the motors, it was not possible to scale the arm down sufficiently to fit smaller individuals. Consequently, the prosthesis is currently more suitable for larger individuals with the present design.

The results of this master's thesis indicate that 3D-printed prothesis with integrated intuitive control are the enabling technology to provide advanced, cost-effective, and broadly accessible solutions for limb-impaired individuals. The insights gained and the challenges encountered pave the way for future studies to develop prosthetic technologies to enhance the individuals' quality of life.

Future work could focus on redesigning the prosthesis to enhance its applicability and functionality, by creating a more reliable thumb movement and using springs for a tighter finger movement. Key areas for improvement the design include integrating motors into the hand to increase space for the residual limb and making the prosthesis scalable for smaller individuals or children. It is recommended to migrate the control software to a compatible framework, such as Python, to enable real-time, stand-alone applications on the Raspberry Pi. Furthermore, adapting the existing CLS to achieve compatibility with the Raspberry Pi could be an interesting aspect to explore.
Further research could investigate enhancing intuitive control by considering other ma-

chine learning algorithms, such as the LR classifier, to determine the most suitable approach for gesture recognition. A comparative study of predefined gestures versus intuitive control could provide valuable insights into which gestures should be implemented to achieve high accuracy and a good user experience. To achieve simultaneous control of multiple DOFs, two separate machine learning models could be trained to recognize each DOF independently.
Testing with limb-impaired individuals could be conducted to assess the design and control system and to identify necessary adjustments for everyday use, thereby maximizing user experience.

# Bibliography

[1] *144W Universal Einstellbares Netzteil Adapter 100V-240V AC to DC 3V-24V 6A Konverter Netzteil,Einstellbarer Netzadapter mit 14 Tipps & Polaritätskabel-6A Max.* Amazon. https://www.amazon.de/Universal-Einstellbares-Einstellbarer-Netzadapter-Polarit%C3%A4tskabel-6A/dp/B0C53QP1SY. – Accessed: 2024-03-17 [Online]

[2] *3D-printable Open-source Bionic Arm.* HACKberry. https://www.exiii-hackberry.com/. – Accessed: 2024-03-15 [Online]

[3] *Accuracy, precision, and recall in multi-class classification.* EVIDENTLY AI. https://www.evidentlyai.com/classification-metrics/multi-class-metrics. – Accessed: 2024-06-16 [Online]

[4] *Amplitude Analysis: Normalization of EMG to Maximum Voluntary Contraction (MVC).* DELSYS. https://delsys.com/emgworks-analysis-techniques-using-emgscript/. – Accessed: 2024-05-10 [Online]

[5] *DAS MYO VON THALMIC LABS IM VERGLEICH ZUM KINEMIC BAND.* Kinemic. https://kinemic.com/de/band/kinemic-band-im-vergleich/thalmic-labs-myo-kinemic-band/. – Accessed: 2024-02-02 [Online]

[6] *DEBO MOTODRIVER4 Entwicklerboards - Servotreiber, 16 Kanal, 12 Bit, PCA9685.* Reichelt. https://www.reichelt.de/entwicklerboards-servotreiber-16-kanal-12-bit-pca9685-debo-motodriver4-p235525.html. – Accessed: 2024-03-15 [Online]

[7] *Dextrus V1.1 Robotic Hand.* AUTODESK Instructables. https://www.instructables.com/Dextrus-v11-Robotic-Hand/. – Accessed: 2024-03-15 [Online]

[8] *diymore 6 Stück digitaler Servomotor 13KG*. Amazon. https://www.amazon.de/Female-Female-Male-Female-Male-Male-Steckbr%C3%BCcken-Drahtbr%C3%BCcken-bunt/dp/B01EV70C78?language=en_GB&currency=EUR. – Accessed: 2024-03-15 [Online]

[9] *ELEGOO Jumper Wire 40x 20cm, Male-Female, Kabel Steckbrücken 28AWG Drahtbrücken für Arduino (3er Set)*. Amazon. https://www.amazon.de/-/en/dp/B09KZRPJ41/ref=twister_B0BM51BGSH?_encoding=UTF8&psc=1. – Accessed: 2024-03-15 [Online]

[10] *Erster Druck mit PrusaSlicer*. Prusa Research. https://help.prusa3d.com/de/article/erster-druck-mit-prusaslicer_1753. – Accessed: 2024-02-02 [Online]

[11] *Gripping force calculation for parallel grippers*. PR – Intelligente Peripherien für Roboter GmbH. https://en.iprworldwide.com/calculation-of-gripping-force/. – Accessed: 2024-03-15 [Online]

[12] *HACKberry HANDBOOK*. Mission ARM Japan. https://www.exiii-hackberry.com/_files/ugd/5b7df8_9e8ac5e0c4604273b8f7c87dc82ebe04.pdf. – Accessed: 2024-03-15 [Online]

[13] *Hand and Forarm assembly 3D views*. InMoov. https://inmoov.fr/build-yours/hand-and-forarm-assembly-3d-views/. – Accessed: 2023-11-15 [Online]

[14] *HERCULES Super Cast 100 m - 2000 m Yards Braided Fishing Line 10 lb - 300 lb Test for Saltwater Freshwater PE Braid Fish Wire Superline 8 Strands*. Amazon. https://www.amazon.de/HERCULES-Super-Cast-100m-Geflochtene/dp/B0791F5XJG?th=1&psc=1. – Accessed: 2024-06-30 [Online]

[15] *Linear Interpolation Formula*. CUEMATH. https://www.cuemath.com/linear-interpolation-formula/. – Accessed: 2024-06-26 [Online]

[16] *MATLAB*. MathWorks. https://de.mathworks.com/products/matlab.html. – Accessed: 2024-02-02 [Online]

[17] *Mehrere Servo Motoren gleichzeitig per Raspberry Pi steuern (PCA9685)*. Tutorials for Raspberry Pi. https://tutorials-raspberrypi.de/mehrere-servo-

motoren-steuern-raspberry-pi-pca9685/. – Accessed: 2024-04-22 [Online]

[18] *MG996R 55g Metal Gear Torque Digital Servo 15KG For RC Helicopter Car Robot*. Diymore. https://www.diymore.cc/products/diymore-mg996r-metal-gear-high-speed-torque-servo-motor-digital-servo-55g-for-rc-helicopter-airplane-car-boat-robot-controls. – Accessed: 2024-03-15 [Online]

[19] *Michelangelo Hand*. Ottobock. https://www.ottobock.com/de-de/product/8E500. – Accessed: 2024-03-15 [Online]

[20] *Original Prusa i3 MK3S+ 3D-Drucker*. Prusa Research. https://www.prusa3d.com/de/produkt/original-prusa-i3-mk3s-3d-drucker/#downloads. – Accessed: 2024-02-02 [Online]

[21] *Prothetik für die obere Extremität – Armprothesen und Handprothesen*. Friedrich Georg Streifeneder KG. https://www.streifeneder.de/armprothetik. – Accessed: 2023-11-23 [Online]

[22] *PrusaSlicer 2.7.1*. Prusa Research. https://www.prusa3d.com/de/page/prusaslicer_424/. – Accessed: 2024-02-02 [Online]

[23] *Raspberry Pi® 3 B+ 1 GB 4 x 1.4 GHz Raspberry Pi®*. Conrad. https://www.conrad.de/de/p/raspberry-pi-3-b-1-gb-4-x-1-4-ghz-raspberry-pi-1668026.html?hk=SEM&WT.mc_id=google_pla&gclid=Cj0KCQjwqP2pBhDMARIsAJQ0Czog_DCx6rCh86U0adKiNmaFvbbMol_ZCh4HuavGnUDKsHBovHu99vEaAujXEALw_wcB&refresh=true. – Accessed: 2024-03-15 [Online]

[24] *Raspberry Pi® RPI-12.5 USB-MB Steckernetzteil, Festspannung Passend für (Entwicklungskits): Raspberry Pi Ausgangsstrom (*. Conrad. https://www.conrad.de/de/p/raspberry-pi-rpi-12-5-usb-mb-steckernetzteil-festspannung-passend-fuer-entwicklungskits-raspberry-pi-ausgangsstrom-2483210.html. – Accessed: 2024-03-15 [Online]

[25] *Raspberry Pi Support from MATLAB*. MathWorks. https://de.mathworks.com/hardware-support/raspberry-pi-matlab.html. – Accessed: 2024-02-02 [Online]

[26] *Raspberry Pi Support from Simulink*. MathWorks. https://de.mathworks.com/hardware-support/raspberry-pi-simulink.html. – Accessed: 2024-02-02 [Online]

[27] *sourcing map Dowel Pin 304 Stainless Steel Pegs Support Shelves Silver Tone 4 mm x 50 mm Pack of 10*. Amazon. https://www.amazon.de/-/en/sourcing-Stainless-Support-Shelves-Silver/dp/B07NYP9FKD. – Accessed: 2024-06-30 [Online]

[28] *Trilancer Webbing straps with Velcro fasteners, 3 sizes (61/46/30 cm x 5 cm), elastic straps, Velcro straps and packing straps for organising your extension cables, hoses, bicycle, workshop, garage*. Amazon. https://www.amazon.de/-/en/Trilancer-fasteners-organising-extension-workshop/dp/B09T5YDMTR. – Accessed: 2024-06-30 [Online]

[29] *Der ultimative Leitfaden für den lebensmittelechten 3D-Druck: Behördliche Vorgaben, Technologien, Materialien und mehr*. Formlabs. https://formlabs.com/de/blog/leitfaden-lebensmittelechtheit-3d-druck/. – Accessed: 2024-02-02 [Online]

[30] *Why You Don't Want Your Arms at 90 Degrees at a Standing Desk*. QuittingSitting. https://quittingsitting.com/dont-want-arms-90-degrees-standing-desk/. – Accessed: 2024-06-05 [Online]

[31] *Standards for Prosthetics and orthotics Part 1: Standards*. World Health Organization, 2017. – URL https://iris.who.int/bitstream/handle/10665/259209/9789241512480-part1-eng.pdf?isAllowed=y&&sequence=1. – ISBN 978-92-4-151248-0

[32] *Feature Space*. University of Twente - Faculty ITC. https://ltb.itc.utwente.nl/498/concept/81578. 2020. – Accessed: 2024-06-19 [Online]

[33] *3D Printing in Prosthetics: History, Benefits, and Materials*. Xometry. https://www.xometry.com/resources/3d-printing/3d-printing-in-prosthetics/. 2022. – Accessed: 2024-02-02 [Online]

[34] *What Is Electromyography (EMG)?* TMSi. https://info.tmsi.com/blog/what-is-emg#:~:text=A%20measure%20often%20used%20in,muscle%20or%20group%20of%20muscles.&text=The%20MVC%20is%20used%

20to,provides%20a%20physiological%20reference%20point. 2022. – Accessed: 2024-06-19 [Online]

[35] *Raspberry Pi 3 Model B+*. Raspberry Pi Ltd. https://datasheets.raspberrypi.com/rpi3/raspberry-pi-3-b-plus-product-brief.pdf?_gl=1*6uoixd*_ga*OTQ3NTIwNjAyLjE3MTAzNDk0MTY.*_ga_22FD70LWDS*MTcxMDM0OTQxNS4xLjAuMTcxMDM0OTQxNS4wLjAuMA.. 2023. – Accessed: 2024-03-13 [Online]

[36] *What is linear discriminant analysis (LDA)?* IBM. https://www.ibm.com/topics/linear-discriminant-analysis. 2023. – Accessed: 2024-05-10 [Online]

[37] *Lineare Regression*. DATAtab e.U. https://datatab.de/tutorial/lineare-regression. 2024. – Accessed: 2024-05-10 [Online]

[38] Artal-Sevil, J. S. ; Acón, A. ; Montañés, J. L. ; Domínguez, J. A.: Design of a Low-Cost Robotic Arm controlled by Surface EMG Sensors. In: *XIII Technologies Applied to Electronics Teaching Conference (TAEE)* (2018). – URL https://doi.org/10.1109/TAEE.2018.8476126

[39] Aumüller, Gerhard A. ; Aust, Gabriela ; Conrad, Arne ; Engele, Jürgen ; Kirsch, Joachim ; Maio, Giovanni ; Mayerhofer, Artur ; Mense, Siegfried ; Reissig, Dieter ; Salvetter, Jürgen ; Schmidt, Wolfgang ; Schmitz, Frank ; Schulte, Erik ; Spanel-Borowski, Katharina ; Wennemuth, Gunther ; Wolff, Werner ; Wurzinger, Laurenz J.: *Duale Reihe Anatomie*. Thieme, 2020. – URL https://doi.org/10.1055/b-007-170976

[40] Avilés-Mendoza, Karla ; Gaibor-León, Neil G. ; Asanza, Víctor ; Lorente-Leyva, Leandro L. ; Peluffo-Ordóñez, Diego H.: A 3D Printed, Bionic Hand Powered by EMG Signals and Controlled by an Online Neural Network. In: *Biomimetics* (2023). – URL https://doi.org/10.3390/biomimetics8020255

[41] Bauer, Alexander: *Druckdauer 3D Druck: Wie lange dauert ein Ausdruck und warum?* AB3D. https://www.ab3d.at/druckdauer-3d-druck-wie-lange-dauert-ein-ausdruck-und-warum/. 2024. – Accessed: 2023-11-26 [Online]

[42] Beetz, Matthias: *Grundlagen: Der Servomotor – Funktionsweise, Kühlung und Anwendungsgebiete.* Baumüller Nürnberg GmbH. https://www.baumueller.com/de/insights/grundlagen/servomotor-funktionsweise-eigenschaften-anwendungsgebiete#:~:text=Der%20Servoantrieb%20bietet%20vor%20allem,Abbremsungen%20auf%20bestimmte%20Drehzahlen%20durchf%C3%BChren.. – Accessed: 2024-03-17 [Online]

[43] Bertram, Boris: *Allgemein - Was ist das?* Armprothetik.Info. https://armprothetik.info/?prothetik. – Accessed: 2023-11-26 [Online]

[44] Biggs, John: *Two Makers Come Together To Make A Robotic Hand For A Boy In South Africa.* TechCrunch. https://techcrunch.com/2013/02/04/two-global-makers-come-together-to-make-a-robotic-han-for-a-boy-in-south-africa/. 2013. – Accessed: 2024-02-09 [Online]

[45] Blough, David K. ; Hubbard, Sharon ; McFarland, Lynne V. ; Smith, Douglas G. ; Gambel, Jeffrey M. ; Reiber, Gayle E.: Prosthetic cost projections for servicemembers with major limb loss from Vietnam and OIF/OEF. In: *Journal of Rehabilitation Research & Development (JRRD)* (2010). – URL https://doi.org/10.1682/jrrd.2009.04.0037

[46] Bolic, Miodrag: *Pervasive Cardiovascular and Respiratory Monitoring Devices: Model-Based Design.* Academic Press, 2023. – URL https://doi.org/10.1016/C2019-0-00743-1. – ISBN 978-0-12-820947-9

[47] Carolo, Lucas: *3D Printer Material Cost in 2023.* All3DP. https://all3dp.com/2/3d-printer-material-cost-the-real-cost-of-3d-printing-materials/#google_vignette. 2023. – Accessed: 2023-11-19 [Online]

[48] Choi, Seoyoung ; Cho, Wonwoo ; Kim, Keehoon: Restoring natural upper limb movement through a wrist prosthetic module for partial hand amputees. In: *Journal of NeuroEngineering and Rehabilitation* (2023). – URL https://doi.org/10.1186/s12984-023-01259-9

[49] Coldewey, Devin: *5-year-old gets 3-D printed 'Robohand' from Internet collaborators.* NBC NEWS. https://www.nbcnews.com/tech/tech-news/5-year-old-gets-3-d-printed-robohand-internet-collaborators-flna1b8242915. 2013. – Accessed: 2024-02-09 [Online]

[50] Dosen, Strahinja ; Markovic, Marko ; Hartmann, Cornelia ; Farina, Dario: Sensory Feedback in Prosthetics: A Standardized Test Bench for Closed-Loop Control. In: *IEEE Transactions on Neural Systems and Rehabilitation Engineering* 23 (2015). – URL https://doi.org/10.1109/TNSRE.2014.2371238

[51] Dr. McGimpsey, Grant ; Bradford, Terry C.: Limb Prosthetics Services and Devices Critical Unmet Need: Market Analysis. In: *Bioengineering Institute Center for Neuroprosthetics Worcester Polytechnic Institution*. – URL https://www.nist.gov/system/files/documents/2017/04/28/239_limb_prosthetics_services_devices.pdf

[52] Earl, Bill: *Adafruit PCA9685 16-Channel Servo Driver*. Adafruit Industries. https://cdn-learn.adafruit.com/downloads/pdf/16-channel-pwm-servo-driver.pdf. 2024. – Accessed: 2024-03-15 [Online]

[53] Freitag, Regina: *Gangrän*. DRACO. https://www.draco.de/gangraen/#:~:text=Eine%20Gangr%C3%A4n%20bezeichnet%20man%20auch,peripheren%20arteriellen%20Verschlusskrankheit%20(pAVK). 2024. – Accessed: 2024-03-04 [Online]

[54] Gallagher, Sean: *Robohand: How cheap 3D printers built a replacement hand for a five-year old boy*. Ars Technica. https://arstechnica.com/information-technology/2013/02/robohand-how-cheap-3d-printers-built-a-replacement-hand-for-a-five-year-old-boy/. 2013. – Accessed: 2024-02-25 [Online]

[55] Gorski, Filip ; Suszek, Ewa ; Wichniarek, Radoslaw ; Kuczko, Wieslaw ; Zukowska, Magdalena: Rapid Manufacturing of Individualized Prosthetic Sockets. In: *Advances in Science and Technology Research Journal* (2020). – URL https://doi.org/10.12913/22998624/113425. – ISSN 2080-4075

[56] Gretsch, Kendall F. ; Lather, Henry D. ; Peddada, Kranti V. ; Deeken, Corey R. ; Wall, Lindley B. ; Goldfarb, Charles A.: Development of novel 3D-printed robotic prosthetic for transradial amputees. In: *The International Society for Prosthetics and Orthotics* (2015). – URL https://doi.org/10.1177/0309364615579317. – ISSN 1746-1553

[57] Hagedorn-Hansen, Devon ; Oosthuizen, G. A. ; Gerhold, Tristan: Resource-Efficient process chains to manufacture patient-specific prosthetic fingers. In: *The*

*South African Journal of Industrial Engineering* (2016). – URL https://doi.org/10.7166/27-1-1279

[58] Hussaini, Ali ; Hill, Wendy ; Kyberd, Peter: Clinical evaluation of the refined clothespin relocation test: A pilot study. In: *Prosthetics and Orthotics International* (2019). – URL https://doi.org/10.1177/0309364619843779

[59] Hussein, Mahdi E. ; Brooker, Graham M. ; Hussein, Mahdi J.: 3D Printed Myoelectric Prosthetic Arm. (2014). – URL https://static1.squarespace.com/static/5fdf30e82dcd53187f20b7f4/t/5fe09c7ef5f64226567c5b9e/1608555676841/Low+Cost+Prosthetic+Arm+Thesis.pdf

[60] James, Michelle A. ; Bagley, Anita M. ; Brasington, Katherine ; Lutz, Cheryl ; McConnell, Sharon ; Molitor, Fred: Impact of prostheses on function and quality of life for children with unilateral congenital below-the-elbow deficiency. In: *J Bone Joint Surg Am* (2006). – URL https://doi.org/10.2106/JBJS.E.01146

[61] Kallenberg, Laura A. ; Hermens, Hermie J.: Behaviour of motor unit action potential rate, estimated from surface EMG, as a measure of muscle activation level. In: *Journal of NeuroEngineering and Rehabilitation* (2006). – URL https://doi.org/10.1186/1743-0003-3-15

[62] Kushki, Yusof: *CRITICAL TIMES FOR INDUCTION MOTORS: The starting time and The stalling time.* Linkedin. https://www.linkedin.com/pulse/critical-times-induction-motors-starting-time-stalling-yusof-kushki/?articleId=6691273980512366592. 2020. – Accessed: 2024-03-14 [Online]

[63] Langevin, Gael: *Hand and Forarm.* InMoov. https://inmoov.fr/hand-and-forarm/. – Accessed: 2023-11-15 [Online]

[64] Langevin, Gael: *The new InMoov Hand is here!* InMoov. https://inmoov.fr/inmoov-hand/. 2020. – Accessed: 2024-06-21 [Online]

[65] Lehmann, Isabelle ; Kraxner, Markus: Das grobe Geschick - Block and Box Test. In: *Physiopraxis - Das Fachmagazin für Physiotherapie* (2017). – URL https://www.thieme-connect.com/products/ejournals/pdf/10.1055/s-0043-113982.pdf

[66] Markovic, Marko: *mmarkov87/CLS*. MathWorks. https://de.mathworks.com/matlabcentral/fileexchange/64273-mmarkov87-cls. 2017. – Accessed: 2024-03-13 [Online]

[67] Mathiowetz, Virgil ; Volland, Gloria ; Kashman, Nancy ; Weber, Karen: Adult Norms for the Box and Block Test of Manual Dexterity. In: *The American Journal of Occupational Therapy* (1985). – URL https://doi.org/10.5014/ajot.39.6.386

[68] Niethard, Fritz U. ; Pfeil, Joachim ; Biberthaler, Peter: *Duale Reihe Orthopädie und Unfallchirurgie*. Thieme, 2022. – URL https://doi.org/10.1055/b000000573

[69] P., Regina: *Was ist ein G-Code und welche Rolle spielt dieser für den 3D-Druck?* 3Dnatives. https://www.3dnatives.com/de/was-ist-ein-g-code-3d-druck-290920211/#! 2021. – Accessed: 2024-02-02 [Online]

[70] Prof. Dr. Wurzinger, Laurenz J.: *Handgelenke*. Thieme via medici. https://viamedici.thieme.de/lernmodul/554586/529603/handgelenke#n5b9adf1ca3f041f0. 2019. – Accessed: 2024-02-25 [Online]

[71] Prof. Dr. Wurzinger, Laurenz J.: *Unterarmmuskulatur*. Thieme via medici. https://viamedici.thieme.de/lernmodul/554595/529604/unterarmmuskulatur#_A76654B6_01CA_43F0_AE22_7EDEF7EEFD3A. 2019. – Accessed: 2024-02-25 [Online]

[72] Prof. Dr. Wurzinger, Laurenz J.: *Bewegungsapparat im Überblick*. Thieme via medici. https://viamedici.thieme.de/lernmodul/554476/528713/bewegungsapparat+im+%C3%BCberblick#section_zl5_cbl_mjb_20191023171226565. 2022. – Accessed: 2024-02-25 [Online]

[73] Rosestein, Niklas: *myo-python 1.0.5*. Python Software Foundation. https://pypi.org/project/myo-python/. 2021. – Accessed: 2024-06-26 [Online]

[74] Rudder, J.: *What is the Lifespan of Prosthetics?* Medical Center Orthotics & Prosthetics. https://opcenters.com/what-is-the-lifespan-of-prosthetics/. 2023. – Accessed: 2024-02-02 [Online]

[75] Said, Sherif ; Boulkaibet, Ilyas ; Sheikh, Murtaza ; Karar, Abdullah S. ; Alkork, Samer ; Nait-Ali, Amine: Machine-Learning-Based Muscle Control of a

3D-Printed Bionic Arm. In: *Sensors (Basel)* (2020). – URL https://doi.org/10.3390/s20113144

[76] Schünke, Michael ; Schulte, Erik ; Schumacher, Udo ; Voll, Markus V. ; Wesker, Karl H.: *Prometheus LernAtlas - Allgemeine Anatomie und Bewegungssystem*. Thieme, 2022. – URL https://doi.org/10.1055/b000000613

[77] Simons, M.: *Ada V1.1 - Datasheet*. openbionics. https://static1.squarespace.com/static/56376cfde4b078ea32822fff/t/5739983122482e97a8563a0d/1463392308072/Ada_v1_1_Datasheet.pdf. 2017. – Accessed: 2023-11-15 [Online]

[78] Simons, M.: *Brunel V1.0 - Datasheet*. openbionics. https://static1.squarespace.com/static/56376cfde4b078ea32822fff/t/5b39eed11ae6cf7909b8a51c/1530523347117/Brunel%2BV.10%2BDatasheet.pdf. 2017. – Accessed: 2023-11-15 [Online]

[79] Stokosa, Jan J.: *Limb Prostheses Options*. MSD Manual. https://www.msdmanuals.com/home/special-subjects/limb-prosthetics/limb-prostheses-options. 2024. – Accessed: 2023-07-01 [Online]

[80] Tkach, Dennis ; Huang, He ; Kuiken, Todd A.: Study of stability of time-domain features for electromyographic pattern recognition. In: *Journal of NeuroEngineering and Rehabilitation* (2010). – URL https://doi.org/10.1186/1743-0003-7-21

[81] Toledo-Pérez, D. C. ; Rodríguez-Reséndiz, J. ; Gómez-Loenzo, R. A.: A Study of Computing Zero Crossing Methods and an Improved Proposal for EMG Signals. In: *IEEE Access* (2020). – URL https://doi.org/10.1109/ACCESS.2020.2964678

[82] Valdez, Jonathan ; Becker, Jared: *Understanding the $I^2C$ Bus*. Texas Instruments. https://www.ti.com/lit/an/slva704/slva704.pdf?ts=1714930951605&ref_url=https%253A%252F%252Fwww.google.com%252F. 2015. – Accessed: 2023-05-06 [Online]

[83] VanZandt, Paul: *Was ist ein UML-Diagramm? Definition, Anwendungsfälle und deren Umsetzung*. Ideascale. https://ideascale.com/de/der-blog/uml-diagramm-definition/. 2022. – Accessed: 2024-06-06 [Online]

[84] Villoslada, Alvaro: *Dextra Open-source myoelectric hand prothesis*. AUTODESK Instructables. https://hackaday.io/project/9890-dextra. 2016. – Accessed: 2024-03-15 [Online]

[85] Wetsch, Wolfgang A. ; Hinkelbein, Jochen ; Spöhr, Fabian: *Kurzlehrbuch Anästhesie, Intensivmedizin, Notfallmedizin und Schmerztherapie*. Thieme, 2018. – URL https://doi.org/10.1055/b-006-149436

[86] Xen, Shido: *Hand and Forarm*. InMoov. https://inmoov.fr/wp-content/uploads/2021/01/Forearm.png#main. 2021. – Accessed: 2024-03-18 [Online]

[87] Zhang, Daniel: *Hauptfunktionen und Vorteile von Servomotoren*. STEPPERONLINE. https://www.omc-stepperonline.com/de/support/hauptfunktionen-und-vorteile-von-servomotoren. – Accessed: 2024-03-17 [Online]

[88] Zuniga, Jorge M. ; Young, Keaton J. ; Peck, Jean L. ; Srivastava, Rakesh ; Pierce, James E. ; Dudley, Drew R. ; Salazar, David A. ; Bergmann, Jeroen: Remote fitting procedures for upper limb 3d printed prostheses. In: *Expert Rev Med Devices* (2019). – URL https://doi.org/10.1080/17434440.2019.1572506

# A Appendix

## A.1 Cost of the Prosthesis

Table A.1: Total cost of the constructed prosthesis. The MyoBand is not included as it is no longer available for purchase and was only provided for the purposes of this master's thesis.

| **Required component** | **Selected component** | **Price** |
|---|---|---|
| Servomotors | Diymore servomotor 13 kg (Pack of 6) [8] | 31.99 € |
| Cables | ELEGOO Jumper Wire [9] | 5.94 € |
| Fishing line | Hercules Supercast 10lb/0.12mm/100m [14] | 11.64 € |
| Bolts | Sourcing map 3.5 x 20 mm Dowel Pins 304 Stainless Steel [27] | 9.99 € |
| Elastic cable ties | Trilancer Webbing straps with Velcro fasteners, 3 sizes (61/46/30 cm x 5 cm) [28] | 8.49 € |
| Power supply unit servomotors | Towisituati 144W Universal Adjustable Power Supply Adapter 100V-240V AC to DC 3V-24V [1] | 35.99 € |
| Motor driver | Adafruit PCA9685 16-Channel Servo Driver [6] | 18.80 € |
| Microcontroller | Raspberry Pi 3B+ [23] | 59.99 € |
| Power supply unit Microcontroller | Raspberry Pi 15.3W USB-C Power Supply [24] | 9.49 € |
| Prosthesis | PLA printing of the prosthesis parts | 23.00 € |
| **Total** | | **215.32 €** |

## A.2 Ethics Approval and Related Documents

# Antrag auf Stellungnahme der HAW-Ethikkommission zu einem Forschungsvorhaben

## Hinweise

Zeitpunkt der Antragstellung:
Grundsätzlich prüft die Ethikkommission nur Anträge, die VOR Beginn der Forschungsarbeiten gestellt werden. Anträge, die nachträglich eingereicht werden, können nicht berücksichtigt werden.

Formales:
Bitte reichen Sie den Antrag nach Möglichkeit mit allen Anlagen als ein PDF-Dokument. Bei einer Überarbeitung/Ergänzung kennzeichnen Sie die geänderten Stellen gegenüber der Vorversion bitte farblich.

Vollständige Unterlagen:
Ein positives Ethikvotum zu einem Forschungsvorhaben setzt eine vollständige Vorlage von Fragebögen, Einverständniserklärungen, Leitfäden etc. voraus. Falls diese Vorlage bei Antragstellung noch nicht möglich ist, sollte dies begründet und die Unterlagen als Ergänzung entsprechend zeitnah nachgereicht werden. Bis zur vollständigen Vorlage kann ein positives Votum unter Vorbehalt ausgesprochen werden.

Zweitvoten:
Unter der Voraussetzung, dass bei bereits vorliegendem positiven Erstvotum einer anderen Ethikkommission ein Zweitvotum von der Ethikkommission der HAW Hamburg begründetermaßen erwünscht wird, kann ein solches Zweitvoten angefertigt werden.

Folgeforschung / neue Forschungsfragen:
Die ethische Bewertung neuer Forschungsfragen, welche im Verlauf des Forschungsprozesses auftreten können und zu entsprechender Folgeforschung führen, muss von den Forschenden beantragt werden. Das Bewertungsergebnis kann anschließend durch eine Ergänzung im Ausgangsantrag in das bereits vorliegende positive Votum integriert werden.

**Gesetzliche Bestimmungen:**
Anträge, die unter die gesetzlichen Bestimmungen der § 40 Abs. 1 Arzneimittelgesetz (AMG), § 20 Abs. 1 Medizinproduktegesetz (MPG) oder § 8 / § 9 Stammzellgesetz (StZG) fallen, sind an die dafür gesetzlich vorgesehenen Ethikkommissionen zu richten. Weiterhin können standesrechtliche Bestimmungen für verschiedene Berufsgruppen, wie zum Beispiel Ärzte, weitere Vorschriften und Zuständigkeiten festlegen.

## Antrag auf Stellungnahme der HAW-Ethikkommission zu einem Forschungsvorhaben

### Antragstellerin/Antragsteller[1]

Name: Lara Borsdorf
Fakultät und Department: Faculty of Life Science/Medizintechnik
ggf. Competence Center oder Forschungs- und Transferzentrum:
Position: Master Student
[redacted]

### Bei Qualifikationsarbeiten[2]:

Namen der betreuenden Professor*innen: Prof. Dr. Meike Wilke
Fakultät und Department: Faculty of Life Science/Medizintechnik
ggf. Competence Center oder Forschungs- und Transferzentrum:
Position: Professorin für Mathematik und Informatik
Anschrift: Ulmenliet 20, 21033 Hamburg
[redacted]

*Kurztitel (Akronym) des Forschungsvorhabens (maximal 50 Zeichen):*

*Titel des Forschungsvorhabens: Design and Implementation of a 3D Printed Arm Prosthetic with a Rotational Wrist Joint Controlled by EMG*

*Datum des Antrags: 19.09.2023*

[1] Die/der Antragsteller*in sollte auch die/der verantwortliche Forscher*in (Projektleiter*in) sein.
[2] Zum Beispiel Promotion, Masterthesis, Bachelorthesis

## 1. Allgemeine Angaben

*Handelt es sich bei dem Forschungsvorhaben[3] um…*

Primärforschung ☒
Sekundärforschung ☐

eine Qualifikationsarbeit ☐

Anderes ☐ bitte erläutern:

Klicken oder tippen Sie hier, um Text einzugeben.

*Wurde das geplante Forschungsvorhaben bereits bei einer anderen Ethikkommission eingereicht?*

*Nein* ☒ *Ja* ☐

Falls ja, wann und wo?[4]

Klicken oder tippen Sie hier, um Text einzugeben.

*Wurde das Vorhaben von der o.g. Kommission befürwortet? (bitte eine Kopie der Stellungnahme beifügen)*
*Nein* ☐ *Ja* ☐

Ggf. Kommentar:

Klicken oder tippen Sie hier, um Text einzugeben.

*Ist das hier beantragte Forschungsvorhaben eine Teilstudie im Rahmen eines umfangreicheren Forschungsprojekts?*

*Nein* ☒ *das Forschungsvorhaben ist eine eigenständige Studie*
*Ja* ☐ *das Forschungsvorhaben ist eine Teilstudie im Rahmen des folgenden Projekts*
*Titel des übergeordneten Projekts:*

_____

*Falls ja, erläutern Sie bitte das übergeordnete Gesamtprojekt und die Rolle der Teilstudie:*

Klicken oder tippen Sie hier, um Text einzugeben.

**Weitere Information:**

Ein positives Ethikvotum zu einem Forschungsvorhaben setzt eine vollständige Vorlage von Fragebögen, Einverständniserklärungen, Leitfäden etc. voraus. Falls diese Vorlage bei Antragstellung noch nicht möglich ist, sollte dies begründet und die Unterlagen als Ergänzung entsprechend zeitnah nachgereicht werden. Bis zur vollständigen Vorlage kann ein positives Votum unter Vorbehalt ausgesprochen werden.

[3] Die Begriffe Forschungsvorhaben, Forschungsprojekt und Studie werden hier synonym gebraucht.
[4] Studien die derzeit von einer anderen deutschen Ethikkommission begutachtet werden, werden von der HAW Ethikkommission erst nach Abschluss des anderen Verfahrens geprüft.

## Fragestellung/Zielsetzung, Rahmen und Methodik des Forschungsvorhabens

*Beschreiben Sie Fragestellung bzw. Zielsetzung des Forschungsvorhabens, die wissenschaftliche Rechtfertigung (theoretischer Rahmen, Relevanz)[5], Design und vorgesehene Methodik (möglichst nicht mehr 1000 Worte; bitte verweisen Sie hierbei nicht auf andere umfangreichere Dokumente; Literaturverzeichnis bitte unter dem entsprechenden Punkt am Ende des Antrags einfügen)[6]*

Laut der WHO hat nur einer von zehn Menschen, die eine Prothese benötigen, Zugang zu einer solchen [1]. Prothesen für die oberen Gliedmaßen kosten zwischen 40.000 € und 60.000 € [2] und können je nach Typ zwischen Wochen und Monaten in der Herstellung benötigen [3]. Es ist daher von großer Bedeutung, kostengünstige Prothesen zu entwickeln, die für jeden zugänglich sind. Gleichzeitig sollten Übergangslösungen angeboten werden, um die Zeiten bis zur Fertigstellung komplexer Prothesen zu überbrücken.

Eine erfolgsversprechende Lösung für dieses Problem können 3D-gedruckte Prothesen sein. Es gibt bereits Forschungen in diesem Bereich und auch Versuche an Patient*innen, in denen 3D-gedruckte Prothesen angewendet wurden. In einigen Experimenten konnten diese mit Hilfe eines MyoBandes über EMG-Signale der Armmuskulatur gesteuert werden [4].

Der Vorteil einer 3D-gedruckten Prothese liegt darin, dass diese schneller produziert werden kann, da die Herstellung der mechanischen Teile im 3D-Drucker vergleichsweise wenig Zeit in Anspruch nimmt. Die Druckzeit der Teile hängt von den Einstellungen des Druckers ab, wie beispielsweise den Durchmesser der Düse, der Schichthöhe oder auch des Füllgrades. Ebenfalls ist sie vom Material des Filamentes abhängig. So dauert zum Beispiel der Druck eines Kalibrierungswürfels mit einer Größe von 20x20x20 mm ungefähr 30 Minuten, wenn eine 0,4 mm Düse, 0,2 mm Schichthöhe und ein Füllgrad von 20% verwendet wird [8]. Die Prothese besteht aus vielen kleinen und teilweise hohlen Einzelteilen. Die Druckzeit kann also weiter optimiert werden, wenn mehrere Drucker gleichzeitig verwendet werden. Ebenfalls sind die Kosten im Vergleich zu herkömmlichen Prothesen erheblich geringer. Betrachtet man beispielsweise die 3D-gedruckte Prothese aus der Arbeit von S. Said et al. „Machine-Learning-Based Muscle Control of a 3D-Printed Bionic Arm“, belaufen sich die Kosten auf ca. 300 € [4].

Das Hauptziel dieser Arbeit ist es eine 3D-gedruckte Handprothese zu entwickeln und diese mithilfe eines MyoBandes zu steuern. Im Rahmen dieser Masterarbeit werden zunächst die Einzelteile der Handprothese mithilfe eines 3D-Druckers gefertigt. Als Vorlage kann zum Beispiel der Roboterarm Inmoove [5] dienen, der entsprechend angepasst wird, damit dieser als Prothese verwendet werden kann. Im Gegensatz zu bisherigen 3D-gedruckten Handprothesen wird diese Prothese auch mit einem rotierenden Handgelenk ausgestattet, um eine höhere Funktionalität bieten zu können. Dies ist in dem Bereich der 3D-gedruckten Handprothesen bislang nicht umgesetzt worden und ermöglicht somit mehr Freiheitsgrade. Das gibt den Patient*innen mehr Freiheiten und schützt vor Haltungsschäden.
Eine zusätzliche Vorrichtung am hinteren Ende der Prothese wird es ermöglichen, diese sicher am Arm zu befestigen.
Die 3D-gedruckten Teile sollen aus Kunststoffen wie PLA und ABS gedruckt werden. PLA sowie einige Marken von ABS gelten als lebensmittelecht. Das bedeutet, dass diese

[5] In Leitlinie 9 der „Leitlinien zur Sicherung guter wissenschaftlicher Praxis. Kodex“ der DFG heißt es dazu: Wissenschaftlerinnen und Wissenschaftler berücksichtigen bei der Planung eines Vorhabens den aktuellen Forschungsstand umfassend und erkennen ihn an. Die Identifikation relevanter und geeigneter Forschungsfragen setzt sorgfältige Recherche nach bereits öffentlich zugänglich gemachten Forschungsleistungen voraus.

[6] Die Darstellung soll es ermöglichen, dass sich die Mitglieder der Ethikkommission ein ausreichend klares Bild über das Forschungsvorhaben machen können, um dieses zu bewerten. Die Darstellung sollte auch für wissenschaftliche gebildete Menschen verständlich sein, die nicht auf dem speziellen Fachgebiet des Forschungsvorhabens tätig sind.

Materialien mit Lebensmitteln in Berührung kommen können und dadurch kein Lebensmittelrisiko entsteht [7].
Nach dem Druck erfolgt der Zusammenbau und die Integration der elektrischen Komponenten, die die Steuerung der Prothese ermöglichen sollen. Jeder Finger der Prothese wird mit einem Schrittmotor ausgestattet, um eine individuelle Ansteuerung zu ermöglichen. Zudem wird ein weiterer Motor für das Handgelenk eingebaut. Die Motoren werden über Leitungen mit einem Mikrocontroller verbunden. Versorgt werden die elektrischen Bauteile der Prothese mit einer Batterie.
Die elektrischen Bauteile arbeiten im Bereich der Sicherheits-Kleinspannung. In Deutschland ist diese bei 50 V Wechselspannung und 120 V Gleichspannung festgelegt. Bei Geräten mit einer Sicherheits-Kleinspannung müssen metallische Gehäuse nicht geerdet werden. Bei medizinischen Geräten hingegen dürfen nach dem Medizinproduktegesetz Werte von 25 V Wechselstrom und 60 V Gleichstrom nicht überschritten werden. Diese Spannungen gelten für Tiere und Kinder als ungefährlich, auf einen Schutz kann also komplett verzichtet werden [6]. Obwohl die genannten Werte in den verwendeten Bauteilen nicht überschritten werden, wird die Prothese so aufgebaut, dass kein direkter Kontakt zwischen Patient*innen und elektrischen Bauteilen besteht. Ebenfalls sind die 3D-gedruckten Teile der Prothese aus Kunststoff, also nichtleitend.
In einem weiteren Schritt werden mithilfe eines MyoBandes EMG-Signale der Armmuskulatur erfasst. Dabei werden über 8 Kanäle insgesamt 8 Signale aufgezeichnet. Diese Signale werden für verschiedene Hand- und Handgelenksgesten aufgenommen. Anschließend wird ein Programm entwickelt, das diese Signale verarbeitet und analysiert. Auf dieser Grundlage sollen Muster in den Signalen gefunden und somit die verschiedenen Gesten erkannt werden. Dieses Programm wird unter Verwendung von MATLAB und Simulink entwickelt. Mithilfe dieses Programmes und des MyoBandes soll die Prothese dann in Echtzeit gesteuert werden. Zunächst werden die Signale zur Überprüfung an uns selbst aufgenommen und mit unseren Armen getestet. Dabei wird die Prothese auf den Tisch gelegt und lediglich das MyoBand an einen unserer Arme angelegt. Um die Funktionalität weiter zu validieren, erfolgt schließlich ein Test an bis zu zehn Patientinnen/ Patienten mit amputierten Arm. Dabei wird ebenfalls der Tragekomfort und die Alltagstauglichkeit getestet.

*Wurde die wissenschaftliche Qualität des Forschungsvorhabens durch eine/n Dritte/n überprüft?*

| | |
|---|---|
| *Unabhängige externe Überprüfung* | ☐ |
| *Überprüfung innerhalb eines Unternehmens* | ☐ |
| *Überprüfung innerhalb einer multizentrischen oder interdisziplinären Forschergruppe* | ☐ |
| *Überprüfung durch die hauptverantwortliche Institution oder Gastinstitution* | ☐ |
| *Überprüfung innerhalb des Forschungsteams* | ☐ |
| *Überprüfung durch eine Betreuerin bzw. einen Betreuer* | ☒ |
| *Keine Überprüfung durch Dritte* | ☐ |
| *Anderes (bitte erläutern)* | ☐ |

Klicken oder tippen Sie hier, um Text einzugeben.

## 2. Forschung an und mit Menschen

*Sind in dem Forschungsprojekt Menschen als Teilnehmende beteiligt?*[7]

Nein ☐ weiter mit Punkt 3.
Ja ☒

*Wie werden die potenziell Teilnehmenden ausgesucht? Benennen Sie Einschluss- und Ausschlusskriterien.*

*Bei den Teilnehmenden handelt es sich im ersten Schritt um die Experimentatoren, im zweiten dann um Personen, welche eine Amputation oberhalb des Handgelenkes haben. Dies ist wichtig, da es sich bei der Prothese um eine Prothese mit Handgelenk handelt. Außerdem muss die Amputation der Personen unterhalb des Ellbogens erfolgt sein (transradial), da es sich um eine Unterarmprothese handelt und diese über den Ellbogen an den Arm des Teilnehmenden befestigt wird.*

*Wie werden die potenziell Teilnehmenden angesprochen (Anwerbung)?*

*Betroffene werden per Aushang oder Pressemitteilung oder auch auf Grund der bestehenden Forschungszusammenarbeit mit Dr. Jennifer Ernst am NIFE in Hannover (https://nife-hannover.de/category/aktuelles/) rekrutiert. Die Personen werden gefragt, ob sie im Rahmen einer Masterarbeit eine 3D-gedruckte Handprothese testen wollen. Dabei wird ihnen erklärt, dass diese mithilfe von EMG-Signalen, also ihrer Muskelbewegung im Arm, gesteuert wird.*

*Wie werden die potenziell Teilnehmenden in die Studie aufgenommen (siehe auch „Einverständnis einholen" in Punkt 2.1.)*

*Mithilfe eines schriftlichen Formulars, welche vor dem Teilnehmen ausgefüllt werden muss.*

*Ist für Anwerbung und Aufnahme in die Studie die Zusammenarbeit mit anderen Institutionen/Partnern erforderlich?*

Nein ☐
Ja ☒ falls ja, bitte erläutern Sie dies näher.

*Evtl. werden Betroffene wie oben beschrieben oben Dr. Ernst vom NIFE rekrutiert.*

## 2.1 Einwilligung

*Werden Daten über Personen erhoben, ohne dass diese wissen, dass Daten oder Informationen über sie erhoben werden?*

*Nein* ☒

[7] In Anlage 2 (Ethikkommission an der HAW Hamburg) der Satzung zur Sicherung guter wissenschaftlicher Praxis an der HAW Hamburg wird ausdrücklich betont, dass »ethische Standards des humanen Umgangs, der Würde, der Selbstbestimmung und Autonomie des Menschen« zur berücksichtigen sind. Zur näheren Ausgestaltung sei auf die Deklaration von Helsinki verwiesen, die sich zwar auf medizinische Forschung bezieht, aber soweit möglich analog bei Forschung an und/oder mit Menschen anzuwenden ist. Insbesondere die Prinzipien der Privatsphäre und Vertraulichkeit (Ziffer 24) und der informierten Einwilligung (Ziffern 25 bis 32) sind zu berücksichtigen.

*Ja* ☐ falls ja, wodurch ist das gerechtfertigt?

Klicken oder tippen Sie hier, um Text einzugeben.

*Liegt eine freiwillige, informierte Einwilligung[8] zur Studienteilnahme vor?*

*Ja* ☒ bitte fügen Sie die Studieninformation und die Einwilligungserklärung in der Anlage bei.

*Nein* ☐ falls nein, legen Sie bitte die genauen Gründe dafür dar.

Klicken oder tippen Sie hier, um Text einzugeben.

In welcher Form erfolgt eine Aufklärung der Teilnehmenden über das Forschungsvorhaben? Werden außer des Aufklärungs-/Informationsbogens noch andere Arten der Aufklärung (z.B. Videos, interaktive Medien) genutzt? *Eine Kopie des Aufklärungs-/Informationsbogens oder andere geeignete Belege sind diesem Antrag beizufügen.*

Potentielle Teilnehmende werden telefonisch über die Details der Studie informiert. Bei Interesse folgt dann eine Demo vor Ort. Dabei wird Ihnen die 3D gedruckte Prothese gezeigt sowie Videos, wie diese gesteuert wird. Die Videos zeigen die Prothese wie sie von uns Experimentatoren gesteuert wird. Währenddessen liegt diese auf einem Tisch.

*Wird nach erfolgter Aufklärung eine schriftliche Einverständniserklärung der an der Studie Teilnehmenden eingeholt?*

*Ja* ☒ falls ja, beschreiben Sie bitte folgende Aspekte: Wer holt die Einverständniserklärung wann und wie ein?

*Nachdem die Prothese und das Video gezeigt wurden, wird die Einverständniserklärung von einem der Experimentatoren eingeholt.*

*Nein* ☐ sollte keine Einverständniserklärung der an der Studie Teilnehmenden eingeholt werden, legen Sie hierfür bitte den genauen Grund dar.

Klicken oder tippen Sie hier, um Text einzugeben.

*Wo und wie werden die Einverständniserklärungen aufbewahrt? Wie ist die Vertraulichkeit gewährleistet? Wer trägt die Verantwortung dafür, dass die Erklärungen nach spätestens 10 Jahren datenschutzkonform vernichtet/gelöscht werden[9]?*

Die Einverständniserklärungen werden in einem abgeschlossenen Schrank von Prof. M. Wilke an der HAW aufbewahrt. Wir sind verantwortlich, sie nach spätestens 10 Jahren datenschutzkonform zu vernichten.

[8] m Sinne der Grundsätze 25-32 der Deklaration von Helsinki des Weltärztebundes: https://www.bundesaerztekammer.de/fileadmin/user_upload/downloads/pdf-Ordner/International/Deklaration_von_Helsinki_2013_20190905.pdf

[9] Nach den Erläuterungen zu Leitlinie 17 der „Leitlinien zur Sicherung guter wissenschaftlicher Praxis. Kodex“ der DFG werden Forschungsdaten »in der Regel für einen Zeitraum von zehn Jahren zugänglich und nachvollziehbar in der Einrichtung, wo sie entstanden sind, oder in standortübergreifenden Repositorien aufbewahrt.

*Wie viel Zeit steht den potenziell Teilnehmenden zur Verfügung, über ihre Teilnahme/Nicht-Teilnahme an der Studie zu entscheiden?*

Teilnehmende haben nach der ersten Information mindestens eine Woche Zeit, um sich zu entscheiden.

*Werden die Teilnehmenden darüber informiert, dass sie jederzeit (ohne Nachteile) die Teilnahme verweigern bzw. von der Studie zurücktreten können (bis zum Zeitpunkt der Anonymisierung der Daten)?*

*Nein* ☐
*Ja* ☒

*Werden Anreize finanzieller oder anderer Art an die Proband*innen gezahlt?*

*Nein* ☐
*Ja* ☒ falls ja, spezifizieren Sie bitte die Art und Höhe der Zahlungen

Teilnehme (außer den Experimentatoren) werden mit 13 Euro pro Stunde vergütet als Aufwandsentschädigung. Bei Betroffenen wird auch die Anreise bezahlt.

## 2.2 Vulnerable Gruppen

*Sind im Forschungsvorhaben Versuchspersonen involviert, die nicht in der Lage sind, eine informierte Einwilligung[10] zu geben?*

*Nein* ☒

*Ja* ☐ falls ja, Zutreffendes bitte markieren

*Handelt es sich um Kinder/Minderjährige?* ☐

*Handelt es sich um Patient*innen in ärztlicher oder medizinischer Behandlung?* ☐

*Erwachsene, die bewusstlos oder schwer krank sind* ☐

*Erwachsene mit unheilbaren Erkrankungen* ☐

*Erwachsene in Notfallsituationen* ☐

*Erwachsene mit psychischen Erkrankungen* ☐

*Erwachsene mit Demenz* ☐

Welche präventiven Maßnahmen werden Sie ergreifen, um den größtmöglichen Schutz der Personen zu gewährleisten? (Bitte detailliert darlegen)

Klicken oder tippen Sie hier, um Text einzugeben.

[10] Vergl. Anmerkung 8 oder weitere Ergänzung durch https://www.forschungsdaten-bildung.de/einwilligung

*Liegen im Forschungsvorhaben Umstände vor, durch die eine Verweigerung der Teilnahme erschwert wird (z.B. Abhängigkeitsverhältnisse, auch wenn potenziell an der Studie Teilnehmende zugleich Studierende der/des Forschenden sind)?*

*Nein* ☒

*Ja* ☐ falls ja, erläutern Sie bitte die Gründe, die eine Verweigerung erschweren können und wie Sie damit umgehen wollen.

Klicken oder tippen Sie hier, um Text einzugeben.

## 2.3 Forschungsprozess

*Werden in Gesprächen, Interviews oder Fragebögen des Forschungsvorhabens Themen angesprochen, die sensibel, peinlich oder übergriffig sind oder als stigmatisierend wahrgenommen werden können? (Bitte fügen Sie den Fragebogen/Interviewleitfaden oder Ähnliches als Anlage bei[11])*

*Nein* ☒

*Ja* ☐ falls ja, bitte erläutern Sie dies näher und erläutern Sie, wodurch dies gerechtfertigt ist und wie damit umgegangen wird.

Klicken oder tippen Sie hier, um Text einzugeben.

*Können im Rahmen des Forschungsvorhabens möglicherweise kriminelle oder andere Taten offenkundig werden, die entsprechende Maßnahmen erfordern (z.B. Untersuchung auf Drogenkonsum)?*

*Nein* ☒

*Ja* ☐ falls ja, bitte erläutern Sie das näher und erläutern Sie wodurch ist das gerechtfertigt ist und wie damit umgegangen wird?

Klicken oder tippen Sie hier, um Text einzugeben.

*Ist das Forschungsvorhaben mit körperlichen Eingriffen (invasiven Verfahren) an den Studienteilnehmer*innen verbunden?*

*Nein* ☒

*Ja* ☐ falls ja, welche Maßnahmen werden zum Schutz und zur Sicherheit der Teilnehmenden getroffen? Besteht eine ausreichende Qualifikation zur Durchführung?

*Klicken oder tippen Sie hier, um Text einzugeben.*

[11] Sofern der endgültige Fragebogen/Interviewleitfaden erst im weiteren Verlauf des Forschungsvorhabens entsteht, ist dieser rechtzeitig vor Beginn der Datenerhebung der Ethikkommission zur ergänzenden Begutachtung vorzulegen.

*Können durch die Befragung / die Untersuchung körperliche, psychische oder soziale Schädigungen (z.B. Traumata) auftreten?*

*Nein* ☒

*Ja* ☐ falls ja, womit ist zu rechnen und wie verfahren Sie damit? (Gibt es z.B. Nachbetreuung?)

Klicken oder tippen Sie hier, um Text einzugeben.

*Beinhaltet die Forschung eine Täuschung bezüglich der Ziele oder Absichten?*

*Nein* ☒

*Ja* ☐ falls ja, werden die Teilnehmenden hierüber aufgeklärt? Wann? Wie? Von wem?

*Klicken oder tippen Sie hier, um Text einzugeben.*

## 2.4 Forschungsdaten von Menschen

*Dürfen die gesammelten Daten laut geltendem Datenschutzrecht genutzt werden? Bitte erläutern Sie auf welcher Grundlage.*

Die Nutzung gesammelter Daten soll durch die Berücksichtigung datenschutzrechtlicher Grundprinzipien, das Einholen informierter Einwilligungen, der Anonymisierung anfallender Forschungsdaten und der sicheren Aufbewahrung der Daten ermöglicht werden. Es werden lediglich Alter, Geschlecht sowie Zeitraum seit Amputation der Personen innerhalb der Arbeit verwendet, sodass diese nicht identifiziert werden können. Es werden keine Bilder verwendet, mit denen die Person identifiziert werden könnten, ausschließlich ein Bild wie die Prothese am Arm verwendet wird. Das Gesicht ist nicht zu sehen. Sollte es allerdings Auffälligkeiten am Arm selbst geben (Tattoos, besondere Narbenbildung, etc.), könnte der Arm dadurch evtl. erkannt werden. Diese werden dann retuschiert, um diesem vorzubeugen.

*Werden in Ihrem Forschungsvorhaben personenbezogene Daten aus eigenen oder fremden Quellen erhoben, gespeichert oder verarbeitet, die nicht anonymisiert[12] sind?*

*Nein* ☒ weiter mit Punkt 3.

*Ja* ☐

[12] Für eine Einschätzung, ob es sich um ein datenschutzrelevantes Vorhaben handelt, sollte die DSGVO beachtet werden. Es findet sich dort keine Definition von **Anonymisierung**, es gibt hierzu lediglich Hinweise: „Die Grundsätze des Datenschutzes sollten […] nicht für anonyme Informationen gelten, d.h. für Informationen, die sich nicht auf eine identifizierte oder identifizierbare natürliche Person beziehen, oder personenbezogene Daten, die in einer Weise anonymisiert worden sind, dass die betroffene Person nicht oder nicht mehr identifiziert werden kann."(Erwägungsgrund 26 DSGVO)
**Pseudonymisierung** ist die Verarbeitung personenbezogener Daten in einer Weise, dass die personenbezogenen Daten ohne Hinzuziehung zusätzlicher Informationen nicht mehr einer spezifischen betroffenen Person zugeordnet werden können, sofern diese zusätzlichen Informationen gesondert aufbewahrt werden und technischen und organisatorischen Maßnahmen unterliegen, die gewährleisten, dass die personenbezogenen Daten nicht einer identifizierten oder identifizierbaren natürlichen Person zugewiesen werden (Art 4 DSGVO).

*Werden die Proband*innen über Ihre Rechte zum Datenschutz aufgeklärt? (bitte Beleg beifügen)*

Klicken oder tippen Sie hier, um Text einzugeben.

*Wo, wie und von wem werden die personenbezogenen Daten gespeichert und verarbeitet? Wer hat Zugang zu diesen Daten? An wen werden eventuell welche personenbezogenen Daten weitergegeben?*

*Klicken oder tippen Sie hier, um Text einzugeben.*

*Bei Kooperationen: durch welche vertraglichen Vereinbarungen wird die Einhaltung der datenschutzrechtlichen Bestimmungen gewährleistet?*

Klicken oder tippen Sie hier, um Text einzugeben.

*Welche Maßnahmen werden angewendet, um die Vertraulichkeit der persönlichen Daten zu gewährleisten? Beschreiben Sie bitte, ob eine Pseudonymisierung (Kodierliste) oder andere Form der Anonymisierung vorgenommen werden, und wenn ja, welche und in welchem Stadium.*

Klicken oder tippen Sie hier, um Text einzugeben.

*Wer ist für die Einhaltung der Vertraulichkeit verantwortlich?*

Klicken oder tippen Sie hier, um Text einzugeben.

*Wann werden personenbezogene Daten gelöscht oder anonymisiert (ggf. wie erfolgt die Anonymisierung)? Wer trägt dafür die Verantwortung und wie wird die Löschung oder Anonymisierung sichergestellt?*

Klicken oder tippen Sie hier, um Text einzugeben.

*Wird eine Nachnutzung der Daten für andere Zwecke geplant (z.B. Open Data)? Wenn ja, für welchen Nutzerkreis? Wie wird der Zugang geregelt? Welche Vorkehrungen werden gegen eine Deanonymisierung getroffen? Wie wird darüber in der Einverständniserklärung aufgeklärt?*

Klicken oder tippen Sie hier, um Text einzugeben.

## 3. Forschung an und mit menschlichen Zellen / Gewebe [13]

*Planen Sie mit menschlichen Zellen oder Gewebe zu forschen?*

*Nein* ☒

*Ja* ☐ falls ja, aufgrund welcher ethischen Abwägung ist diese Forschung gerechtfertigt? Bitte erläutern Sie ggf. rechtliche Aspekte (z.B. Richtlinie 2004 /23/EG).

Klicken oder tippen Sie hier, um Text einzugeben.

[13] Die Ethikkommission behält sich vor, auf die Zuständigkeit einer anderer Ethikkommission zu verweisen.

## 4. Forschung an und mit menschlichen Embryonen / Föten [14]

*Planen Sie an menschlichen embryonalen Stammzellen zu forschen?*

*Nein* ☒

*Ja* ☐ falls ja, bitte erläutern Sie auf welcher Rechtsgrundlage dies zulässig ist? Aufgrund welcher ethischen Abwägungen ist diese Forschung gerechtfertigt?

Klicken oder tippen Sie hier, um Text einzugeben.

[14] Die Ethikkommission behält sich vor, auf die Zuständigkeit einer anderer Ethikkommission zu verweisen.

## 5. Nachhaltigkeit

*Sind durch das Forschungsvorhaben und die damit gesetzten Ziele Konflikte mit Nachhaltigkeit absehbar (insbesondere im Kontext der Nachhaltigkeitsziele der Vereinten Nationen oder des Übereinkommens von Paris)?*

*Nein* ☒

*Ja* ☐ falls ja, bitte erläutern Sie dies genauer. Beschreiben Sie auch, wie Sie mit diesen Konflikten umgehen wollen.

Klicken oder tippen Sie hier, um Text einzugeben.

## 6. Menschenrechte

*Sind durch das Forschungsvorhaben und die damit gesetzten Ziele Konflikte mit Menschenrechten absehbar?*

*Nein* ☒

*Ja* ☐ falls ja, bitte erläutern Sie dies genauer. Beschreiben Sie auch, wie Sie mit diesen Konflikten umgehen wollen.

Klicken oder tippen Sie hier, um Text einzugeben.

## 7. Umweltschutz und Ökologie

*Sind durch das Forschungsvorhaben und die damit gesetzten Zielen Konflikte mit Umwelt- und/oder Klimaschutz absehbar (insbesondere im Kontext der Nachhaltigkeitsziele der Vereinten Nationen oder des Übereinkommens von Paris)?*

*Nein* ☒

*Ja* ☐ falls ja, bitte erläutern Sie dies genauer. Beschreiben Sie auch, wie Sie mit diesen Konflikten umgehen wollen.

Klicken oder tippen Sie hier, um Text einzugeben.

*Beinhaltet das Forschungsvorhaben Elemente, welche die Umwelt, Tiere oder Pflanzen beeinträchtigen?*

*Nein* ☒

*Ja* ☐ falls ja, bitte erläutern Sie dies genauer. Stellen Sie dar, warum dies gerechtfertigt ist und welche Schutzmaßnahmen Sie vorsehen.

Klicken oder tippen Sie hier, um Text einzugeben.

*Planen Sie an oder mit geschützten Arten zu forschen?*

*Nein* ☒

*Ja* ☐ falls ja, bitte erläutern Sie dies genauer. Stellen Sie dar, warum dies gerechtfertigt ist, auf welcher Rechtsgrundlage dies zulässig ist und welche Schutzmaßnahmen Sie vorsehen. Sind dafür weitere Genehmigungen notwendig?

Klicken oder tippen Sie hier, um Text einzugeben.

## 8. Technikfolgeabschätzung

*Planen Sie neue Technologien zu entwickeln oder bestehende weiterzuentwickeln?*

*Nein* ☒

*Ja* ☐ *falls ja, bitte beschreiben Sie Ihrer Einschätzung nach relevante Felder, in denen Ihr Forschungsvorhaben Auswirkungen haben könnte. Hierfür können Sie sich beispielsweise an folgenden Beschreibungsperspektiven orientieren: (insgesamt* ***maximal*** *750 Wörter)*

- Juristische Aspekte (z.B. tierschutzrechtliche Aspekte)
- Ökonomische Aspekte (z.B. Geschäftsmodelle)
- Gesellschaftliche Aspekte (z.B. Einfluss auf Sozialstrukturen / politische Folgen)
- Ökologische Aspekte (z.B. Einfluss auf Umweltfaktoren)
- Technikethische Dimension (z.B. Daten-, Medien- oder Maschinenethik)
- Interaktionen zwischen den genannten Dimensionen

Klicken oder tippen Sie hier, um Text einzugeben.

Falls es Ihrer Einschätzung nach mögliche gesellschaftliche Konfliktfelder im Hinblick auf die Akzeptanz der Ergebnisse Ihres Forschungsvorhabens geben sollte, beschreiben Sie diese bitte kurz:

Klicken oder tippen Sie hier, um Text einzugeben.

## 9. Autonome Technologien und Künstliche Intelligenz

*Beinhaltet oder entwickelt das Forschungsvorhaben Technologien, von denen zu erwarten ist, dass sie die ethischen Prinzipien der Achtung der menschlichen Autonomie, Schadensverhütung, Fairness und Erklärbarkeit[15] verletzen können?*

*Nein* ☒

*Ja* ☐ falls ja, bitte erläutern Sie dies genauer. Stellen Sie dar, warum dies gerechtfertigt ist und welche Schutzmaßnahmen Sie dafür vorsehen. Wie ist die Verantwortung für die Folgen der Anwendung geklärt?

Klicken oder tippen Sie hier, um Text einzugeben.

*Beinhaltet oder entwickelt das Forschungsvorhaben Technologien (in Hardware oder Software), von denen zu erwarten ist, dass sie ethisch relevante Entscheidungsunterstützung oder -vorbereitung zur Aufgabe haben, bzw. die künftig ethisch relevante Entscheidungen treffen könnten bzw. sollen?*

*Nein* ☒ weiter mit Frage 10.

*Ja* ☐ falls ja, bitte erläutern Sie dies genauer.

Klicken oder tippen Sie hier, um Text einzugeben.

*Wie ist die Verantwortung für die Folgen der Anwendung geklärt?*

Klicken oder tippen Sie hier, um Text einzugeben.

*Auf welcher Datengrundlage werden die o.g. Entscheidung vorbereitet und/oder getroffen? Wie wird gewährleistet, dass die Entscheidungsfindung gerecht, fair und nicht-diskriminierend stattfindet.*

Klicken oder tippen Sie hier, um Text einzugeben.

[15] insbesondere im Hinblick auf: • Vorrang menschlichen Handelns und menschliche Aufsicht • Technische Robustheit und Sicherheit • Datenschutz und Datenqualitätsmanagement • Transparenz • Vielfalt, Nichtdiskriminierung und Fairness • Gesellschaftliches und ökologisches Wohlergehen • Rechenschaftspflicht.
https://www.demographie-netzwerk.de/site/assets/files/5064/ethicsguidelinesfortrustworthyai-depdf.pdf

## 10. Forschung in Länder mit niedrigem und mittlerem Einkommen

*Werden für das Forschungsvorhaben Ressourcen aus Ländern mit niedrigem oder mittlerem Einkommen genutzt?*

*Nein* ☒

*Ja* ☐ falls ja, wie ist ein Benefit-Ausgleich eingeplant?

Klicken oder tippen Sie hier, um Text einzugeben.

*Werden bei dem Forschungsvorhaben Daten in Ländern mit niedrigem oder mittlerem Einkommen erhoben?*

*Nein* ☒

*Ja* ☐ falls ja, wie wird den betroffenen Ländern Zugang zu den Daten und Forschungsergebnissen gewährt?

Klicken oder tippen Sie hier, um Text einzugeben.

## 11. Dual-Use[16]

*Gibt es Bedenken oder eine nicht nur geringe Wahrscheinlichkeit, dass die Forschungsergebnisse für militärische Zwecke genutzt werden können?*

*Nein* ☒ weiter mit Frage 12.

*Ja* ☐ falls ja, bitte erläutern Sie dies genauer.

Klicken oder tippen Sie hier, um Text einzugeben.

*Welche Vorkehrungen werden gegen eine militärische Nutzung getroffen?*

Klicken oder tippen Sie hier, um Text einzugeben.

*Beinhaltet das Forschungsvorhaben Dual-Use-Güter (Güter mit doppeltem Verwendungszweck gemäß EG-Verordnung 428/2009, d.h. Güter, die einschließlich Datenverarbeitungsprogramme und Technologie sowohl für zivile als auch für militärische Zwecke verwendet werden können)?*

*Nein* ☒ weiter mit Punk12.

*Ja* ☐ falls ja, bitte erläutern Sie dies genauer.

Klicken oder tippen Sie hier, um Text einzugeben.

*Wie ist die Verantwortung für die Folgen der Anwendung geklärt? Bitte erläutern Sie dies kurz.*

Klicken oder tippen Sie hier, um Text einzugeben.

[16] In der Präambel der Grundordnung der HAW heißt es hierzu: „Die HAW Hamburg sieht sich in der Verpflichtung, in ihrem wissenschaftlichen und didaktischen Wirken und Verwaltungshandeln gesellschaftliche Verantwortung zu übernehmen und sich in Lehre, Forschung und Weiterbildung nachhaltig für die friedliche soziale, gerechte, demokratische, politische, technische, ökologische und ökonomische Entwicklung der Gesellschaft einzusetzen.
Forschung, Lehre und Studium an der HAW Hamburg sind friedlichen Zielen verpflichtet und sollen zivile Zwecke erfüllen; die Forschung, insbesondere die Entwicklung und Optimierung technischer Systeme, sowie Studium und Lehre sind auf eine zivile Verwendung ausgerichtet.“

## 12. Missbrauch von Forschungsergebnissen

Hat Ihre Forschung ein Potenzial für den Missbrauch von Forschungsergebnissen[17]?

*Nein* ☒ weiter mit Frage 13.

*Ja* ☐ falls ja, bitte erläutern Sie dies genauer.

Klicken oder tippen Sie hier, um Text einzugeben.

*Welche Vorkehrungen werden gegen einen Missbrauch von Forschungsergebnissen getroffen?*

Klicken oder tippen Sie hier, um Text einzugeben.

[17] Z.B.: Könnten die Materialien / Methoden / Technologien und das Wissen, das oder die erzeugt wurden, Menschen, Tieren, Pflanzen oder der Umwelt schaden, wenn sie verändert oder weiterentwickelt werden?

## 13. Durchführung des Projekts

*Wo findet das Forschungsprojekt statt? (Setting, Ort)*

Fakultät Life Sciences oder Fakultät TI, HAW Hamburg; ansonsten zu Hause bzw. im Alltag der PatientInnen

*Wer trägt die Kosten des Forschungsprojektes?*

Die Hochschule für Angewandte Wissenschaften Hamburg, Fakultät Life Science.

*Bitte legen Sie alle potenziellen Interessenkonflikte dar, die sich für das Projekt, die Projektverantwortlichen und Projektbeteiligten ergeben könnten.*

Klicken oder tippen Sie hier, um Text einzugeben.

*Bitte legen Sie alle weiteren möglichen ethisch zu berücksichtigenden Aspekte dar, von denen das Beratungsgremium Kenntnis haben sollte.*

Klicken oder tippen Sie hier, um Text einzugeben.

*Wie ist die Veröffentlichung der Forschungsergebnisse geplant? Werden Forschungsdaten aus dem Projekt für weitere Nutzung zur Verfügung gestellt, ggf. welche Lizenz ist hierfür angedacht?*

Angedacht ist idealerweise eine Publikation in einem wissenschaftlichen peer-reviewed Journal, wahrscheinlicher aber erstmal ein kleinerer Vortrag, z.B. auf der Hamburger Studierendentagung

## 12. Verzeichnis der Anlagen

Welche Anlagen/Dokumente sind dem Antrag beigefügt?

| | |
|---|---|
| Informationsmaterial / Broschüren etc. für mögliche Studienteilnehmende | ☐ |
| Einwilligungserklärung für die Teilnehmenden | ☒ |
| Datenschutzerklärung | ☐ |
| Anschreiben an die Teilnehmenden | ☐ |
| Anschreiben an die Eltern / Erziehungsberechtigten etc. | ☐ |
| Bewilligungsschreiben des Ethikkomitees oder andere Genehmigungsschreiben | ☐ bitte benennen: Klicken oder tippen Sie hier, um Text einzugeben. |
| Kopie des Studienprotokolls | ☐ |
| Andere relevante Dokumente | ☒ bitte benennen: Patienteninformation |

## 13. Unterschriften

- Die Angaben in diesem Antrag habe ich nach bestem Wissen und Gewissen korrekt angeführt.
- Ich versichere, dass mit den Forschungsarbeiten, die Gegenstand dieses Antrags sind, noch nicht begonnen wurde.
- Änderungen oder Ergänzungen zu diesem Antrag werde ich der Ethikkommission rechtzeitig zur Kenntnis und/oder Begutachtung vorlegen.
- Im Fall einer Publikation der Forschungsergebnisse werde ich der Ethikkommission eine elektronische Kopie der Publikation unter Angabe der Vorgangsnummer zeitnah zukommen lassen (gilt nicht für Qualifikationsarbeiten)[18].

Unterschrift des/der hauptverantwortlich Forschenden:

……[redacted]……

Datum: 04.10.2023

Unterschrift der betreuenden Professorin/des betreuenden Professors an der HAW bzw. der Studienleitung (falls vorhanden):
Ich habe den Antrag geprüft und befürworte ihn in der vorliegenden Form.

[redacted]

Datum: 6.10.23

[18] Sofern die Publikation als Monografie erfolgt und eine elektronische Fassung nicht zur Verfügung steht, genügt eine Information der Ethikkommission über die bibliographischen Angaben. Es ist erwünscht, dass ein Exemplar der Monografie der Bibliothek der Hochschule zur Verfügung gestellt wird.

## Quellenangaben


1. WHO – Standards for Prosthetics and Orthotics https://apps.who.int/iris/bitstream/handle/10665/259209/9789241512480-part1-eng.pdf?sequence=1&isAllowed=y
2. Zweites Deutsches Fernsehen – High-Tech- Armprothese https://www.zdf.de/gesellschaft/volle-kanne/high-tech-armprothese-100.html#:~:text=Die%20Kosten%20f%C3%BCr%20moderne%20High,Krankenkassen%20oder%20der%20Berufsgenossenschaft%20%C3%BCbernommen.
3. Friedrich Georg Streifender KG – Prothetik für die obere Extremität – Armprothesen und Handprothese https://www.streifeneder.de/armprothetik
4. Said S, Boulkaibet I, Sheikh M, Karar AS, Alkork S, Nait-Ali A. - Machine-Learning-Based Muscle Control of a 3D-Printed Bionic Arm https://pubmed.ncbi.nlm.nih.gov/32498289/
5. Gaël Langevin – French InMoov designer https://inmoov.fr/
6. Sicherheitsingenieur.NRW - Schutzkleinspannung https://sicherheitsingenieur.nrw/glossar/schutzkleinspannung/
7. Formlabs – Der ultimative Leitfaden für den lebensmittelechten 3D-Druck: Behördliche Vorgaben, Technologien, Materialien und mehr https://formlabs.com/de/blog/leitfaden-lebensmittelechtheit-3d-druck/
8. AB3D – Druckdauer 3D Druck: Wie lange dauert ein Ausdruck und warum? https://www.ab3d.at/druckdauer-3d-druck-wie-lange-dauert-ein-ausdruck-und-warum/

HAW HAMBURG

# Probandeninformation zur Studie:

## Design and Implementation of a 3D Printed Arm Prosthetic with a Rotational Wrist Joint Controlled by EMG

**Verantwortliche Leiterin der wissenschaftlichen Studie:**

Prof. Dr. Meike Wilke [redacted]

Lara Borsdorf [redacted]

Sehr geehrte Studienteilnehmerin, sehr geehrter Studienteilnehmer,

hiermit bitten wir Sie um die Teilnahme an unserem Forschungsprojekt, die an der HAW Hamburg, entweder an der Fakultät LS oder TI, oder zu Hause bzw. im Alltag durchgeführt werden. Ihre Teilnahme ist freiwillig und Sie können Ihre Zustimmung jederzeit ohne Angabe von Gründen und ohne Einfluss auf derzeitige oder zukünftige Behandlungen widerrufen.

Zur Abgabe Ihrer Einverständniserklärung haben Sie das Recht Ihre Entscheidung zu bedenken, sowie eine Vertrauensperson während der mündlichen Aufklärung hinzuzuziehen.

### Ziel der Studie

Nicht jeder, der eine Prothese benötigt, hat Zugang zu einer solchen. Dies liegt sowohl an den Kosten als auch an der Zeit, die für die Herstellung von Prothesen benötigt wird. Eine vielversprechende Lösung für dieses Problem könnten 3D-gedruckte Prothesen sein, wie bereits durch vorhandene Forschung und Experimente in diesem Bereich gezeigt wurde.

Das Ziel dieser Studie ist es, die Funktionalität einer 3D-gedruckten Armprothese zu testen, die mithilfe von EMG-Signalen über die Armmuskulatur gesteuert wird. Dabei sollen auch der Tragekomfort und die Alltagstauglichkeit getestet werden.

Die Studie wird an Proband/innen durchgeführt, die oberhalb des Handgelenks amputiert sind, da es sich um eine Prothese mit Handgelenk handelt. Außerdem muss die Amputation unterhalb des Ellbogens (transradial) erfolgt sein, da es sich um eine Unterarmprothese handelt, die am Arm über den Ellbogen befestigt wird. In dieser Studie soll zunächst die Funktionalität anhand einiger Handgesten wie dem Öffnen und Schließen der Hand oder der Rotation des Handgelenks getestet werden. Die Erkenntnisse aus dieser Studie werden dazu beitragen, die Prothese in Zukunft weiterzuentwickeln, beispielsweise durch die Implementierung zusätzlicher Gesten oder die Integration von Feedback-Mechanismen.

## Versuchsdurchführung

Die Studie wird individuell durchgeführt. Zunächst werden Muskelkontraktionen im Arm mithilfe der Elektromyografie (EMG) gemessen. Dafür wird ein MyoBand, welches acht Elektroden besitzt, verwendet. Das MyoBand zeichnet ein 8-kanaliges EMG-Signal auf. Das Band wird über den Arm gezogen und auf die Haut gelegt, um die Signale nicht-invasiv aufzunehmen. Je nach Körperbehaarung oder Hautbeschaffenheit kann es notwendig sein, Haare zu entfernen und die Haut mit einem Hautreinigungsgel (Everi, Fa. Spes medica) zu behandeln, um die elektrische Leitfähigkeit zu verbessern. Diese Methode entspricht dem medizinischen Standard, der im klinischen Betrieb täglich verwendet wird. Es werden keine Daten gespeichert, die zur Identifizierung der Proband/innen verwendet werden können.

Nach dieser Vorbereitung werden die Proband/innen gebeten, ihre Armmuskulatur so zu kontrahieren, wie sie es bei den vorgegebenen Gesten tun würden. Gegebenenfalls wird dieser Prozess auch am nicht-amputierten Arm durchgeführt. Mithilfe dieser Signale wird die Armprothese "trainiert" und an die Muskelkontraktionen des jeweiligen Proband/innen angepasst. Im zweiten Schritt wird die Armprothese gemeinsam mit dem MyoBand am Arm angelegt. Nun sollen die Armmuskeln genutzt werden, um die Prothese mithilfe des MyoBandes zu steuern. Dabei sollen die Proband/innen versuchen, Objekte zu greifen und zu bewegen, um die Funktionalität, Alltagstauglichkeit und den Komfort zu testen.

## Risiken

Die Risiken der zuvor beschriebenen Schritte sind minimal.

Die nicht-invasiven Schritte zur Applizierung der Oberflächenelektroden (EMG) können zu leichtem Unbehagen durch Abrieb an der Haut führen. Das zur Verbesserung des Haut-Elektroden-Kontaktes verwendete Hautreinigungsgel kann in sehr seltenen Fällen zu allergischen Reaktionen in Form von lokalen Rötungen führen.

## Persönliche Daten

Während der Studie werden personenbezogene Daten erhoben und nur in pseudonymisierter Form aufgezeichnet. Pseudonymisierung bedeutet Verschlüsselung von Daten ohne Namensnennung, nur mit Buchstaben oder Nummern codiert. Die Zuordnung der Daten oder Proben zu einer Person ist nur möglich, wenn hierfür der Schlüssel eingesetzt wird, mit dem die Daten pseudonymisiert wurden. Die personenbezogenen Daten/Proben werden unter besonderen Schutzvorkehrungen getrennt von der Schlüsselliste aufbewahrt. Eine Entschlüsselung ist nur durch die für die Studie verantwortlichen Personen möglich. Dritte erhalten keinen Einblick in die Originalunterlagen. Die Datenspeicherungszeit beträgt 10 Jahre. Eine Datenweitergabe an personenbezogenen Daten an Dritte findet nicht statt. Bei Widerruf der Studienteilnahme werden die personenbezogenen Daten gelöscht. Eine Veröffentlichung findet nur mit pseudonymisierten Daten statt. Die experimentellen Ergebnisse können einer dritten Person für Forschungszwecke weitergegeben werden. In diesem Fall werden die Daten nur verschlüsselt und der Privatbereich der Teilnehmenden völlig geschützt sein.

Die Ergebnisse dieser Studie werden im Rahmen einer Masterarbeit und evtl. wissenschaftlicher Publikationen sowie Kongressbeiträgen verwendet. Dabei werden ausschließlich Altersangaben, Geschlecht und der Zeitraum seit der Amputation der Teilnehmenden verwendet, um sicherzustellen, dass diese nicht identifiziert werden können. Es werden keine Bilder verwendet, auf denen die Personen identifiziert werden könnten. Stattdessen wird lediglich ein Bild gezeigt, auf dem die Prothese am

Arm zu sehen ist, ohne das Gesicht der Person erkennbar zu machen. Sollten auffällige Merkmale am Arm vorhanden sein, wie etwa Tattoos oder besondere Narbenbildung, die zur Identifizierung führen könnten, werden diese Merkmale retuschiert, um jegliche Identifikation zu verhindern.

## Teilnahme an der Studie

Voraussetzung für die Teilnahme an der Studie ist die Einwilligung und Einwilligungsfähigkeit. Sollte eine der folgenden Punkte auf Sie zutreffen, ist eine Teilnahme an der Studie nicht möglich.

- Neuromuskuläre Erkrankung
- Schwangerschaft
- Drogen-, Medikamenten- und/oder Alkoholmissbrauch
- Ansteckende Erkrankungen

## Abbruch der Studie

Falls bei Ihnen unerwartet Rötungen, allergische Reaktionen, Herz-Kreislauf-Symptome während des Versuches auftreten oder Sie im Verlauf Ausschlusskriterien aufweisen, dann kann jeder einzelne Versuchsschritt jederzeit abgebrochen werden. Sie erhalten dann eine Bezahlung entsprechend dem Zeitaufwand, an dem Sie tatsächlich teilgenommen haben. Sie können zu jedem Zeitpunkt die Teilnahme am Forschungsprojekt abbrechen. Natürlich würden wir dann gerne von Ihnen wissen wollen, warum Sie die Teilnahme abbrechen. Aber Sie brauchen uns keine Gründe nennen, wenn Sie nicht möchten.

## Genehmigung des Versuchs

Die Versuchsdurchführung, die wir Ihnen hier vorstellen, wurde von der zuständigen Ethik-Kommission unter der Bearbeitungsnummer XXXXXX zustimmend bewertet.

## Aufwandsentschädigung

Zur Aufwandsentschädigung für die Teilnahme an der Studie erhalten Sie einen Betrag von 13 €/h. Im Falle eines vorzeitigen Abbruchs der Studie erhalten Sie ebenfalls eine Aufwandsentschädigung, entsprechend der bis dahin beanspruchten Zeit. Für durch Anreise entstandene Kosten werden Spritkosten in der Höhe von 0,20 €/km oder entsprechend die Kosten für ein Bahnticket der 2. Klasse übernommen.

## Weitere Fragen

Sollten Sie weitere Fragen haben, zögern Sie nicht die Prüfdurchführenden anzusprechen.

Bei Fragen stehen wir Ihnen gerne zur Verfügung.

Ihr Studien-Team

# Einwilligungserklärung zur Studie:

# Design and Implementation of a 3D Printed Arm Prosthetic with a Rotational Wrist Joint Controlled by EMG

**Verantwortliche Leiterin der wissenschaftlichen Studie:**

Prof. Dr. Meike Wilke [redacted]
Lara Borsdorf [redacted]

Angaben zur Person:

Name, Vorname : _____

Geburtsdatum: _____

Hiermit bestätige ich, dass ich freiwillig an der o.g. Studie teilnehme.

Ich wurde über Nutzen und Risiko der Studie vor der Versuchsdurchführung aufgeklärt und habe die Erklärungen verstanden.

Mir wurde ein Exemplar der Probandeninformation aushändigt, die ich die gelesen und verstanden habe. Ich konnte alle offenen Fragen klären, sodass ich vor Beginn der Studie keine weiteren Fragen mehr habe. Darüber hinaus wurde ich über mein Widerrufsrecht dieser Einwilligungserklärung und dessen Folgen informiert.

Für die Studie wurde eine Aufwandsentschädigung von 13 €/h vereinbart, die mir auch im Falle eines vorzeitigen Abbruchs der Studie entsprechend der bis dahin beanspruchten Zeit ausbezahlt wird.

**Datenschutzpassus:**

**Mir ist bekannt, dass im Rahmen dieses Forschungsvorhabens personenbezogene Daten erhoben und in pseudonymisierter (verschlüsselter) Form aufgezeichnet und gespeichert werden. Die Datenspeicherzeit beträgt 10 Jahre. Die personenbezogenen Daten werden nicht an Dritte weitergegeben. Ich weiß, dass ich mein Einverständnis zur Speicherung der personenbezogenen Daten jederzeit widerrufen kann. Im Falle des Widerrufs werden alle personenbezogenen Daten gelöscht.**

| | |
|---|---|
| Ort, Datum | Unterschrift Proband/in |
| Ort, Datum | Unterschrift Versuchsdurchführende/r |

# Einverständniserklärung

**I.** **DIE PARTEIEN**. Diese Einverständniserklärung ("Formular") wurde am 19.09.2023 erstellt, und zwar zwischen:

Teilnehmende: _____ mit der E-Mail-Adresse _____ (“Teilnehmende”) ist sich vollständig über das Verfahren und die möglichen Folgen der Teilnahme an dem Experiment bewusst, bei dem die im Rahmen der Masterarbeit "Design and Implementation of a 3D Printed Arm Prosthetic with a Rotational Wrist Joint Controlled by EMG" entwickelte 3D-gedruckte Armprothese getestet werden soll. Der/die Teilnehmende erklärt sich bereit, an dem Experiment teilzunehmen, indem er seine informierte Zustimmung gibt und die Erlaubnis erteilt, dass:

Experimentierende: Lara Borsdorf, Studentin der Hochschule für Angewandte Wissenschaften in Hamburg, mit der E-Mail-Adresse lara.borsdorf@haw-hamburg.de ("Experimentierende") sowie Prof. Dr. Meike Wilke, meikeannika.wilke@haw-hamburg.de die hier genannten Handlungen vornehmen dürfen:

**II.** **ERLAUBTE HANDLUNGEN**. Die Experimentierenden haben die uneingeschränkte Befugnis, die folgenden Handlungen vorzunehmen:

Durchführung der Evaluation einer 3D-gedruckten Armprothese, die im Rahmen der Masterarbeit "Design and Implementation of a 3D Printed Arm Prosthetic with a Rotational Wrist Joint Controlled by EMG" entwickelt wurde. Dies beinhaltet das Anbringen eines MyoBands an meinem Arm, um nicht-invasive EMG-Signale von meiner Armmuskulatur zu erfassen. Anschließend wird die 3D-gedruckte Armprothese angelegt, um ihre Steuerbarkeit basierend auf den zuvor aufgezeichneten Muskelbewegungsdaten zu bewerten. Mein Alter, Geschlecht und die Zeit seit der Amputation werden ausschließlich zu Forschungszwecken aufgezeichnet, ohne dass persönliche Daten preisgegeben werden. Die aus der Analyse meiner Daten gewonnenen Ergebnisse dürfen ausschließlich für Bildungs- und Forschungszwecke verwendet werden.

**III.** **NUTZERRECHTE**. Der/die Teilnehmende hat das Recht, jederzeit während des Experiments seine/ihre Teilnahme zu beenden. Die oben genannten Handlungen können von den Experimentierenden durchgeführt werden, solange der/die Teilnehmende dieses Formular nicht widerruft. Als Aufwandsentschädigung für die Teilnahme erhält der/die Teilnehmende 13 Euro pro Stunde. Darüber hinaus werden die Kosten für den Transport, entweder mit öffentlichen Verkehrsmitteln oder dem eigenen Auto, erstattet.

**IV.** **OFFENLEGUNG**. Der/die Teilnehmende erklärt sich bereit, den Experimentierende von jeglicher rechtlichen, finanziellen und sonstigen Haftung freizustellen, einschließlich seiner Beauftragten, Angestellten, Nachfolger und Bevollmächtigten sowie deren Erben, persönlichen Vertretern, verbundenen

Unternehmen, Nachfolgern und Bevollmächtigten sowie aller Personen, Firmen oder Unternehmen, die haftbar sind oder als haftbar bezeichnet werden könnten, unabhängig davon, ob sie hier genannt sind oder nicht, wobei keiner von ihnen eine Haftung gegenüber dem Unterzeichner anerkennt, die jedoch alle ausdrücklich jede Haftung ablehnen, von allen Ansprüchen, Forderungen, Schäden, Klagen, Klagegründen oder Prozessen jeglicher Art, die sich aus allen Verletzungen und Schäden jeglicher Art, sowohl an Personen als auch an Eigentum, ergeben oder in Zukunft ergeben könnten, sowie von allen Verletzungen und Schäden, die sich in Zukunft aus den hier zulässigen Handlungen ergeben oder in irgendeiner Weise damit zusammenhängen könnten.

**Unterschrift des Empfängers: _____**

**Datum**: _____

HAW HAMBURG

Ethikkommission

29.11.2023

Ethikantrag 2023-26

*„Design and Implementation of a 3D Printed Arm Prosthetic with a Rotational Wrist Joint Controlled by EMG“*

vom 06.10.2023

Antragstellerin: Lara Borsdorf, MA-Studentin
Betreuerin: Prof. Meike Wilke

Sehr geehrte Frau Borsdorf,

das o.g. Vorhaben wurde nach Prüfung durch die Ethikkommission der HAW Hamburg als grundsätzlich „ethisch unbedenklich“ bewertet.

Mit freundlichen Grüßen

[redacted]

Dr. Christiane Stange (Koordination Ethikkommission)

## Erklärung zur selbstständigen Bearbeitung

Hiermit versichere ich, dass ich die vorliegende Arbeit ohne fremde Hilfe selbständig verfasst und nur die angegebenen Hilfsmittel benutzt habe. Wörtlich oder dem Sinn nach aus anderen Werken entnommene Stellen sind unter Angabe der Quellen kenntlich gemacht.

| Ort | Datum | Unterschrift im Original |
|---|---|---|